Biophysical Characterization of the Photoreceptor Synapse

A thesis submitted for the degree of Doctor of Philosophy of the Australian National University

Amy K. Berntson, June 2001

Statement of Authorship

All research presented in this thesis is original, and carried out by myself under the supervision of Dr. Rowland Taylor.

Amy Berntson

Acknowledgements

It is a daunting, and surely impossible task to express in words the gratitude and warmth that I feel toward my supervisors, Rowland and Catherine. Firstly, I would like to thank Rowland and Catherine for all of their dear friendship and support over the years. I very much appreciate the time and effort that Rowland has spent in teaching me. In particular, I am very grateful to learn the skills and techniques that Rowland has developed and perfected throughout his career. If I must choose, the most important lesson I have learned from Rowland is probably dogged, stubborn persistence. In the many instances where I nearly gave up, it was Rowland's infinite persistence, and constant encouragement which brought success. In addition, I would like to thank Rowland for all of the long and interesting discussions, many of which were digression. And I really enjoyed the time we spent bashing out ideas on the white-board. I must say that those moments (sometimes turning into hours) going head to head to solve a problem were the highlight of my Ph.D.

I also very much appreciate Catherine's friendship and support. I have never worked with, nor met someone so creative and quick-witted. I appreciate her so much as a role model for me both in terms of scientific achievement, and as a woman who really can "have it all". There was not one single moment throughout my Ph.D. that I did not feel 100% supported by both Rowland and Catherine. They are an incredible, and formidable team.

I would also like to thank John Bekkers for helpful insight into what goes on outside the retina. And I truly appreciate the time he spent reading my thesis, and making comments. The three of them, Rowland, Catherine, and JB, were the most influential people in my scientific development, and set very high standards for me. Thank you.

I would also like to thank my family for encouragement and support while I've been overseas. In particular I'd like to thank my mom and Jim for dealing with all of the little niggling and annoying details on my behalf while I've been away. Thanks Dad for all of your encouragement, and advice on presentations. I owe a thanks to all of my friends, especially Sam, Deb, Nathan, Nicolas, Danny Mac, and Tim, all of whom put up with me when things got really stressful. And I'd like to extend a special thanks Daniel who was

supportive and encouraging while I was writing my thesis, which was a very busy and stressful time. Thanks for making me laugh so much, and thanks just for being tuff.

Publications Arising From Data Presented in this Thesis

Papers appearing in refereed journals

Berntson, A. and Taylor, W. R. (2000). "Response characteristics and receptive field widths of on-bipolar cells in the mouse retina." J Physiol (Lond) **524 Pt 3**: 879-89.

Conference abstracts

Berntson,A and Taylor, W.R. (2000) "Light response properties of Bipolar Cells in the Mouse Retina." Proceedings of the Australian Neuroscience Society. Volume 11, abstract 1-145.

Abstract

The present study establishes the dark-adapted mouse retinal slice as a new preparation for the study of neuronal light responses. This study also represents the first systematic study of bipolar cell response properties in the mammalian retina. The bipolar cells in the retina form the direct connection between photoreceptors, which capture light, and ganglion cells which send their axons to the brain. The response properties of the bipolar cells will largely determine the nature of the input received at the ganglion cell level, thus bipolar cell response properties are of keen interest.

First, the properties of the voltage-gated calcium currents in bipolar cells were examined, since they will in large part determine the nature of the bipolar cell output onto amacrine and ganglion cells. This was accomplished by making whole-cell recordings from bipolar cells in the light-adapted mouse retinal slice preparation. Two voltage-gated calcium currents were observed: a sustained calcium current with kinetics resembling an L-type current, and a classical T-type calcium current. Measurements of the inactivation range of the T-type current indicate that it would be almost completely inactivated within the voltage operating range of the bipolar cells. As bipolar cells are generally assumed to be non-spiking neurons, it is unclear what the role of the T-type calcium channel is.

The sustained L-like calcium current of the mouse bipolar cells had a reduced sensitivity to dihydropyridines compared to the L-type currents found in skeletal or cardiac muscle, or in the nerve terminals of goldfish bipolar cells. In addition, the sustained calcium currents are activated by much lower voltages than "classical" L-type currents. This result challenges the dogma that all sustained calcium currents are high voltage activated. The unusual properties of the sustained calcium currents suggests they may be mediated by a novel calcium channel simliar to an L-type calcium channel. The bipolar cell calcium channel may contain the recently cloned α1F calcium channel subunit, which has been shown to be involved in congenital stationary night blindness. The sustained calcium current is probably responsible for the regulation of synaptic vesicle exocytosis, as is the case for the L-type calcium current found in goldfish bipolar cells.

Second, a characterization of mammalian bipolar cell light responses was undertaken. Light responses from on-cone bipolar, off-cone bipolar, and rod bipolar cells were recorded from the dark-adapted mouse retinal slice preparation. The bipolar cells were filled with lucifer yellow during recording in order to identify them morphologically. When exposed to saturating light intensities, on- and off-cone bipolar cells responded with sustained inward and outward currents, respectively, while the rod bipolar cell responded with an inward current which inactivated to a

smaller plateau current. The current-voltage relation of the light evoked current was measured by flashing a light at a series of holding potentials. For the three main classes of bipolar cells, the current voltage relation was linear, and reversed around 0mV indicating that under dark adapted conditions bipolar cells receive primarily glutamatergic input from the photoreceptors. This is surprising, given that anatomical studies have shown that bipolar cells receive a large number of amacrine cell inputs onto their axons, and axon terminals. Spontaneous inhibitory input was frequently seen in bipolar cell recordings, however light evoked inhibitory input was only occasionally observed. This may be due either to a lower sensitivity of the inhibitory surround mechanism, or to the fact that much of the surround may have been cut away during the slicing procedure.

The receptive field profiles were measured for the three classes of bipolar cells. For the rod bipolar cells, an estimated dendritic spread of 20μm and a coverage factor of 3 would mean they would contact around 37 rods, close to the 25 rods per rod bipolar cell estimated from electron microscopic studies. However, the physiological receptive field size was measured to be 67μm (n=6), just over three times larger than the estimated dendritic spread. This suggests that while rod bipolar cells make direct contacts with only 20-30 rods, they receive input from around 750 rods, perhaps via mild signal spread in the OPL.

The receptive field profiles measured for cone bipolar cells was 43μm for on-cone bipolar cells (n=5), and 40μm for off-cone bipolar cells (n=1). This is also slightly larger than the bipolar cell dendritic spread measured in rat retina and, assuming mouse bipolar cells have similar dendritic fields, indicates that there is mild spread of cone signals, as well as rod signals, in the outer plexiform layer. A receptive field size of 40μm would mean cone bipolar cells receive input from 8-12 cones. Since the mouse retina is approximately 3mm in diameter, a 40μm receptive field equates to about 1.5 degrees of visual angle. Thus the highest predicted spatial frequency that the cone bipolar cells could resolve is about 0.3 cycles per degree. This is consistent with behavioral studies which indicate that the highest frequency that the mouse visual system can resolve is <0.5 cycles/degree. This result indicates that the bipolar cell array may limit the spatial resolution of the visual system, and that at least one class of ganglion cells preserves the spatial acuity of the cone bipolar cells.

The intensity response relation of the rod bipolar cell photocurrent to 400ms light steps could be fit by a saturation function with a Hill coefficient of 1.1 (n=5), while the relation of the photovoltage was slightly steeper with a Hill coefficient of 1.46 (n=5). The intensity response relations of on-and off-cone bipolar cells showed evidence for dual rod and cone input. The rod component of the intensity response relations could be fit with a Hill coefficient of 1.1, while the

cone component had a Hill coefficient of 2.25 (n=3) for the on-cone bipolar cell photocurrent, and 1.59 (n=3) for the off-cone bipolar cell photocurrent. The light intensities required to evoke half saturating responses are 1.7- 1.9 log units higher for cone bipolar cells compared to rod bipolar cells, similar to the different sensitivities measured for mammalian rod and cone photoreceptors.

All three classes of bipolar cells displayed an increase and subsequent decrease in variance as the intensity of light stimuli was increased from darkness to saturating intensities. Fitting the change in variance of 4 on-cone bipolar cells to a parabolic function yielded an estimate of the elementary event size of -3.3pA, and the number of synaptic sites as 24. Channel noise can account for at most 18% of the variance, thus most of the variance must arise from synaptic sources. The elementary event size of the rod bipolar cells was estimated to be about -3.5pA, and is presumably due to the capture of a single photon in a rod photoreceptor.

During the characterization of the rod bipolar cell light responses, it was noticed that they rapidly inactivated to light intensities just below half-saturating, and higher. This observation was made in every rod bipolar cell recorded from which responded to light. The inactivation was prevented by including 10mM BAPTA in the recording electrode, indicating that it is mediated by a rise in intracellular calcium. The inactivation was found to be voltage dependent indicating that it is a post-receptoral phenomenon. The inactivation occurred rapidly with a time constant τ of 60ms, which was independent of both light intensity and voltage. The magnitude of the inactivation was slightly voltage dependent, being slightly larger at negative holding potentials. Including 10mM BAPTA in the recording electrode caused the intensity response relation to light steps to be steeper (Hill 1.96) than in control conditions (Hill 1.1). This suggests that calcium may play a role in regulating the operating range of the rod bipolar cell.

Since recovery from inactivation followed an exponential time course (τ = 240ms), it was concluded that the rod bipolar cell response will be maximal when each connecting rod captures one photon every 720ms, or 1.39 photons/rod/ s or fewer. If rod bipolar cells collect from approximately 25 rods, this translates into 35 single photon events per rod bipolar cell per second (1.39 photons/rod/s times 25 rods). Inactivation of the rod bipolar cell light response may be a mechanism for post-receptoral adaptation. Alternatively, the inactivation may effectively shut down the rod bipolar cell- AII amacrine cell pathway when the light intensities exceed a threshold, leaving the direct rod to cone pathway as the main pathway for the transmission of rod signals.

List of Abbreviations

AP-4	2-amino-4-phosphonobutyric acid
AMPA	amino-3-hydroxy-5-methylisoxazole-4-proprionic acid
BAPTA	1,2-bis(2-aminophenoxy)-ethane-N,N,N',N'-tetraacetic acid
CaM	Calmodulin
CaMKII	Calcium/calmodulin-dependent kinase, type II
Co	Cobalt
CSNB	Congenital stationary night blindness
DHP	Dihydropyridine
DMSO	Dimethyl sulfoxide
EGTA	Ethylene glycol-bis(-aminoethyl ether)-N,N,N',N'-tetraacetic acid
ERG	Electroretingram
$GABA_A$	δ-aminobutyric acid receptor, type A
$GABA_B$	δ-aminobutyric acid receptor, type B
$GABA_C$	δ-aminobutyric acid receptor, type C
GCL	Ganglion cell layer
HVA	High voltage activated
INL	Inner nuclear layer
IPL	Inner plexiform layer
KA	Kainate
LVA	Low voltage activated
mGluR6	Metabotropic glutamate receptor, type 6

NMDA	N-methyl-D-aspartic acid
ONL	Outer nuclear layer
OPL	Outer plexiform layer
V_m	Membrane voltage

If there's one thing a rod can do well,

it's telling a bipolar cell

that a light was turned on

and it sees a photon.

Oh! The quantal secrets they tell!

Chapter 1

General Introduction

As the first stage of visual processing, the retina extracts features from the visual environment and translates them into a neural image. The transduction of light into electrical signals begins at the photoreceptors which sample the light intensity at each point within the visual scene. Some processing of the light information occurs in the photoreceptors themselves. For instance, the kinetics of the photoreceptor response filters the signal temporally, and the light input is spatially filtered by virtue of the spacing of the photoreceptors within the retina (Rieke and Baylor, 1998). Moreover, in some species lateral signal flow occurs between neighboring photoreceptors due to gap-junctional coupling; hence mild convergence of signals is possible even within the first cell layer (Burkhardt, 1977). The synapse between the photoreceptors and bipolar cells in the retina represents the first opportunity for extensive information processing such as signal convergence and divergence, temporal and spatial filtering, modulation of inhibition and excitation, and feature extraction. The properties of the synaptic transmission between the photoreceptors and bipolar cells will limit the capabilities of the rest of the visual system, and thus are of keen interest.

In the present study, synaptic transmission across the first synapse was monitored by stimulating the photoreceptors with light while recording the bipolar cell responses. This set-up is ideal, since the photoreceptors will be responding to their natural stimulus. A number of such studies have been performed on the photoreceptor/bipolar cell synapse in fish and amphibian retina (Ashmore and Falk, 1979; Ashmore and Copenhagen, 1983; Copenhagen et al., 1983; Belgum and Copenhagen, 1988; Hare and Owen, 1990). However, several differences exist between mammalian and non-mammalian retina, which warrant a specific study of mammalian bipolar cells. For example, there is more signal convergence at the first synapse in non-mammalian retinas due to extensive gap-junctional coupling among photoreceptors (reviewed by Attwell, 1986; Sterling, 1990). Such coupling is largely absent from mammalian retina (Schneeweis and Schnapf, 1995). Furthermore, in non-mammalian retina, bipolar cells frequently receive mixed rod- and cone- input (although there are cone-specific bipolar cells in some species; Ishida et al., 1980), whereas bipolar cells in mammalian retina restrict their dendrites either to rod or to cone photoreceptors. Lastly, photoreceptor kinetics and synaptic transmission are generally faster in the mammalian retina presumably due to the higher body temperature.

The focus of the present study was to characterize mammalian bipolar cell response properties. The bipolar cells were grouped into three main classes consisting of rod bipolar, on-cone bipolar, and off-cone bipolar cells. First, voltage-gated calcium currents were examined in each class of bipolar cell, since the calcium current at the nerve terminals of bipolar cells will control neurotransmitter release onto the bipolar cells' postsynaptic targets. This was accomplished by recording from bipolar cells in the light-adapted mouse retinal slice preparation, and is the topic

of Chapter 3. Second, we wished to characterize the light response properties of the three classes of bipolar cells, which was accomplished by stimulating the photoreceptors with light while recording from the bipolar cells in the dark-adapted retinal slice. In these experiments we measured a number of basic biophysical light response properties including the light response kinetics, the intensity-response relation, the current-voltage relation, the receptive-field profile, and noise characteristics. These topics will be discussed in Chapter 4. The third goal was to look for calcium-feedback in the mouse rod bipolar cells as was reported in dogfish (Shiells and Falk, 1999) and salamander (Nawy, 2000). This topic is discussed in Chapter 5.

The following introduction will review the current understanding of the photoreceptor/bipolar cell synapse. The photoreceptors will be reviewed first, include the anatomy and physiology of the photoreceptor synapse, the phototransduction cascade, and the spectral sensitivity of rods and cones. The bipolar cell section will describe the pre- and post-synaptic contacts of bipolar cells, the parallel rod and cone pathways, and the on-bipolar cell signal-transduction cascade. The other three types of neurons in the retina, namely the horizontal, amacrine, and ganglion cells will be reviewed only briefly. The types and mechanisms of light adaptation will be discussed, and finally, the last section will briefly describe the intricacies that are peculiar to the mouse retina.

Organization of the retina

The retina is organized into three cellular layers separated by two synaptic layers. The Nomarski image (Figure 1.1) is of the mouse retinal slice preparation as it appears under the microscope during an experiment, and the schematic (right) shows the morphology and connectivity of the neurons in the retina. The rods and cones in the outer nuclear layer (ONL) detect light and relay the signals to the second-order bipolar and horizontal cells. The synapse between the photoreceptors and the second-order neurons occurs in the very narrow outer plexiform layer (OPL), where the bipolar and horizontal cells send their processes into invaginations in the photoreceptor terminals. The bipolar and horizontal cell bodies, along with amacrine cell bodies, reside in the inner nuclear layer (INL). Horizontal cells make feedback synapses onto the photoreceptors, and form a lateral inhibitory network at the OPL. Bipolar cells form the vertical pathway for excitatory signals in the retina and synapse onto amacrine and ganglion cells in the inner plexiform layer (IPL). The amacrine cells form lateral inhibitory networks in the IPL where they synapse onto bipolar, ganglion, and other amacrine cells. Action potentials are first generated by some classes of amacrine cells, while the remaining amacrine cells signal via graded polarizations. All ganglion cells generate action potentials, and as the final output of the retina their axons bundle together at the optic disc and project to the brain.

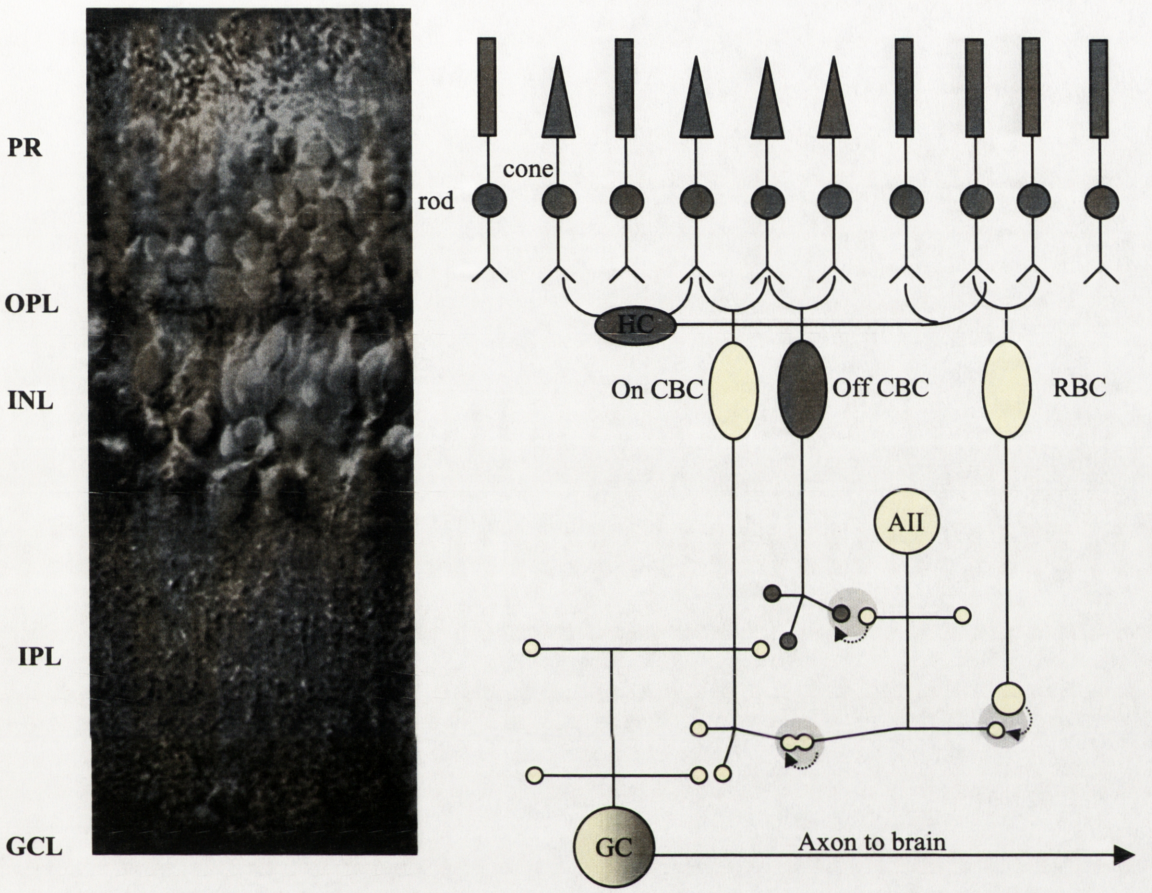

Figure 1.1 Organization of the mammalian retina. On the left is a Nomarski image of the mouse retinal slice preparation as it appears during an experiment. The schematic on the right illustrates the morphology and connectivity of neurons within the retina. Neurons which hyperpolarize in response to light are colored grey, while neurons which depolarize in response to light are colored yellow. The ganglion cell depicted is an on-off ganglion cell and receives excitatory input from cone bipolar cells at light onset and offset. The synapses involved in the AII amacrine cell pathway (discussed later in text) are highlighted by the light grey circles. PR photoreceptors; OPL outer plexiform layer; INL inner nuclear layer;IPL inner plexiform layer; GCL ganglion cell layer; HC horizontal cell; RBC rod bipolar cell; On CBC On-cone bipolar cell; Off CBC Off-cone bipolar cell; AII AII amacrine cell; GC ganglion cell.

Photoreceptors

The rod and cone photoreceptors share the task of transducing light into electrical signals. Rod photoreceptors mediate vision under very dim (scotopic) conditions, while the cones mediate vision at high (photopic) intensities. There is an overlapping (mesopic) region of light intensities where both rods and cones are active. The relative light intensity ranges in which rods and cones operate are shown in Figure 1.2.

The photoreceptors respond to light with graded polarizations. Changes in light intensity translate into graded changes in the membrane voltage, which ultimately regulates the rate of neurotransmitter release via the activation of voltage-gated calcium channels. Photoreceptors are maximally depolarized in darkness and release glutamate continuously, while light causes hyperpolarization and a decrease in the rate of neurotransmitter release (Dowling, 1987). Second order neurons, such as the bipolar and horizontal cells, are tonically exposed to high concentrations of glutamate in the dark, while light is signaled by the fall of the glutamate concentration in the synaptic cleft.

Morphology of the Photoreceptor Synapse

The photoreceptor synapse is optimized for maintaining high rates of neurotransmitter release. First, the presence of non-inactivating L-type calcium channels at the active zone ensures a constant influx of calcium at depolarized potentials. A constant calcium influx is necessary to support prolonged bouts of neurotransmitter release. Second, the photoreceptor terminal contains a synaptic ribbon, which is an electron-dense structure lying just above and perpendicular to the active zone believed to recruit synaptic vesicles for release. Electron micrographic studies show that synaptic vesicles are tethered to the ribbon, providing support for the hypothesis that the ribbon captures vesicles from the cytosol and transports them to the active zone (Rao-Mirotznik et al., 1995). And third, the photoreceptor axon terminals are filled with thousands of synaptic vesicles, providing sufficient synaptic vesicles for continuous release. It is estimated that photoreceptors are capable of maintaining release rates of at least 40 vesicles/s and as high as 400 vesicles per second (Rao et al., 1994). Such a high rate of release is much greater than that which occurs at conventional boutons (typically only one synaptic vesicle per action potential Korn and Faber, 1991). While other synapses can also exocytosis synaptic vesicles at a high rate, such as the frog neuromuscular junction (Betz and Bewick, 1993), they rarely sustain such a release rate for prolonged periods. In contrast, the photoreceptors are tonically depolarized in the dark, and release glutamate continuously.

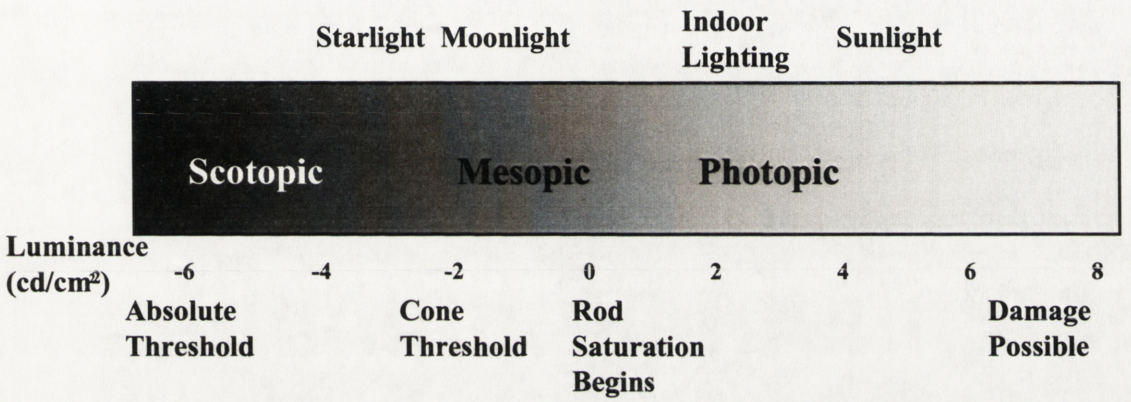

Figure 1.2 Operating range of the visual system. The rod system mediates vision under scotopic conditions while cones mediate photopic vision. Both the rods and cones operate under mesopic conditions. The light stimuli used in the present experiments ranged over 6 log units from absolute threshold into the mesopic region. The values in this figure are taken from Hood and Finkelstein (1986).

Photoreceptors also differ from conventional neurons in their use of a single active zone with a high release rate, as opposed to multiple active zones with a low release rate. Rao et al (1994) speculate that since rods are by far the most numerous neuron in the retina, this design is the most efficient use of space, which is at a premium in the retina. Since rods have only a single active zone (and a single synaptic ribbon) divergence is low, and only four post-synaptic elements (two rod bipolar cell and two horizontal cell dendrites) invaginate the rod spherule (Sterling et al., 1988; Rao-Mirotznik et al., 1995).

In contrast, the corresponding structure of the cone (the cone pedicle) has between 12-20 active zones in cat (Boycott and Kolb, 1973; Sterling and Harkins, 1990) and up to 38 in monkey (Hopkins and Boycott, 1997), each with its own ribbon. Consequently, the size of the cone pedicle is considerably larger than that of the rod spherule, occupying ~8 times the volume (Sterling and Harkins, 1990). Cones are less numerous (27,000 per sq. mm in cat retina; Sterling et al., 1988) and unlike the rod spherule, the cone pedicles form basal, as well as invaginating synapses with post-synaptic neurons (reviewed in Kolb, 1994; Hopkins and Boycott, 1995).

The Phototransduction Cascade

The photoreceptors respond to light through a second messenger system which couples photon absorption to the closure of cation channels. The phototransduction cascade will be discussed in some detail here because (i) it strongly influences the photoreceptor response properties, and (ii) it is the current model for the on-bipolar cell signal transduction cascade, which will be discussed later.

The phototransduction cascade begins with the absorption of a photon by one of several photopigments contained in the outer segments of rods and cones. The best studied photopigment is rhodospin, which is found in rods. Rhodopsin contains a vitamin A chromophore, 11-*cis*-retinal, attached to a protein, opsin, which is embedded in the membranes of the discs found in the outer segment. The energy of a photon isomerizes 11-*cis*-retinal, causing it to go through a series of conformational changes until it becomes meta-rhodopsin II (or activated rhodospin). Activated rhodopsin (R*) acts as the catalyst for the first step in the phototransduction cascade, which ultimately leads to the closure of cation channels in the outer segment.

In darkness, high concentrations of cGMP hold cation-selective cyclic nucleotide gated channels open. These outer-segment channels are highly permeable to Ca^{2+}, Na^{+}, and K^{+} ions (Yau and Nakatani, 1984; Hodgkin et al., 1985; Yau and Nakatani, 1985; Picones and Korenbrot, 1992; Picones and Korenbrot, 1995) and in darkness there is a constant flow of cations into the outer-segment. The resulting inward current is referred to as the dark current and keeps the cell

depolarized in darkness. When the absorption of a photon isomerizes rhodopsin, the newly formed R* forms a complex with the G-protein, transducin. R* catalyzes the exchange of GTP for bound GDP on the α subunit of transducin. Once bound to GTP, α-transducin-GTP dissociates from R* leaving it free for another round of transducin activation. α-transducin diffuses freely in the membrane and activates a cGMP-preferring phosphodiesterase (PDE) by binding to the γ-subunit, thereby removing an inhibitory constraint. PDE cleaves cGMP into 5'-GMP, leading to a drop in cGMP concentration and closure of the cyclic nucleotide-gated channels in the outer segment. This channel closure blocks the standing inward current, while continued efflux of K^+ hyperpolarizes the rod photoreceptor.

The G-protein mediated phototransduction cascade allows for a large gain of the signal, and in fact rod photoreceptors are capable of detecting and signaling single photons. There are two amplification steps in the cascade, the first stage occurring when a single molecule of activated rhodopsin activates of up to 150 molecules of α-transducin (Leskov et al., 2000). It has been estimated that R* and transducin collide with one another at a rate of 4000/s, but the actual activation of transducin by R* is much lower (Lamb and Pugh, 1992; Lamb, 1994). The activation may be limited by the rate of activation of transducin, or by the time required to exchange GTP for bound GDP, or a combination of these factors. Transducin activates PDE in a 1:1 ratio. However, PDE exists as a holomer, so two transducins will then activate a PDE holomer, which can then hydrolyze up to 5000 molecules of cGMP. PDE is one of the most efficient effectors and this second stage of amplification is limited only by diffusion (Lamb and Pugh, 1992; Rieke and Baylor, 1998).

Although rods and cones use essentially the same signal transduction cascade, cone responses are faster, less sensitive, and exhibit more robust features of adaptation than do rod responses (for review see Miller 1994). Cone responses are noisier than rods probably due to the instability of the cone photopigments (Schneeweis and Schnapf, 1999). These differences are thought to partially arise from differences in the protein-protein interactions in the phototransduction cascade, although the nature of these differences is poorly understood.

Cytoplasmic calcium plays a major role in both rod and cone adaptation (Matthews et al., 1988; Nakatani and Yau, 1988; Matthews et al., 1990; Menini, 1999; Pugh et al., 1999). While it affects many steps in the signal transduction cascade, there are three main consequences to a drop in calcium concentration, which account for many adaptive effects. First, guanylate cyclase (GC), which synthesizes cGMP, is inhibited by high concentrations of calcium. The fall in calcium concentration that occurs in the presence of light is sufficient to increase GC activity 10-fold (koch and stryer 1988). The increased production of cGMP will re-open the outer-segment

channels and re-establish the dark current. Second, when the calcium concentration drops, the calcium-calmodulin complex unbinds from the cGMP-gated channel, thus reducing the $K_{1/2}$ of the channel for cGMP. Thus cGMP unbinds more easily, and the cGMP-gated current will increase (be larger at a given cGMP concentration). Lastly, two other proteins involved in the inactivation of R*, recoverin and arrestin, are also influenced by the calcium concentration. Most recoverin is bound to calcium in the dark, but the drop in calcium concentration in the light leads to higher levels of Ca^{2+}-free recoverin. Once calcium unbinds, recoverin can phosphorylate arrestin, which then binds to and quenches the activity of R*. Thus the drop in calcium reduces the lifetime of R*, shortening the duration of the light response.

Spectral Cone Types

The cone photoreceptors are well known for their role in color vision. A particular photopigment absorbs photons most efficiently across a narrow band of wavelengths. Most cones express a single photopigment, although in some animals cones express multiple photopigments. In primates (including humans) there are three cone photoreceptor types (Marks et al., 1964), each expressing a photopigment tuned to either short (~450nm), medium (~500nm), or long (~600nm) wavelengths. These cones are often referred to as S-, M-, and L- cones, respectively. Primates are unusual in their trichromacy however, as most mammals express only S- and M-photopigments. There is a single spectral type of rod photoreceptor in all mammals which is tuned to medium wavelengths (~500nm) (Bridges and Quilliam, 1973; Baylor et al., 1984).

The biochemical explanation for the spectral tuning of photopigments resides in its molecular structure. The photopigment is composed of a chromophore (11-*cis*-retinal) and an opsin. The chromophore is the same in all photoreceptors, but the opsin to which it is attached differs (Leibovic 1990, from Science of Vision). The molecular structure of the opsin determines the wavelength of light to which the pigment is most sensitive. The photoreceptor responses themselves, however, are invariant with regard to wavelength. While each photopigment will absorb photons most efficiently of a particular wavelength, the photoreceptors response only reports the catching of quanta, not the nature of quanta caught. Color signals are extracted at later stages in the retina by comparing responses from different spectral cone types.

Bipolar cells

Like the photoreceptors, bipolar cells respond via graded polarizations, although instead of responding to light, they respond to graded changes in the glutamate concentration in the synaptic cleft. Also like the photoreceptors, the bipolar cell axon terminals are filled with hundreds of thousands of synaptic vesicles (von Gersdorff et al., 1996), and the active zones are

characterized by the presence of a synaptic ribbon (Heidelberger et al., 1994; von Gersdorff and Matthews, 1994). In other words, bipolar cells have several of the specializations that the photoreceptors have to allow them to maintain a very high rate of transmitter release. During prolonged depolarizations, some bipolar cells can maintain release rates exceeding 1000 vesicle s^{-1} (Neves and Lagnado, 1999).

Types of Bipolar Cells

Bipolar cells in the mammalian retina come in three functional classes: on-cone, off-cone, and rod bipolar cells. The cone bipolar cells receive direct input from the cone photoreceptors, and split the retina into on- and off- pathways. On-cone bipolar cells depolarize to increases in illumination, while off-cone bipolar cells depolarize to decreases in illumination. There have been 8-11 morphological types of cone bipolar cells described, depending on the species, which are distinguished based upon the stratification of their axon terminals in the IPL (Famiglietti, 1981; Kolb et al., 1981; McGuire et al., 1984; Pourcho and Goebel, 1987; Boycott and Wässle, 1991; Euler and Wässle, 1995; Hartveit, 1997). The on-cone bipolar cells stratify in the inner 2/3 of the IPL, while the off-cone bipolar cell axons stratify in the outer 1/3 of the IPL (Famiglietti and Kolb, 1976; Nelson et al., 1978; Bloomfield and Miller, 1986).

The ability to split the retina into on- and off- pathways results from the differential expression of glutamate receptors on the bipolar cell dendrites. Off-cone bipolar cells have AMPA/Kainate receptors that open in the presence of glutamate (Dvorak, 1984; Peng et al., 1995; Schultz et al., 1997; Brandstätter et al., 1998; Lo et al., 1998; DeVries and Schwartz, 1999; Morigiwa and Vardi, 1999). In contrast, on-cone and rod bipolar cells express the inhibitory metabotropic glutamate receptor, mGluR6, which closes channels in the presence of glutamate (Slaughter and Miller, 1981; Attwell et al., 1987; Shiells and Falk, 1990; Nakajima et al., 1993; Vardi and Morigiwa, 1997). When glutamate disappears from the cleft (in response to light), the inhibition on the mGluR6-linked channel is relieved and the channels open, depolarizing the cell. Ionotropic glutamate receptors have also been localized to on-bipolar cells(Hughes, 1997; Morigiwa and Vardi, 1999) but there have been no reports that they are functional.

In contrast to the morphological variations seen in cone bipolar cells, rod bipolar cells constitute a single population of cells with uniform coverage across the retina and homogenous physiological response properties (Wassle and Boycott, 1991; Berntson and Taylor, 2000). Rod bipolar cells are all of the on-type, and thus depolarize in response to light. Rod bipolar cells receive input exclusively from rod photoreceptors (Dowling and Boycott, 1966) thus the separation of the rod signal initiated by the photoreceptors is maintained across the first synapse.

Synaptic Contacts of Bipolar Cells

Bipolar cells receive a mixture of inputs, including glutamatergic input from the photoreceptors onto their dendrites, and inhibitory GABA and glycinergic input from amacrine cells onto their axon terminals. The light responses recorded from bipolar cells are therefore likely to represent a mixture of non-specific cation (glutamatergic) currents, and chloride (GABA and glycinergic) currents. A description of the number, and nature of the synaptic inputs onto the different classes of bipolar cells is introduced below.

Rod Bipolar Cells

Rod bipolar cells receive glutamatergic input in the OPL exclusively from the rod photoreceptors. Estimates of rod convergence onto rod bipolar cells varies among species. In the rabbit retina, 80-115 rods converge on each rod bipolar cell (Dacheux and Raviola, 1986; Young and Vaney, 1991), whereas in other species convergence is much lower: 20 rods/rod bipolar cell in cat retina (Boycott and Kolb, 1973), 20-60 rods/rod bipolar in primate retina (Grunert and Martin, 1991), and 25 rods/rod bipolar cell in mouse retina (Y. Tsukomoto, personal communication).

In addition to glutamatergic input from the photoreceptors in the OPL, rod bipolar cells also receive inhibitory input from GABA- and glycinergic amacrine cells in the IPL (Vaughn et al., 1981; Suzuki et al., 1990; Gillette and Dacheux, 1995; Pan and Lipton, 1995). Most of these synapses occur at the axon terminal near the ribbon synapses, but amacrine cells also make conventional synapses along the rod bipolar cell axon (Sterling and Lampson, 1986). Inhibitory inputs onto rod bipolar cells are mediated mostly by $GABA_c$ receptors, although $GABA_A$ receptors are also expressed on the axon terminals, and have also been shown to mediate inhibitory input onto rod bipolar cells (Greferath et al., 1994; Enz et al., 1996; Euler and Wässle, 1998).

$GABA_B$ receptors have been reported on salamander bipolar cells, and have been shown to modulate bipolar cell calcium current via G-protein activation (Shen and Slaughter, 1999). However, Pan and Lipton (1995) failed to find evidence for $GABA_B$ mediated responses on rod bipolar cells of the rat retina. Furthermore, antibodies directed against $GABA_B$ receptors fail to label bipolar cells in the rat retina, while strongly labeling populations of horizontal, amacrine, and ganglion cells (Koulen et al., 1998). Therefore it is unlikely that $GABA_B$ receptors play a large role in mediating inhibitory input onto rod bipolar cells in the mouse retina.

The axon terminals of rod bipolar cells have around 25-60 active zones, each with it's own ribbon (McGuire et al., 1984; von Gersdorff et al., 1996). The output synapse of the rod bipolar

cell is often referred to as a "dyad" (Dowling and Boycott, 1966), which refers to the presence of two postsynaptic amacrine cells dendrites. One member of the dyad forms a reciprocal synapse with the rod bipolar cell near the active zone (Sandell et al., 1989), and is frequently the A17 subclass of amacrine cell (although other types of amacrine cells, such as the A8, A11, and A13 have also been reported) (Kolb and Nelson, 1983; McGuire et al., 1984; Sterling and Lampson, 1986). The reciprocal input from the A17 represents at least one GABAergic input onto bipolar cell axons. The other member of the dyad is almost invariably an AII amacrine cell, which is exclusively found postsynaptic to rod bipolar cells, and forms an integral part of the rod pathway (discussed in a later section). Rod bipolar cells only rarely make direct outputs onto ganglion cells (Strettoi et al., 1990; Strettoi et al., 1994), but rather send their signals through the AII amacrine cells to the axon terminals of the cone bipolar cells.

Cone Bipolar Cells

Cone bipolar cells receive glutamatergic input in the OPL from 4-10 cones and. Diffuse cone bipolar cells, except for the diffuse blue-cone selective bipolar cell found in monkey (Mariani, 1984; Kouyama and Marshak, 1992), collect from all cones within reach and transfer an achromatic signal to the ganglion cells (Sterling et al., 1988; Boycott and Wässle, 1991; Calkins et al., 1996; Euler et al., 1996; Merighi et al., 1996; DeVries and Schwartz, 1999). In the primate retina, midget bipolar cells contact a single cone, and synapse onto a single ganglion cell (Calkins et al., 1996). Like the rod bipolar cells, cone bipolar cells also respond robustly to the neurotransmitters GABA and glycine (Suzuki et al., 1990; Kaneko et al., 1991; Euler and Wässle, 1998), and receive a number of GABA- and glycinergic inputs in the IPL from amacrine cells (Sterling and Lampson, 1986; Strettoi et al., 1994).

Also like rod bipolar cells, the output synapses of cone bipolar cells are dyads (Sterling et al., 1988; Strettoi et al., 1994). Cone bipolar cells, unlike the rod bipolar cells, directly contact ganglion cells. Cone bipolar cells terminals have around ~150 active zones, each with it's own synaptic ribbon, and make synapses onto ~50 ganglion cells and ~50-90 amacrine cells (Strettoi et al., 1994). About 30% of these amacrine cells make reciprocal synapses back onto the cone bipolar cells terminals (Strettoi et al., 1994). Cone bipolar cells stratifying in different layers of the IPL are likely to contact different populations of postsynaptic cells, possibly giving rise to functional specializations. However, the specific postsynaptic contacts of each subtype of cone bipolar cell have not been determined.

Three Rod Pathways in the Retina

The rod bipolar cell is an integral member of the rod pathway, and is exclusively devoted to transmitting rod signals. However, this is not the only way rod signals can reach the ganglion

cells. Despite the fact that rods are thought to contact only rod bipolar cells (but see below), rod signals appear both in the cone bipolar cells, and in the cone photoreceptors. In the present study, evidence for rod signals in cone bipolar cells was frequently seen. There are at least two, and possibly three pathways in the retina that carry rod signals, all of which would result in a rod signal being apparent in the cone bipolar cells.

The most well-studied rod pathway is the rod bipolar cell-AII amacrine cell pathway. In this pathway, the rod signal travels from the rod→ rod bipolar cell → AII amacrine cell → cone bipolar cell (Famiglietti and Kolb, 1975; Strettoi et al., 1994). The AII amacrine cells, which are bistratified neurons whose lobular dendrites make glycinergic synapses with off-cone bipolar cells and electrotonic synapses with on-bipolar cells, form the pivotal link in this pathway. The rod signal is transmitted to the rod bipolar cell, and is then fed into the cone pathway through a sign-inverting (glycinergic) synapse with off-cone bipolar cells, and a sign-conserving (electrotonic) synapse with on-cone bipolar cells (Chun et al., 1993; Mills and Massey, 1995). Thus, cone bipolar cells function both as second order neurons in the cone pathway, and as fourth order neurons in the rod-AII pathway. Surprisingly, the presence of two additional synapses between the rods and the ganglion cells in this pathway adds very little noise to the rod signal, and single photon events can be detected in the ganglion cells (Barlow et al., 1971; Mastronarde, 1983). Furthermore, psychophysical experiments show that the rod system can effectively count single photons (Sakitt, 1972). Thus the rod bipolar cell-AII pathway is very reliable and well suited to mediating vision under scotopic conditions, where individual rods only catch 1 or 2 photons per minute (Sterling, 1998).

Psychophysical studies lend evidence for the existence of a second pathway for rod signals (Conner and MacLeod, 1977; Conner, 1982). About 48 rods converge onto each cone via gap junctions between the rod spherules and the basal processes of cone pedicles (Kolb, 1977; Nelson, 1977; Smith et al., 1986; Schneeweis and Schnapf, 1995). In this pathway, the rod signal is passed presynaptically from rod → cone → cone bipolar cell. This pathway is believed to predominate under mesopic light intensities where the rods transduce tens to hundreds of photons, a sufficiently high intensity to saturate the rod bipolar cell → AII amacrine cell pathway (Raviola and Gilula, 1973; Sterling, 1998).

Lastly, there is some evidence in mouse retina that rod photoreceptors directly contact off-cone bipolar cells (Soucy et al., 1998). This pathway was suggested when extracellular recordings from ganglion cells in the coneless retina of a transgenic mouse revealed the presence of multi-photon responses (Soucy et al., 1998). In this pathway, the rod signal would travel across a conventional synapse from the rod photoreceptor to the off-cone bipolar cell, by-passing both the rod bipolar cell, and the cone photoreceptors. Whether this is a normal characteristic of all

mammalian retinas, or whether the cone bipolar cells extended dendrites to the rod photoreceptors due to the lack of cones is unknown. The scarcity of reports of rod photoreceptor synapsing directly onto cone bipolar cells in anatomical studies suggests that if these contacts do occur, they are rare.

The On-Bipolar Cell Signal Transduction Cascade

While it is agreed that the on-bipolar cell response is mediated by the metabotropic glutamate receptor mGluR6 (Vardi and Morigiwa, 1997), there are currently two disparate models of the second messenger cascade. In the original model, the on-bipolar cell second messenger system is analogous to the photoreceptor transduction cascade and involves the same intermediates (Nawy and Jahr, 1990; Shiells and Falk, 1990). According to this model, the binding of glutamate to mGluR6 leads to the activation of a transducin homologue, which activates phosphodiesterase (PDE). Hydrolysis of cGMP by PDE leads to a drop in cGMP concentration and a closure of cGMP gated cation channels. Thus, in darkness, when glutamate release from the photoreceptors is high, the mGluR6-linked channels close and the on-bipolar cells hyperpolarize. In the light, glutamate unbinds from mGluR6 and PDE is no longer activated. The subsequent rise in cGMP concentration opens the mGluR6-linked channels, and depolarizes the on-bipolar cell.

Support for this model comes from recordings from dogfish and salamander on-bipolar cells in which the inclusion of cGMP in the recording pipette led to the development of an inward current. This result suggests that cGMP can open the mGluR6-linked channels (Nawy and Jahr, 1990; Shiells and Falk, 1990; de la Villa et al., 1995). In addition, there is some evidence that the on-bipolar cell second messenger pathway is sensitive to pertussis and cholera toxins, which fits the known toxin profile of transducin (Shiells and Falk, 1992). Furthermore, intracellular IBMX (a non-selective inhibitor of PDE) had the same effect on the on-bipolar cell light response as including cGMP in the electrode presumably by preventing cGMP hydrolysis (Shiells and Falk, 1990). These studies suggest that the mGluR6 receptor is coupled to transducin, which activates PDE and causes the closure of cGMP-gated channels, analogous to the photoreceptor transduction mechanism.

However, several lines of evidence have recently suggested an alternate model for the on-bipolar cell signal transduction mechanism. First, antibodies directed against components of the signaling pathway utilized by the photoreceptors (transducin and several isoforms of PDE, and the photoreceptor cGMP gated channels) fail to label on bipolar cells in several mammalian species, while very intensely staining the photoreceptors (Wassle et al., 1992; Vardi et al., 1993). In addition, inclusion of 8-bromo-cGMP (a non-hydrolysable form of cGMP) in the recording pipette did not block the light response of salamander on-bipolar cells, suggesting that cGMP

does not gate the mGluR6-linked channel (Nawy, 1999), although it is clear from other studies that cGMP increases the current amplitude through the mGluR6-gated channels (Nawy and Jahr, 1990; Shiells and Falk, 1990; de la Villa et al., 1995). Thus far, the only G-protein localized to the dendritic tips of the on-bipolar cells is G_o, suggesting that it may be the functional link between the mGluR6 and the channel rather than transducin (Vardi et al., 1993; Vardi, 1998). G_o is sensitive to pertussis toxin, but not cholera toxin (Kikkawa et al., 1993) which conflicts with the bipolar cell toxin sensitivity reported by Shiells (1992). However, it is possible that the sensitivity of the on-bipolar cell pathway to cholera toxin in the dogfish retina may be a species difference, or that G_o has a cholera toxin site which is only exposed upon agonist binding (Vardi, 1998).

Furthermore, the physiological characteristics of the mGluR6-linked cation channel in on-bipolar cells do not fit with the presence of a classical cyclic nucleotide gated channel. The glutamate gated channel in on-bipolar cells have single channel conductances of 11-13pS (Attwell et al., 1987; de la Villa et al., 1995) whereas cyclic nucleotide gated channels in the outer segment have conductances of less than 1pS in the presence of physiological concentrations of divalent cations. This "flicker block" of cyclic nucleotide gated channels reduces the open probability to around 1-2% (Nakatani and Yau, 1988) while the open probability of the on-bipolar cell channels is much higher (P_o between 50-100%) (de la Villa et al., 1995). Thus there are many important differences between the on-bipolar cell signal transduction cascade and that of the photoreceptors. The details of the on-bipolar cell signal transduction cascade still remain to be determined.

Horizontal cells

Inhibitory pathways are established laterally in the retina at the two synaptic layers. In the outer plexiform layer the GABAergic horizontal cells form a large, electrically coupled network with other horizontal cells, and form a feedback pathway to the photoreceptors. Horizontal cells are large and sparse, comprising only 3% of neurons in the INL (Jeon et al., 1998). Mammals generally have two types of horizontal cells, termed A-type (axon-less) and B-type (short axon) horizontal cells (reviewed by Boycott et al., 1987; Boycott, 1988). However, anatomical studies in rat, rabbit, and mouse retinas have revealed the presence of only axon-bearing, B-type horizontal cells. Both types of horizontal cells receive glutamatergic input from photoreceptors through ionotropic glutamate receptors, and have clustered dendritic terminals which make output synapses back onto cone terminals (Kamermans and Spekreijse, 1999). In addition to the dendritic contacts with cones, B-type horizontal cells have an axon terminal system which

contacts exclusively rod terminals (Kolb, 1974). It is not clear at present whether the two types of horizontal cells have different functional roles.

Horizontal cells have been shown to generate an antagonistic surround in cone photoreceptors and in bipolar cells (Werblin and Dowling, 1969; Naka and Nye, 1971; Naka and Witkovsky, 1972; Burkhardt, 1993; Kamermans and Spekreijse, 1999). In non-mammalian retina, the generation of the surround by horizontal cells could be mediated by direct horizontal cell input onto the dendrites of bipolar cells, by horizontal cell feedback onto the photoreceptors, or by a combination of these two mechanisms (Werblin and Dowling, 1969; Baylor et al., 1971; Naka and Nye, 1971; Lasansky, 1973). There is little evidence for direct horizontal cell input onto bipolar cells in mammals, so it is believed that horizontal cells generate the surround of bipolar cells by negative feedback onto the photoreceptor terminals. There are two lines of evidence that support this hypothesis, First, hyperpolarizing current injected into the horizontal cell evokes a hyperpolarizing response in on-bipolar cells, i.e. it mimics a surround response (Marchiafava, 1978; Toyoda and Tonosaki, 1978), and second, the bipolar cell surround can be accounted for by the convolution of the bipolar cell receptive field center with horizontal cell receptive fields (Baylor et al., 1971; Fuortes and Simon, 1974; Attwell et al., 1983; Hare and Owen, 1990). Horizontal cells also contribute to the generation of the antagonistic surround of the ganglion cells, presumably originating in the outer plexiform layer as the bipolar cell surround (Mangel and Dowling, 1987; Mangel, 1991).

There are currently two hypotheses regarding the mechanism of horizontal cell feedback onto photoreceptors. One involves horizontal cell modulation of GABA-gated chloride conductance in the photoreceptors. This is supported by the fact that horizontal cells have been shown to accumulate and release GABA. The other hypothesis involves direct modulation of the calcium current in cone photoreceptors (Verweij et al., 1996). According to this hypothesis, hyperpolarization of the horizontal cells in response to light results in a shift in the activation of the calcium current to more negative potentials in the cone photoreceptor. This results in an increased calcium influx in the cone synaptic terminal, and the cone resumes glutamate release, which had been shut down in response to light. The neurotransmitter involved is not known, although it has been shown that this mechanism is GABA-independent (Verweij et al., 1996).

Amacrine cells

In the inner plexiform layer, amacrine cells (literally "no axon") form networks of inhibitory synapses onto bipolar cell axon terminals, and onto the dendrites of ganglion cells and other amacrine cells. In the mouse retina, amacrine cells make up 39% of the cells in the inner nuclear

layer (Jeon et al., 1998), and as is true of horizontal cells, the dendrites of amacrine cells are both pre-synaptic and post-synaptic to other neurons. There is a tremendous morphological diversity of amacrine cells, with estimates of 20-30 distinct classes (Masland, 1988; Vaney et al., 1991; Wassle and Boycott, 1991; MacNeil and Masland, 1998). Although little is known about the functional roles of specific types of amacrine cells, they are usually inhibitory and release either GABA or glycine (although there are dopaminergic and cholinergic amacrine cells). Amacrine cells are functionally diverse, and there are both spiking and non-spiking types. Amacrine cells are thought to contribute to a number of receptive field properties of ganglion cells including the antagonistic surround, the non-linear responses in Y cells, and to directional selectivity (Barlow and Levick, 1965). This could be achieved either by direct input onto the ganglion cells, or by input onto the bipolar cells terminals pre-synaptic to ganglion cells.

Ganglion cells

The ganglion cells form the last cell layer in the retina, and their axons form the optic nerve which leads to the brain. As a general rule, the receptive fields at successive layers in the retina encode increasingly high-level features of the visual stimulus, and by the time the signal reaches the ganglion cells, significant processing of the light input has already occurred. While each photoreceptor samples only one small point in the visual space and is therefore almost completely insensitive to the spatial structure of the stimulus, the ganglion cell responses are strongly dependent upon the spatial extent of the stimulus. The receptive fields of ganglion cells are almost always organized into concentric, antagonistic center-surround regions (Kuffler, 1953). This organization is prevalent at every layer in the visual system, even as early as the first synapse in the retina (Smith and Sterling, 1990).

There are at least 13 types of ganglion cells (Levick, 1975; and reviewed in Wassle and Boycott, 1991), but the majority of ganglion cells can be grouped into three main functional classes, termed W, X , and Y ganglion cells (Enroth-Cugell and Robson, 1966; Stone and Hoffmann, 1972; Saito, 1983; Rowe and Cox, 1993). These functional classes correspond to the anatomical classes of γ-, α-, and β- ganglion cells, respectively (Boycott and Wassle, 1974; Saito, 1983). X-ganglion cells respond to stimuli with vigorous, sustained spiking, and sum their inputs linearly. They generally have small receptive fields, and are thought to encode the spatial properties of the stimulus. In contrast, Y-cells show strong transient responses to stimuli, and sum their inputs non-linearly. These characteristics make them well suited for detecting change, and they probably encode temporal qualities of the stimulus. W-ganglion cells as a group are much more heterogenous than either X- or Y-cells, but are well-known for their sluggish responses to stimuli (Enroth-Cugell and Robson, 1966; Cleland et al., 1971; Saito, 1983; Enroth-

Cugell and Freeman, 1987). All three functional classes of ganglion cells come in on- and off-varieties, and their receptive fields are organized into concentric center and surround regions.

The axons of the ganglion cells bundle together at the optic disc to form the optic nerve which projects to two brain regions: the lateral geniculate nucleus in the thalamus, and the superior colliculus in the mid-brain (Cleland et al., 1971; Leventhal et al., 1981; Leventhal et al., 1985). Both of these brain regions are organized into layers, each of which receive input from separate populations of ganglion cells. The lateral geniculate nucleus is an important relay station between the retina and higher brain centers, while the superior colliculus is involved in the control of behavioral responses to visual input such as the appropriate orientation of the eyes, head, and whiskers toward a stimulus (Sparks, 1988). In both the lateral geniculate nucleus and the superior colliculus, a topographical map is created in which the precise visual-spatial relations established in the retina are maintained. The neurons in these two brain regions have receptive field properties very much like those of their inputs (i.e. the ganglion cells), including being organized into center and surround regions. The receptive fields become more complicated in the LGN and SC since these neurons are also segregated into "orientation columns". After the lateral geniculate nucleus, the visual signal is sent to the striate cortex and to several other processing centers in the brain.

Adaptation

The process of adaptation is common to sensory systems and allows them to operate over broad ranges of input. In a normal cycle between day and night, the ambient illumination can vary over 12 orders of magnitude (see Figure 1.2) and the visual system is able to operate over such a large range because of its ability to adapt (Hood and Finkelstein, 1986). As a first step in adaptation, the pupil can modulate light input by about 1 log unit, depending upon the minumum and maximum aperatures of the pupil, and the size of the eye. In addition, simply by switching from rod to cone vision, the range over which the retina can respond is increased to about 6 log units. The remainder of the visual response range is achieved by other cellular, and post-receptoral mechanisms of adaptation.

Types of Adaptation

The ultimate goal of adaptation is to prevent neuronal responses from saturating, so that the neurons can respond irrespective of the background light intensity. In other words, adaptation allows the retina to respond to the contrast of a stimulus rather than responding to the absolute light level (Shapley and Enroth-Cugell, 1985). There are two types of adaptation, dark adaptation and light adaptation, which are mediated by different molecular mechanisms. Dark adaptation

refers to the process that occurs when the retina is stepped from high background illumination into very dim conditions. Dark adaptation involves, among other things, the regeneration of the photopigment that has been bleached by light. In contrast, light adaptation refers to the changes which occur when the retina is stepped from dim conditions into bright conditions.

The process of light adaptation reduces the overall sensitivity of the retina, allowing the retina to continue responding in the presence of background illumination. The consequences of no adaptation would be response compression followed by saturation. If a steady background illumination is introduced onto the retina and there is no adaptation, the retina will respond continuously to that background with no change in the maximal response. In other words, the response "floor" would be raised but the response "ceiling" would remain the same. Eventually the background illumination will saturate the system, and added lights will have no effect.

Mechanisms of light adaptation help to overcome response compression by subtracting away the steady-state background, and by reducing the gain of the input-output relation. The latter process is often referred to as multiplicative adaptation since all inputs are effectively scaled by some factor, and the responses to both the background and the signal are attenuated (Adelson, 1982; Geisler, 1983; Hayhoe et al., 1987). Pigment depletion in the cone photoreceptors is an example of a multiplicative adaptation process (Alpern et al., 1970; Boynton and Whitten, 1970). Steady lights deplete some of the cone photopigment, which effectively reduces the number of quanta absorbed due to both the background and the signal. The effect of multiplicative adaptation will be to shift the intensity-response curve to the right (i.e. to higher intensities) by an amount equal to the gain change. Other examples of multiplicative adaptation might involve gain control adjustments at sites distinct from the photoreceptors (post-receptoral adaptation). Multiplicative adaptation restores most, but not all of the response range (Hayhoe et al., 1987).

Subtractive adaptation differs from multiplicative adaptation in that only the adapting field signal is attenuated, while the response to changing signals is relatively unaffected (Adelson, 1982; Hayhoe et al., 1987). High pass filtering of the signal would produce this effect, such that the visual system would respond robustly to changes in light intensity but would not respond at all to a steady background (Adelson, 1982). Subtractive adaptation will effectively lower the floor and expand the response range back toward its original range, without actually shifting the intensity response curve along the intensity axis. In other words, the absolute light intensity required to saturate the system will remain the same in subtractive adaptation, but will be shifted to higher intensities following multiplicative adaptation. Psychophysical and electrophysiological studies have shown that multiplicative and subtractive mechanisms act in concert to adapt the retina.

Adaptation in Rods and Cones

Rod photoreceptors are capable of limited adaptation, but rod responses quickly saturate, and are strongly attenuated even after pigment bleaches of less than 1% (Lamb, 1980; Ashmore and Falk, 1981). There is accumulating evidence that most adaptation in the rod pathway occurs at a site distinct from the rods (Green et al., 1975; Green and Powers, 1982; Shapley and Enroth-Cugell, 1985). Post-receptoral adaptation in the rod system has been suggested both by psychophysical studies and by *in vitro* recordings from ganglion cells (Green and Powers, 1982; Levick et al., 1983, Enroth-Cugell, and Shapely, 1973).

Cone photoreceptors on the other hand, have a large capacity for adaptation, and do not saturate even at the brightest intensities (Burkhardt, 1994). For cone photoreceptors it appears Weber's law applies to all light intensities. An important mechanism of cone adaptation is photopigment bleaching, and cones can continue to operate even after a 95% photopigment bleach (Lamb, 1980; Burkhardt, 1994). The bleaching of the photopigment acts as a multiplicative adaptation process since all cone responses are scaled by some factor (Adelson, 1982; Geisler, 1983; Hood and Finkelstein, 1986). The underlying molecular explanation for this different adaptation behavior in rods and cones is not understood. However, it is known that there are post-receptoral adaptation mechanisms in the cone pathways as well (Crognale and Jacobs, 1988).

The Mouse Retina

The mouse retina is becoming more popular as a model of retinal physiology due to the obvious advantages provided by genetic techniques to examine retinal function. There have been a few anatomical studies examining the anatomy and connectivity of neurons in the mouse retina. As a nocturnal animal, the retina of the mouse is rod dominated, with cones comprising only ~3% of all photoreceptors (Carter-Dawson and LaVail, 1979; Carter-Dawson and LaVail, 1979). This is very similar to rat retina where only 1% of photoreceptors are cones (Szel et al., 1993). Clearly, the mouse retina is an excellent model for rod vision (rod density 437,000 rods per mm2, Jeon et al., 1998). However, in terms of the absolute density of cones, ~12,400 cones/mm^2, the mouse retina is comparable to cat, rabbit, and primate peripheral retina (Jeon et al., 1998). Although the spatial resolution of cone vision is low in mice, 0.125 cycles per degree measured from behavioral studies (Sinex et al., 1979), there is no scarcity of cones in mouse retina. Rather, there are many small, tightly packed rods. Hence, the mouse retina serves as a good system for the study of both rod and cone vision.

Bipolar cells make up 41% of the inner nuclear cells (Jeon et al., 1998), but it is unknown how many are rod bipolar cells and how many are cone bipolar cells. It has been reported that in the

mouse retina rod bipolar cells contact approximately 25 rods, and that each rod diverges onto two rod bipolar cells (Jeon et al., 1998). Thus rods and rod bipolar cells exist in the retina in a 1:14 ratio. An average rod density of 500,000 rods/mm^2 (Jeon et al., 1998), would mean that there are 36,000 rod bipolar cells/mm^2 , which is the average density of rod bipolar cells also reported for the cat retina (Freed et al., 1987). Since there are 50,000 bipolar cells/mm^2 in mouse retina (Jeon et al., 1998), this would mean there are 14,000 cone bipolar cells/mm^2. In other words, the ratio of rod bipolar cells, to cone bipolar cells is about 2.5 to 1. However in rat retina, it has been estimated that at least 50% of bipolar cells are cone bipolar cells (Euler and Wässle, 1995).

The mouse retina contains two types of cone photoreceptors: one with spectral sensitivity peak at 360-365nm (the UV sensitive cone) and the second which peaks at 511nm (the green sensitive cone) (Jacobs et al., 1991; Szel et al., 1992; Deegan and Jacobs, 1993; Chiu et al., 1994; Sun et al., 1997). Interestingly, the cone photoreceptor types are spatially segregated with the UV-sensitive cones localized to ventral retina, and the green sensitive cones located in the dorsal retina (Szel et al., 1992; Calderone and Jacobs, 1995; Ekesten et al., 2000). There is also a central region in which the cones express both the short, and the medium wavelength pigment (Neitz and Neitz, 2001). Such an organization ensures that the different cone types maximally receive their preferred wavelength. The S-cones, situated in the ventral retina, will receive light coming from the sky which is largely composed of short wavelengths, whereas the green sensitive cones receive light reflected off the ground which is abundant in medium wavelengths. The spatial segregation of cone types means that second order neurons, such as the bipolar cells, might receive "pure" cone input from a single spectral cone type depending upon location in the retina.

In the present experiments, no effort was made to determine the eccentricity at which the recordings were made. However, the distribution of neurons within the mouse retina is unusually flat when compared with rabbit, and primate retina (Jeon et al., 1998). In addition to providing information about retinal physiology in general, the work presented below forms a bulk of work with which one can compare genetically altered mice.

Summary, and Questions to be Addressed

The connectivity, and the morphological variety of the neurons within the retina are complex, and numerous circuits process information in parallel, each extracting different components of the stimulus. The bipolar cells form the vertical pathway between photoreceptors and ganglion cells in the retina, and thus an understanding of their response properties is of the great importance. In order to assess the information processing role of the bipolar cells, we have made

whole-cell voltage and current recordings from bipolar cells in the retinal slice preparation. Our first course of action was to examine bipolar cell calcium currents. Since neurotransmitter release is tightly coupled to calcium influx, the properties of the voltage activated calcium currents will strongly influence bipolar cell signaling properties. This is the topic of Chapter 3. We then characterized the light response properties of bipolar cells by recording from bipolar cells while stimulating the photoreceptors with light in the dark-adapted retinal slice. This represents the first systematic study of mammalian bipolar cell light responses, and is the topic of Chapter 4. We then narrowed our focus to a peculiar light response property of the rod bipolar cell, namely, calcium-mediated inactivation. This will be the topic of Chapter 5.

Chapter 2

General Methods

This chapter will describe the experimental methods common to all of the following experiments. A shorter Methods section will also be found in each data chapter, describing the details specific to those experiments.

Preparation of slices

Manipulations and recordings were performed in darkness under infrared illumination. Animals were treated in accordance with institutional animal ethics committee guidelines. Slices of retina were prepared from C57Black6J mice obtained from in-house breeding facilities. Mice were killed by an overdose (0.1ml of 100mg/ml) of pentobarbitone sodium (Nembutal, Rhone Merieux Australia), injected into the peritoneum. The eyes were enucleated and hemisected along the ora-serrata and submerged oxygenated Ames solution at room temperature (Sigma). The pH of the Ames solution was adjusted to 7.4 with sodium bicarbonate. Whole retinas were isolated and placed onto nitrocellulose paper with the ganglion cell side down. The retina was adhered to the nitrocellulose by applying negative pressure underneath the paper. The edges of the nitrocellulose were clamped in place in a custom-built slicer and 200um thick slices were cut by hand with a scalpel blade. While remaining submerged, the nitrocellulose paper with attached retinal slices were transferred to a perspex recording chamber. The slices were fixed to the bottom of the chamber by inserting the ends of the nitrocellulose paper into silicon vacuum grease. The recording chamber containing the slices was then transferred to the experimental apparatus.

Electrophysiology

Experimental apparatus

The experimental apparatus is illustrated in Figure 2.1. The recording chamber was mounted on the stage of an Olympus BX40 microscope (Japan) and illuminated from below with a lamp equipped with a 10nm bandpass infrared filter (850nm). Slices were viewed with a 40X water-immersion objective and Nomarski interference contrast optics, and imaged onto a television monitor by an infrared video camera (Hamamatsu C2400, Japan). Electrodes were positioned using a Burleigh PCS 5000 micromanipulator (Burleigh Instruments, NY).

Identification of Bipolar Cells

Bipolar cells were selected based upon their close proximity to the photoreceptors and the slightly ellipsoid soma. All cells contributing to the results of Chapters 3 and 4 were filled with Lucifer Yellow (0.05%) during the recording, allowing the morphology to be viewed by exposure to short wavelength light. In Chapter 4, only one cell was recorded from each slice preparation since exposure to light bleached the photoreceptors. Cells contributing to the Results section in Chapter 5 were identified solely by their position in the retina, and by their light sensitivity and response waveform, as established in Chapter 4.

Recordings

The recording chamber was continuously perfused at a rate of 3ml/minute with oxygenated Ames solution heated to 35°C. Slices were viable under these conditions for 4-6 hours. Typically, the best recordings were obtained within the first hour after slicing.

Patch pipettes (resistance 14-17MΩ) were fabricated from borosilicate glass (GC150TF, Clarke Electromedical Instruments, UK) on a Flaming/Brown micropipette puller, model P-97 (Sutter Instruments, U.S.A). Due to the small size of bipolar cells, changes in cell capacitance were masked by the capacitance of the recording electrode. During recordings, electrode capacitance was reduced by coating the electrodes with Sylgard (Dow Corning, Michigan), and the remaining capacitance was compensated for automatically by the data acquisition software (HEKA). Synaptic responses were elicited by stimulating the photoreceptors with light from a computer monitor light source (see below). Whole-cell voltage- and current-clamp recordings were amplified with an EPC9 patch clamp amplifier (HEKA elektronics) controlled by Pulse 8.11 software (HEKA Elektronics). Recordings were filtered at 10kHz before being digitized at 5kHz. All potentials were corrected for the liquid junction potential which was measured to be +10mV with the standard Cs-gluconate solution. No series-resistance compensation was applied.

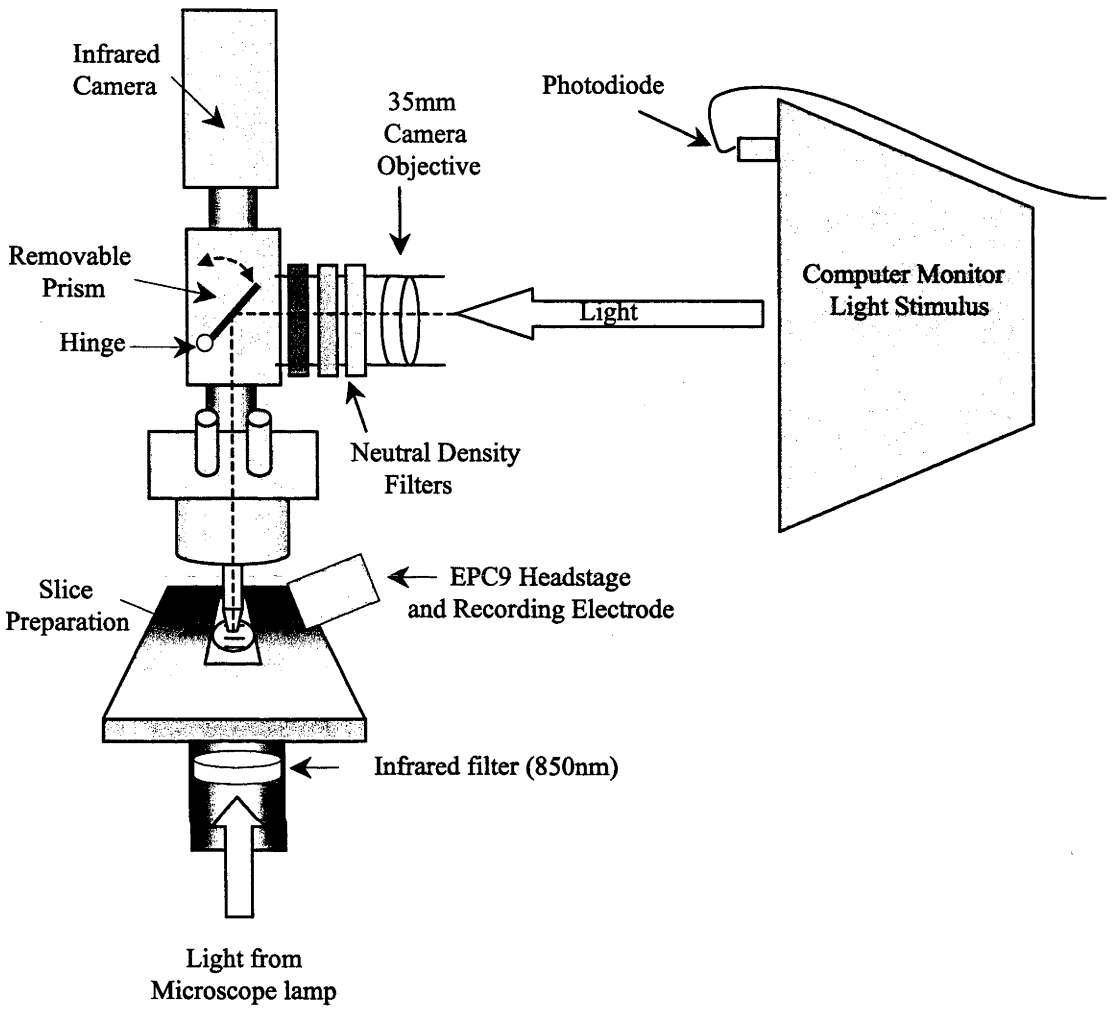

Figure 2.1 Experimental set-up. The light stimulus was generated by a computer monitor, focused through a lens, and directed through the objective by a removable mirror (dotted line). The preparation could be viewed by flipping the mirror into an upright position. For viewing, the preparation was illuminated from below with infrared light which was converted by the infrared camera into a video image, and displayed on a separate computer monitor (not shown).

Bipolar cells were patch clamped under visual control. Due to the small size of the cells, the success rate of recording light responses was quite low. Approximately 1 out of every 5 or 6 cells patched was stable for longer than a few minutes. Of those cells, around a quarter of them displayed a significant light response. Recordings were generally of very short duration (average recording time ~3-5 minutes), presumably due to the fragility of the cell membranes. Recordings of longer duration were occasionally possible, however long recordings of on-bipolar cell light responses were rare presumably due to the wash-out of a critical second messenger.

Light Stimulus

Synaptic responses were elicited by stimulating the retina with light from an Apple Multiple Scan 15AV computer monitor. The screen of the monitor was focused through a 35mm camera objective, and directed through a 40x/0.8NA microscope objective onto the retina (Figure 2.1). The prism could be flipped into and out of position depending on whether the experimenter wished to view, or stimulate the preparation. The light intensity was adjusted by a series of removable calibrated neutral density filters.

Light stimuli were generated using software written in-house in IGOR PRO. All of the light stimulus parameters were controlled using this software including the stimulus timing, spatial profile, and intensity.

Data in Chapter 4 was acquired by stimulating the retina with white light (i.e. the red, green, and blue guns combined), while data in Chapter 5 was acquired by using exclusively the green gun (which has a single peak at 540nm with a half-width of 75nm). The monitor resolution was set to 1064 by 768. The magnification of the light stimulus through the optics was measured to be 1.17 pixels/μm by back-projecting a gradicule onto the computer monitor. Two types of stimuli were used: flashes and steps. Flashes consisted of a single frame, lasting less than 1ms at any one point on the screen, while steps were created by presenting multiple frames. The timing of the light stimulus was recorded by a photodiode, which responded to a small square of light in the top left hand corner of the screen that flashed simultaneously with the stimulus. Since the screen was scanned every 13.3ms (75HZ), the time between light onset at the photodiode, and light onset in the center of the screen was approximately 6.7ms (the time taken to scan the top half of the screen). The timing of light stimuli is adjusted for this delay.

Calibration of the monitor

The computer monitor output was measured with a calibrated UDT detector. The output was linearized by creating a look-up table, and the output from the monitor was periodically checked to ensure it remained linear. All light intensities used to stimulate the retina were measured by

the calibrated UDT detector. The maximum monitor luminance using all three guns (red, green, and blue) was measured to be 55 cd/m^2. At the preparation (i.e. through the 40X objective) the maximum intensity was measured to be 44.6 cd/m^2. This value was converted into photopic lumens by multiplying by the number of steradians, which resulted in a value of 45 lumens/m^2. When only the green gun was used (as in Chapter 5), the maximal intensity measured at the preparation was 31.8 lumens/m^2. All light intensities are reported in units of photopic lumens/m^2.

Using this calibration, the photon density was calculated at the half-saturation point for the rod bipolar cell. Half saturation of the rod bipolar cell flash response occurs at $8e^{-14}$ photopic lumens/m^2 (see Figure 5.7). This is equivalent to $3.4e^{-14}$ scoptoic lumens/m^2. The energy E of a 500nm photon is hc/λ which equals $3.97e^{19}$ Joules. Assuming a scotopic luminous efficiency of 1745 lumens/Watt, then $3.4e^{-14}$ scotpic lumens/m^2 is equivalent to $1.96e^{-17}$ Joules per second per μm^2. Dividing the energy flux by the energy of a photon and the screen refresh rate equals 0.659 photons per μm^2 per frame. The orientation of the outer segments is not taken into account in the above measurement, therefore the number of effective photons will be lower since the retina is being illuminated from the side.

Data analysis

All data analysis was done in IGOR PRO (Wavemetrics) using procedures that were written in-house. Further details are given in the following Results chapters.

Solutions

In all experiments, the extracellular solution was oxygenated Ames solution. The intracellular solutions used were as follows:

Chapter 3		Chapter 4		Chapter 5	
CsCl Intracellular		**Cs-Gluconate Intracellular**		**Control Intracellular**	
CsCl	110	Cs-gluconate	110	Cs-gluconate	110
NaCl	10	NaCl	5	CsCl	5
EGTA	1	$MgCl_2$	0.1	NaCl	5
$MgCl_2$	0.1	EGTA	0.1	EGTA	1
Na-Hepes	5	Na-HEPES	5	$MgCl_2$	0.1
Na-ATP	5	Na-ATP	5	Na-Hepes	5
Na-GTP	0.1	Na-GTP	0.5	Na-ATP	5
				Na-GTP	0.5
Lucifer Yellow	0.05%	Lucifer Yellow	0.05%		
pH adjusted to 7.4 with CsOH		pH adjusted to 7.4 with CsOH		pH adjusted to 7.35 with CsOH.	
calculated Cl^-_{rev} - 0.9mV		calculated Cl^-_{rev} -85mV		calculated Cl^-_{rev} -67mV	
Cs-Gluconate Intracellular		**K-Gluconate Intracellular**		**BAPTA Intracellular**	
Cs-gluconate	120	K-gluconate	110	Cs-gluconate	110
CsCl	5	NaCl	5	CsCl	5
EGTA	0.1	$MgCl_2$	1	NaCl	5
$MgCl_2$	4	EGTA	0.1	BAPTA	10
Na-Hepes	5	Na-HEPES	5	$MgCl_2$	0.1
Na-ATP	5	Na-ATP	5	Na-Hepes	5
Na-GTP	0.5	Na-GTP	0.1	Na-ATP	5
				Na-GTP	0.5
Lucifer Yellow	0.05%	Lucifer Yellow	0.05%		
pH adjusted to 7.4 with CsOH		pH adjusted to 7.4 with KOH		pH adjusted to 7.35 with CsOH.	
calculated Cl^-_{rev} -60mV		calculated Cl^-_{rev} -77mV		calculated Cl^-_{rev} -67mV	
		No Calcium-buffer Intracellular		**No Calcium-buffer Intracellular**	
		K-gluconate	112	K-gluconate	112
		NaCl	5	NaCl	5
		KCl	5	KCl	5
		$MgCl_2$	0.1	$MgCl_2$	0.1
		Na-Hepes	5	Na-Hepes	5
		Na-ATP	5	Na-ATP	5
		Na-GTP	0.5	Na-GTP	0.5
		pH adjusted to 7.35 with KOH		pH adjusted to 7.35 with KOH	
		calculated Cl^-_{rev} -67mV		calculated Cl^-_{rev} -67mV	

Intracellular solutions were aliquoted and stored at -20°C until ready for use. Na-ATP and Na-GTP were prepared as 100mM stock solutions in water, stored at -20°C, and added to the intracellular solution on the day of the experiment.

Chapter 3

Bipolar Cell Calcium Currents

Introduction

Calcium influx through voltage-gated calcium channels in response to membrane depolarization is the critical signal for neurotransmitter release (Katz and Miledi, 1967; Llinas et al., 1981; Augustine et al., 1985). At central synapses, the arrival of an action potential in the nerve terminal briefly depolarizes the plasma membrane, causing the voltage gated calcium channels to open. The influx of calcium triggers a reaction that causes synaptic vesicles to fuse with the plasma membrane, and release neurotransmitter into the synaptic cleft (for review see (Scheller, 1995; Sudhof, 1995; Augustine et al., 1996; Zucker, 1996). However, bipolar cells do not generate action potentials, but respond to changes in glutamate concentration by graded polarizations. In addition, goldfish bipolar cells are known to release neurotransmitter in a sustained fashion (Heidelberger and Matthews, 1992).

There are several types of calcium channels, referred to as N-, P/Q-, R-, T- and L-types, which can be distinguished biophysically by their voltage dependence, conductance, and pharmacology (reviewed in Olivera et al., 1994; Catterall, 1998) (summarized in Table 3.1). Calcium channels can also be defined by the pore forming α1-subunit (see Table 3.1) which confers the calcium selectivity, voltage dependence, and the pharmacological profile to the calcium channel (Catterall, 1991; Catterall, 1995). There are at least three other subunits which associate with the α1 subunit, and influence its biophysical properties: The β subunit modulates both the kinetic and pharmacological profile of the channel (Williams et al., 1992; Williams et al., 1992; Ellinor et al., 1993; Stea et al., 1993; Zhang et al., 1993; Moreno et al., 1997), while expression of the α2 and δ subunits increased the current through the channel (Williams et al., 1992; Gurnett et al., 1996). There is also a fifth subunit (γ) associated with L-type channels expressed in cardiac and skeletal muscle, which influences the expression and the inactivation of L-type currents (Singer et al., 1991). Most of the information on the physiological properties of different subunits comes from the expression of the subunits in cultured cell lines. The specific subunit composition of native calcium channels is largely unknown.

Most neurons in the brain generate action potentials, and in these neurons, N-type (composed of the α1B subunit; see Table 3.1), and P/Q-type (α1A) calcium channels mediate synaptic transmission (Luebke et al., 1993; Regehr and Mintz, 1994; Dunlap et al., 1995; Wu et al., 1998). The N-, and P/Q-type calcium channels are activated by large depolarizations from negative potentials and are thus said to be high voltage activated (HVA), and they repidly inactivate after opening (Tsien et al., 1988). They are blocked by the ω-conotoxins, with N-type channels blocked by ω-conotoxin GVIA and the P/Q type channels blocked by ω-conotoxin MVIIC. The

α1A and α1B subunits have been precisely localized with the proteins involved in neurotransmitter release at presynaptic nerve terminals (Westenbroek et al., 1995), placing them in a good position to control synaptic vesicle exocytosis.

First discovered in cerebellar granule cells (Ellinor et al., 1993), R-type (α1E) calcium channels are so named because they are "resistant" to block by the pharmacological agents which block the other calcium channel types (i.e. the dihydropyrdines, ω-Conotoxin GVIA, and ω-Agatoxin). They have been shown to mediate neurotransmitter release following action potentials (Wu et al., 1998), to evoke neuropeptide release from the neurohypophysis (Albillos et al., 2000), and to mediate calcium entry into dendrites (Kavalali et al., 1997). They mediate HVA currents, and like N- and P/Q-type channels, they rapidly inactivate after opening (Wu et al., 1998; Albillos et al., 2000). They can be blocked by low concentrations (~4nM) of the polypeptide SNX-482 (Wang et al., 1999), and by antisense oligonucleotides directed against the α1E subunit (Piedras-Renteria and Tsien, 1998). As one of the most recently discovered, R-type calcium channels are not well understood.

T-type α1G, α1H, α1I (Cribbs et al., 1998; Perez-Reyes et al., 1998) channels are the only known calcium channels to be activated by low voltages (LVA), and are activated by depolarizations positive to -70mV from holding voltages more negative than -80mV (Catterall, 1998). T-type channels rapidly inactivate during maintained depolarizations in a purely voltage-dependent manner, and inactivation is only removed when the membrane potential is held more negative then -80mV (Nowycky et al., 1985; Tsien et al., 1988). They have been implicated in repetitive firing of neurons, and pacemaker activity in cardiac muscle cells (Nilius et al., 1985; Nowycky et al., 1985). T-type calcium currents have not been shown to be involved in the control of neurotransmitter release.

The L-type calcium channels are the only known calcium channels to mediate sustained calcium currents (Nowycky et al., 1985), and are sensitive to dihydropyridines (Bean, 1984; Nowycky et al., 1985). There are four identified α1 subunits belonging to the L-family, resulting in several functional subtypes of L-type calcium channels. Calcium currents through the α1S and α1C channels serve an important role in excitation-contraction coupling in skeletal and cardiac muscle, respectively. The α1D subunit, specific to neurons, is frequently localized to the dendrites and cell bodies (Chung et al., 2000), where they are thought to be involved in a wide range of functions such as developmental regulation (Kater et al., 1988), gene expression (Bito et al., 1997), and control of excitability and dendritic function (Moyer et al., 1992). There is also a newly cloned α1F subunit, which is exclusively expressed in the retina (Bech-Hansen et al.,

1998; Strom et al., 1998). Since they have been recently cloned, no physiological studies have been performed on the α1F channels, and nothing is known about their biophysical properties.

L	HVA	α1C, α1S, α1D,α1F	Dihydropyridines	25pS
N	HVA	α1B	ω-Conotoxin GVIA	12-18pS
P/Q	HVA	α1A	ω-Agatoxin	10-20pS
R	HVA	α1E	SNX-482, Ni^{2+}	?
T	LVA	α1G, α1H α1I	Ni^{2+}	8pS

Table 3.1. Properties of voltage-activated calcium channels.

There is a general consensus that L-type calcium channels are not involved in action-potential dependent neurotransmitter release (Dunlap et al., 1995). However, L-type calcium currents have been implicated in mediating neurotransmitter release from neurons which respond to stimuli in a graded fashion, such as the photoreceptors and bipolar cells in the retina, and saccular hair cells in the inner ear (Heidelberger and Matthews, 1992; Su et al., 1995; Kollmar et al., 1997; Taylor and Morgans, 1998).

L-type calcium currents have been localized to the axon terminals of goldfish bipolar cells, where they were found to support neurotransmitter release (Tachibana and Okada, 1991; Heidelberger and Matthews, 1992) (Tachibana et al., 1993). Indeed, long-lasting calcium currents seem well-suited for mediating prolonged bouts of synaptic vesicle release characteristic of ribbon synapses (Heidelberger and Matthews, 1992; Rieke and Schwartz, 1994; Rouze and Schwartz, 1998; Neves and Lagnado, 1999). Surprisingly, only a transient T-type calcium current had been reported in mouse bipolar cells (Kaneko et al., 1989). T-type currents have not been shown to support neurotransmitter release in other neurons, so it seemed unlikely that T-type currents were the only calcium currents in mammalian bipolar cells. However, this study had been performed on dissociated bipolar cells, thus it is possible that the dissociation procedure disrupted the axon terminals. This may explain why an L-type calcium current was not seen in this study. The goal of the present study was to re-examine the calcium currents of mammalian bipolar cells to determine if they also had a sustained, L-type current like that reported in goldfish.

During the course of these experiments, two studies were published on mammalian bipolar cell calcium currents, one in rat, and one in mouse, with results very similar to those we had obtained. The results are presented below, with a discussion of the simultaneously published reports in rat (Protti and Llano, 1998) and mouse (de la Villa et al., 1998).

Methods

Preparation

Light-adapted mouse retinal slices were prepared following the procedures summarized in Chapter 2: General Methods. All manipulations were performed under normal room light.

Recordings

Whole cell voltage- and current- recordings were made from bipolar cells in the mouse retinal slice preparation. Cells were held at -70mV and stepped to a number of different membrane potentials in order to evoke calcium currents. The voltage protocols used are described in more detail in the text. For an extensive description of the electrophysiology set-up and preparation see Chapter 2: General Methods.

Bipolar cells were selected for recording by the shape of their cell soma, and by their position in the retina. Electrodes were filled with Lucifer Yellow (0.5%), allowing for visualization and morphological identification of the bipolar cells at the conclusion of the recording. Bipolar cells were classified as either on-cone or off-cone bipolar cells based upon the morphology and stratification of their axon terminals in the IPL. Rod bipolar cells were identified based upon the stratification of the axons in the inner-most part of the IPL, and the presence of 1-3 large lobular axon terminals, characteristic of rod bipolar cells.

Solutions

Ames solution was used as the standard extracellular solution in all experiments. Nifedipine (Sigma) was prepared as a 200mM stock solution in dimethyl sulfoxide (DMSO; Sigma), stored at 4°C, and was added directly to the Ames solution on the day of the experiment. The calcium-free saline solution containing cobalt was composed of (in mM): 115 NaCl, 23 $NaHCO_3$, 3.1 KCl, 1.15 $CoCl_2$, 1.2 $MgCl_2$, and 6 glucose.

Two cesium-based intracellular solutions were used (summarized in Table 2.1 in General Methods). The recordings were made with cesium based intracellular solutions in order to suppress large K^+ currents which may otherwise obscure the calcium currents.

Results

Bipolar cells have a sustained calcium current.

In order to test for the presence of L-type calcium currents, bipolar cells were held at -70mV and stepped for 100ms to a series of different voltages. A sustained calcium current was activated in 18 bipolar cells (7 rod bipolar cells; 3 cone bipolar cells; and 8 unclassified bipolar cells). An example of the sustained calcium current is shown in Figure 3.1A, where a rod bipolar cell was stepped from -70mV to -35mV. Bath application of a calcium-free saline solution containing 1.15mM cobalt, a specific blocker of calcium channels, reversibly abolished this inward current confirming its identity as a calcium current. The sustained calcium current reappeared when the retina was once again bathed in normal Ames solution (blue trace; Figure 3.1A). The time-course of the cobalt block was measured by applying a 100ms voltage step to -35mV approximately every 20-30 seconds over four an a half minutes. The amplitude of the calcium current is plotted against time (Figure 3.1B). The calcium-free/cobalt solution completely blocked the calcium current in all cells tested (n=5).

The peak amplitude of the sustained calcium currents from 7 rod bipolar cells (□) and 3 cone bipolar cells (●) were averaged, and plotted against membrane voltage (Figure 3.1C). Since the sample size of cone bipolar cells was small, no attempt was made to differentiate between morphological subclasses of cone bipolar cells. Both rod and cone bipolar cell calcium currents activated around -50mV and peaked around -25mV (Figure 3.1C). Studies in rat (Protti and Llano, 1998), and mouse (de la Villa et al., 1998; Pan, 2000) bipolar cells also report sustained calcium currents activating around -50mV. The low activation threshold qualifies them, by definition, as low voltage activated currents. The average calcium current seems to be slightly larger in cone bipolar cells than in rod bipolar cells. This is an observation also made in dissociated rat bipolar cells, where the larger cone bipolar cell calcium current was attributed to a larger calcium current density (Pan, 2000).

In addition to the LVA sustained calcium current, (Pan, 2000) also reported a HVA L-type calcium current in rat bipolar cells. The HVA calcium current activated around -30mV, and peaked near -10mV. Such a HVA calcium current was not seen in the present experiments. However, in the study by (Pan, 2000) the HVA L-type current was frequently apparent only following the application of BAYK 8644, which potentiates currents through L-type channels. It is possible that this current was missed in the present experiments since BAYK 8644 was never used. However, a calcium current with that activation range was not reported in the studies by Protti and Llano (1998)or de la Villa, et.al. (1998), despite the use of BAYK 8644 (although

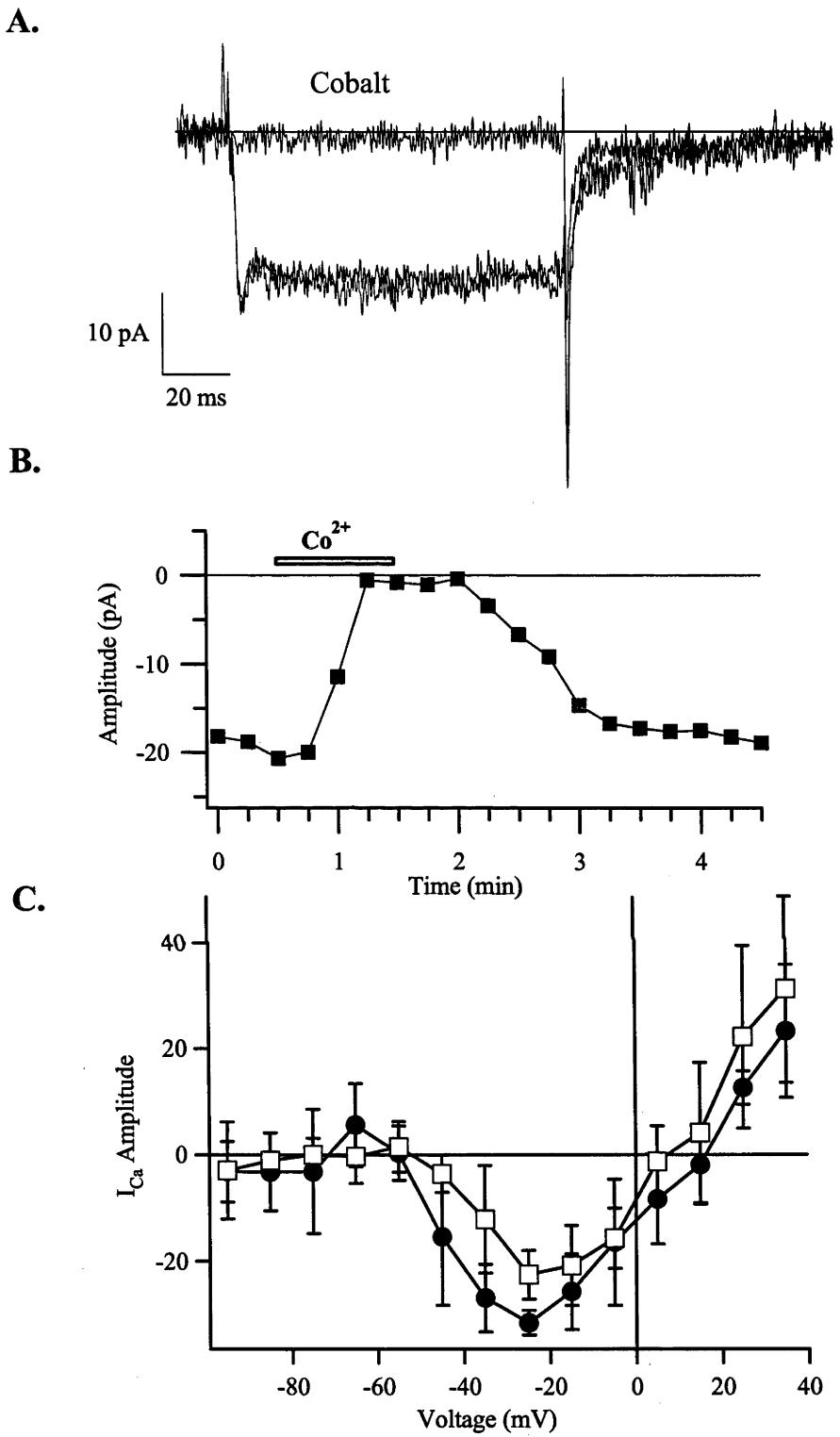

Figure 3.1. Bipolar cells exhibit a sustained low voltage activated calcium current. (A) Whole-cell current recordings from a rod bipolar cell. The bipolar cell was stepped from -70mV to -35mV (timing of voltage step shown under traces) to evoke the calcium current. The current was reversibly abolished when the Ames extracellular solution was replaced with a calcium-free saline containing 1.15mM cobalt. The blue trace shows the reappearance of the calcium current upon exposure to the normal Ames extracellular solution. (B) Time course of the block of the calcium current by extracellular cobalt. Bath application of cobalt shown by the bar in top of graph. (C) The average current-voltage relation of the calcium current from 7 rod bipolar cells (□), and 3 cone bipolar cells (●) activates around -45mV and peaks at about -25mV. Error bars show one standard deviation.

those studies did find that BAYK 8644 potentiated the sustained calcium current which activated at –50mV). It is not clear what underlies this difference.

Pharmacology of the sustained calcium current

The LVA sustained calcium current is sensitive to the dihydropyridine Nifedipine, an L-type channel antagonist. In the rod bipolar cell shown in Figure 3.2A, the calcium current was mildly inactivating, i.e. the early part of the calcium current was slightly larger than the late phase. A one minute bath application of 10μM Nifedipine reduced the amplitude of the calcium current (blue trace; Figure 3.2A), but did not completely block it. This observation was made in 5 bipolar cells while Nifedipine had no effect in a further 5 cells. Dihydropyridines at concentrations of less than 1μM are sufficient to abolish L-type currents in cardiac cells (Bean, 1984).

An early, resistant component of the calcium current following the application of Nifedipine is also apparent in the mouse bipolar cell recordings by de la Villa, et.al., (1998) and in the rat bipolar cell recordings shown by Protti and Llano (1998). The partial block by Nifedipine is also a feature of the sustained calcium currents of the cone photoreceptors in tiger salamander (Wilkinson and Barnes, 1996), and Tupaia retina (Taylor and Morgans, 1998). The reduced sensitivity to dihydropyridines sets the calcium current apart from the L-type calcium currents observed in goldfish bipolar cell terminals, which are completely blocked by 10μM Nifedipine (Heidelberger and Matthews, 1992).

In order to quantify the effect of Nifedipine, the amplitude of the calcium current in this cell was monitored every 20-30 seconds for seven and half minutes. The calcium current was activated by a 100ms voltage pulse to –35mV, and was measured at two time points corresponding to the peak (□) and the late (■) phase of the calcium current (Figure 3.2B). While the late phase of the calcium current was strongly suppressed, a residual calcium current remained, an observation also made by de la Villa (1998). The washout of Nifedipine was also monitored, although the amplitude of the calcium current remained suppressed for the duration of the recording. This was a consistent finding, and recovery from the block of the calcium current was incomplete in all bipolar cells (n=5).

Bipolar cells also have a transient, LVA calcium current

T-type calcium currents, which are generally inactivated at voltages above -70mV, were revealed by applying a -90mV prepulse followed by a -25mV test pulse (black trace, Figure 3.3A). A

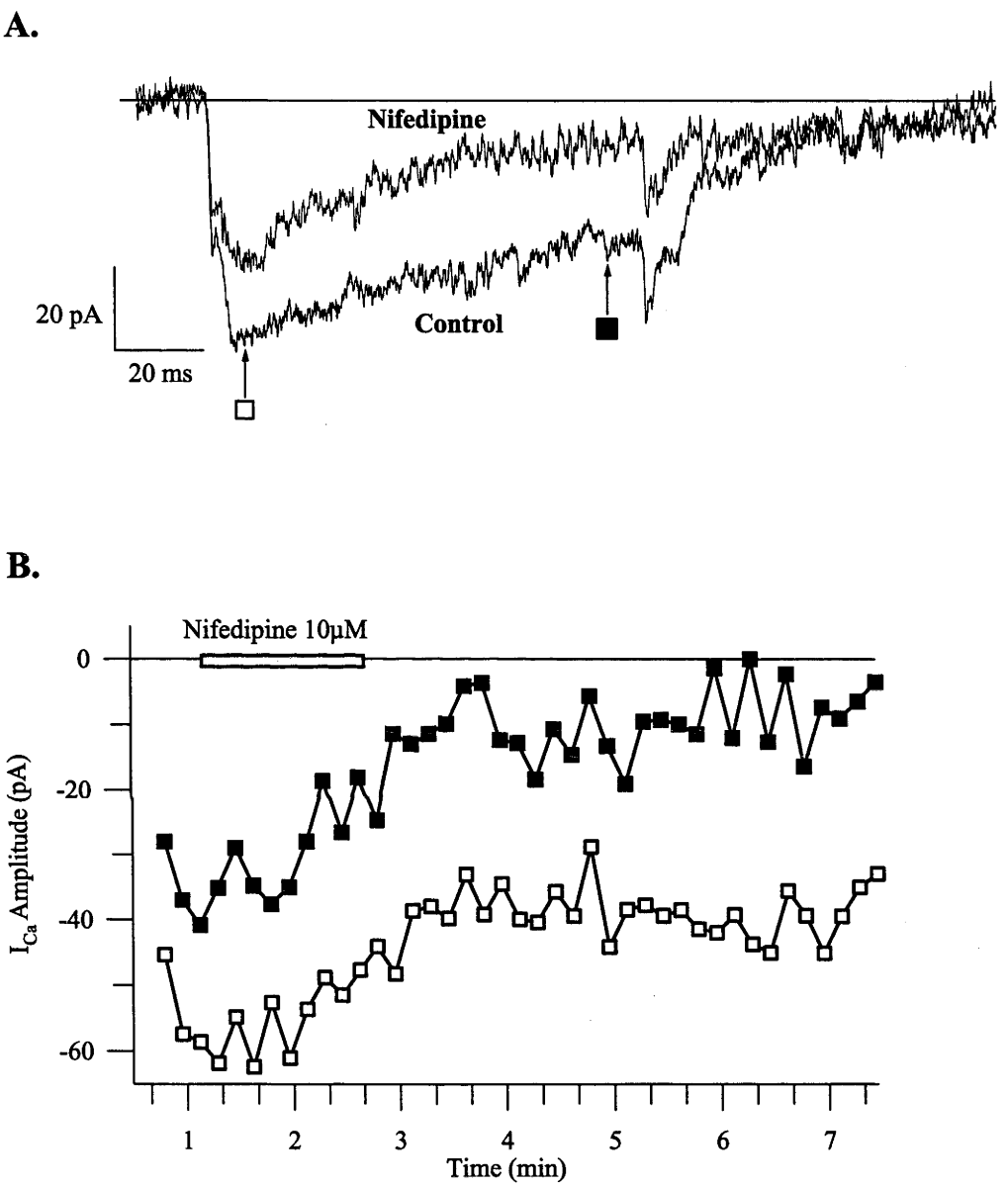

Figure 3.2. 10μM Nifedipine suppressed the sustained calcium current. (A) Voltage-clamp recordings from a rod bipolar cell in control conditions (black trace) and in the presence of 10uM extracellular Nifedipine (blue trace). (B) Time course of current suppression by Nifedipine in a rod bipolar cell (same cell as in A). The application of Nifedipine is shown by bar at top of graph. The amplitude of both the peak (□) and the late (■) phase of the calcium current were plotted as a function of time. The late phase of the calcium current was more completely suppressed than the early phase.

small inward current can be seen during the test pulse, especially when compared to the current following the -50mV prepulse (blue trace). A prepulse to -50mV is ineffective at removing the inactivation, and thus no inward current is apparent during the test pulse. In agreement with the other studies in mouse bipolar cells, LVA transient calcium currents were observed in both rod and cone bipolar cells (Kaneko et al., 1989; de la Villa et al., 1998; Pan, 2000). This is in contrast to a study by (Protti and Llano, 1998) where T-type calcium currents were reported only in cone bipolar cells.

The T-type current in the present study increased in amplitude following more negative prepulse potentials (Figure 3.3B). An off bipolar cell was stepped to a series of negative potentials for 1 second, and then stepped to -35mV. The maximal T-type calcium current in this off-cone bipolar cell is unusually large (~140pA following a prepulse to -120mV). Most of the T-type calcium currents observed in the present experiments were around -20pA following a prepulse to -120mV.

The steady-state inactivation curve for the T-type calcium current is shown for five bipolar cells (Figure 3.3C). The T-type current has a peak amplitude of approximately -20pA, and is 50% inactivated at -91mV. This suggests the T-type calcium channels will be almost completely inactivated in the physiological response range of the bipolar cells (-70mV to -20mV) (Simon et al., 1975; Ashmore and Falk, 1980; Ashmore and Copenhagen, 1983; Saito and Kaneko, 1983). This is in conflict with the activation range reported for dissociated mouse bipolar cells, where the T-type calcium currents were 50% inactivated at -60mV, and half-activated at -35mV (Kaneko et al., 1989; Pan, 2000). It is unclear what underlies this difference. It is possible that the dissociation procedure somehow affected the voltage-dependence of the T-type channels. The activation, and inactivation ranges for the T-type currents measured by de la Villa et.al., (1998) in mouse bipolar cells in the retinal slice preparation were not reported

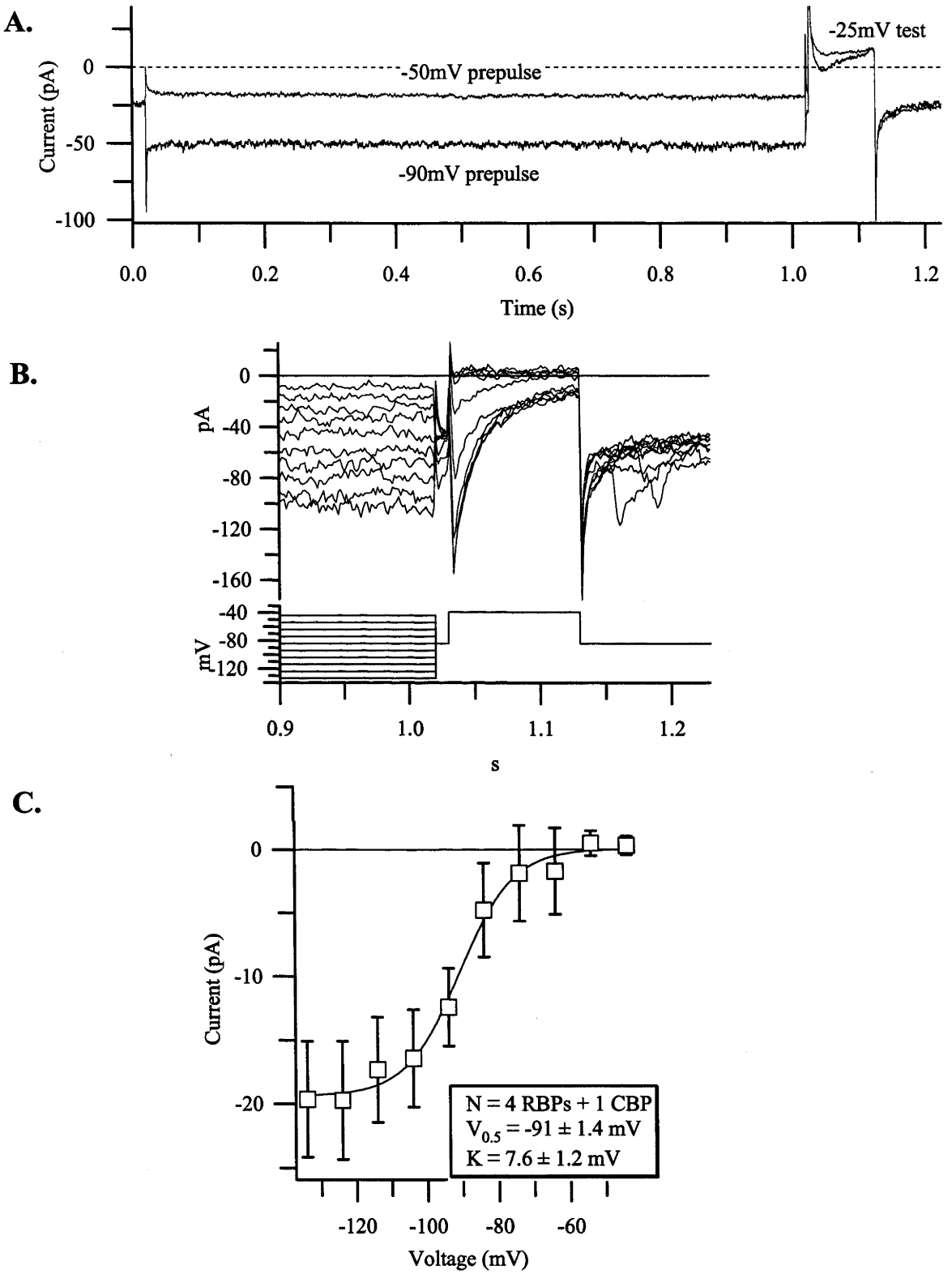

Figure 3.3. Bipolar cells also possess T-type calcium currents. (A) The T-type current from a rod bipolar cell can be seen during test pulse to -25mV following a -90mV prepulse to remove voltage-dependent inactivation. No T-type current is apparent following the -50mV prepulse due to voltage-dependent inactivation of the current. (B) The inactivation of the T-type current in an off-cone bipolar cell can be tracked by presenting prepulses of various voltages. The inactivation protocol (below traces) consisted of a series of 1 second conditioning pulses ranging from -135mV to -40mv, and were followed by a brief repolarization to -80mV, that preceded a 100ms test pulse to -30mV. (C) Steady-state inactivation of the t-type calcium current for 4 rod bipolar cells, and 1 cone bipolar cell. Error bars show one standard deviation.

Discussion

Bipolar cells have at least two calcium currents

The present study reveals two calcium currents in mouse bipolar cells: a transient calcium current with the classical features of T-type currents (i.e. activation by low voltages, and voltage-dependent inactivation), and a sustained calcium current with kinetics resembling an L-type current, but an activation range lower than that of a classical L-type channel, and a relative insensitivity to dihydropyridines. The low voltage activation range of the calcium currents is in line with the operating range of bipolar cells (Simon et al., 1975; Ashmore and Copenhagen, 1980; Ashmore and Copenhagen, 1983; Saito and Kaneko, 1983), and would therefore be well-suited for modulating neurotransmitter release from the terminal.

The results presented above agree with those published by de la Villa et.al., (1998) in bipolar cells of the mouse retinal slice preparation. A similar study in bipolar cells of the rat retinal slice preparation also revealed a sustained calcium current activating at a lower voltage than classical L-type channels (Protti and Llano, 1998). However, the same study failed to find T-type currents in rod bipolar cells, but reported them to be present in some cone bipolar cells. Both of these authors concluded that the sustained calcium currents are mediated by an L-type channel, while the transient currents are mediated by T-type channels.

Identification of the calcium currents

Despite multiple publications on the topic, the identification of the bipolar cell calcium channels is still far from clear. While the transient calcium current shares all of the features of a classical T-type calcium channel, the identification of the sustained calcium current is more of a puzzle. There are several observations in the published studies, and in the present results, which suggest that the sustained calcium current in bipolar cells is mediated by a novel calcium channel. First, the sustained calcium currents observed in bipolar cells of the mouse and rat retina have an unusually low activation threshold of around -50mV (see Figure 3.1C), similar to -60mV found in mouse (de la Villa et al., 1998) and -50mV found in rat (Protti and Llano, 1998; Pan, 2000). Interestingly, two other ribbon-containing neurons also display sustained calcium currents with a low activation threshold: cone photoreceptors in retina (Yagi and Macleish, 1994; Taylor and Morgans, 1998) and saccular hair cells in the inner ear (Su et al., 1995). At present, there are no known α subunits that display the kinetics and activation range of the calcium currents observed in the present study. The low activation threshold qualifies the sustained calcium currents, by

definition, as low voltage activated currents. These results challenge the idea that all L-type calcium currents are high voltage activated.

The calcium currents in the bipolar cells seem to share several of the features of the cone photoreceptor calcium currents. In addition to the similar voltage activation range, the calcium currents of cone photoreceptors and bipolar cells in mammals were unaffected, or only partially blocked by dihydropyridines (Taylor and Morgans, 1998). In the present study, Nifedipine partially blocked the sustained calcium current in some bipolar cells (Figure 3.2A) whereas in other cells Nifedipine seemed to have no effect (data not shown). Similarly, dihydropyridines had little effect on the calcium currents of tupaia cone photoreceptors, even following a prolonged exposure to 50uM of Nifedipine (Taylor and Morgans, 1998). Interestingly, when expressed in oocytes, calcium channels containing the α1D subunit have also been shown to be incompletely blocked by dihydropyridines (Williams et al., 1992). Thus, the variable effect of Nifedepine does not exclude the α1D subunit as the pore-forming subunit of the cone photoreceptor and the bipolar cell calcium channel.

Cone photoreceptor terminals are labeled by antibodies directed against the α1D subunit (Taylor and Morgans, 1998), suggesting that the sustained calcium currents in cones are carried by calcium channels which contain the α1D subunit. However, calcium channels containing the α1D subunit have been shown to be HVA, activating around -30mV (Williams et al., 1992), not LVA like the calcium currents in cone photoreceptors. It is possible that the low voltage activation in cone photoreceptors results from the expression of different auxiliary subunits, which may modulate the voltage sensitivity of α1D calcium channels (Singer et al., 1991). Alternatively, cone photoreceptors could express novel calcium channels with an amino acid sequence similar to the α1D subunit. In contrast, bipolar cells are not labeled by antibodies directed against α1D (Morgans, 1999), suggesting that, while having many physiological similarities, bipolar cells and cone photoreceptors express different calcium channels.

Recently a new L-type calcium channel α subunit, α1F, has been cloned. Mutations in the gene encoding the α1F subunit have been correlated with congenital stationary night blindness (CSNB) (Strom et al., 1998; Naylor et al., 2000). Interestingly, electroretinogram (ERG) recordings of patients with CSNB suggest a decrease in the effectiveness of synaptic transmission between photoreceptors and second-order neurons in the retina (Hood and Greenstein, 1990). An antibody raised against the α1F subunit labels the axon terminals of rod, but not cone photoreceptors, in the rat retina, and the same antibody labeled the nerve terminals of dissociated rod bipolar cells (Morgans, personal communication). It has not yet been confirmed whether cone bipolar cells also express the α1F subunit. Thus, the LVA sustained

calcium currents measured in the bipolar cells of the mouse retina may be mediated by the novel L-type channels expressing the α1F subunit.

The T-type calcium current has been localized to the cell soma in bipolar cells in the mouse (Kaneko et al., 1989; de la Villa et al., 1998), and tiger salamander retina (Maguire et al., 1989). Due to its localization to the soma, and the fact that the currents will be almost completely inactivated positive to -70mV, it is unlikely that it supports synaptic vesicle release from the axon terminal. Since bipolar cells are generally assumed to be non-spiking neurons (but see Protti et al., 2000), it is not clear what role the T-type calcium current plays.

Conclusion

In conclusion, there are two types of calcium currents in bipolar cells: A LVA sustained calcium current possibly mediated by the newly cloned α1F subunit, and a classical T-type calcium current. Bipolar cells may also have a HVA L-type calcium current, as reported by Pan (2000), although such a current was not seen in the present study. The role for the T-type calcium current is unknown, while there is a general consensus that the sustained L-type calcium current mediates synaptic vesicle release from the bipolar cell terminal.

It is possible that there is diversity in calcium channel expression among bipolar cells. Indeed, such diversity is already found among photoreceptors, with only some cones expressing the α1D subunit (Morgans, 1999). Preliminary immunohistochemical evidence in dissociated mouse bipolar cells suggests that rod bipolar cells express calcium channels at their nerve terminals which contain the α1F subunit (Morgans, personal communication). Patients with complete CSNB show a severe loss in rod function, while cone function is unaffected (Bech-Hansen et al., 1998). If the rod bipolar cells also express the α1F subunit, then perhaps both rod and rod bipolar cell functioning is compromised in CSNB. Since cone vision is unaffected in CSNB it is possible that cone bipolar cells express either a different calcium channel than the rod bipolar cells, or that they coexpress the α1F channel and a second calcium channel. Future light- and electronmicroscopic studies may reveal the localization the α1-subunits to the different classes of bipolar cells, while expression of the subunit in oocytes may make it possible to study the physiological and pharmacological properties of these calcium channels.

Chapter 4

Characteristic Bipolar Cell Light Response Properties

Introduction

Bipolar cells form the vertical pathway for excitatory signals in the retina, and an understanding of their basic light response properties is essential for assessing their information processing role. There are three main functional classes of bipolar cells in the mammalian retina. The rod bipolar cells comprise a single morphological and functional class, with the specific role of transmitting rod signals. The two other functional classes of bipolar cells, the on-cone bipolar and the off-cone bipolar cells, come in multiple morphological subtypes. In mammalian retina, 8-11 morphologically distinct cone bipolar cells have been identified, and it has long been speculated that the subtypes have distinct functional roles. Thus far, the only known example of this is the blue-cone bipolar cell in primate retina which contacts only blue cones, and therefore transmits spectral information. The goal of the present study was to characterize the light response properties of the different types of bipolar cells, and to look for possible differences in their response characteristics.

Light Response Kinetics

Initially the basic response waveforms, and the light response kinetics of the three main classes of bipolar cells were characterized. In the cone bipolar cells, the second messenger signal transduction mechanism may introduce delays in the light response compared to the ionotropic mechanisms utilized by off-cone bipolar cells. Indeed, temporal differences have been noted between the on- and off- pathways in other species, including mudpuppy (Kim and Miller, 1993), cat (Victor, 1988) and turtle (Copenhagen et al., 1983). In contrast, presynaptic mechanisms may contribute to kinetic differences between the rod bipolar cells and on-cone bipolar cells, due to the slow kinetics of the rod photoreceptors compared to cone photoreceptors (Schneeweis and Schnapf, 1995). The kinetics of light responses were examined by measuring their rise time, and latency in the three classes of bipolar cells.

Intensity-Response Relation

For neurons in the visual system, the intensity-response relation describes the neurons operating range, and sensitivity of the neurons to light. The intensity-response relation of the rod and cone bipolar cells would be expected to reflect the intensity-response relations of the rod and cone photoreceptors, both of which have been well characterized. Since the rods are more sensitive than the cones, it is expected that the intensity-response relation of the rod bipolar cells will also be shifted to lower intensities relative to the intensity-response relation of the cone bipolar cells.

The intensity-response relation of cone bipolar cells should also reflect dual rod cone input, since cone bipolar cells are known to receive rod input by at least two, and perhaps three, pathways: (i) the rod bipolar cell- AII amacrine cell pathway (Kolb and Famiglietti, 1974; Kolb and Nelson, 1983), (ii) rod to cone coupling (Nelson, 1977; Smith et al., 1986; Schneeweis and Schnapf, 1995), and (iii) direct rod input onto cone bipolar cells (Soucy et al., 1998). We wished to know the magnitude of the rod signal in cone bipolar cells, and at what light intensity it would appear.

Light-evoked excitatory and inhibitory input

Several anatomical and physiological studies have shown that on-bipolar cells express the metabotropic glutamate receptor mGluR6 (Nakajima et al., 1993; Vardi and Morigiwa, 1997), while off-bipolar cells express AMPA and KA receptors (Peng et al., 1995; Schultz et al., 1997; Brandstätter et al., 1998; Lo et al., 1998; DeVries and Schwartz, 1999; Morigiwa and Vardi, 1999). Application of glutamate to acutely dissociated bipolar cells, and to bipolar cells in the light-adapted retinal slice preparation, have shown that both the metabotropic and the ionotropic glutamate receptors gate currents through non-specific cation channels, and that glutamate evokes robust outward currents in on-bipolar cells, and inward currents in off-bipolar cells (Yamashita and Wässle, 1991; de la Villa et al., 1995). Since light turns glutamate release from the photoreceptors *off*, the bath application of glutamate has an effect opposite to light (which depolarizes on-bipolar cells and hyperpolarizes off bipolar cells).

In addition to glutamatergic input, all three classes of bipolar cells express GABA and glycine receptors on their axon terminals where they receive input from amacrine cells (Sterling and Lampson, 1986). Application of GABA and glycine to acutely dissociated cells, and to bipolar cells in the light-adapted retinal slice preparation show that GABA and glycine evoke robust chloride conductances (Karschin and Wässle, 1990; Kaneko et al., 1991; Shiells and Falk, 1994; de la Villa et al., 1995; Euler et al., 1996; Hartveit, 1997; Euler and Wässle, 1998). Since bipolar cells receive multiple inputs, the bipolar cell light responses are likely to be a mixture of excitatory and inhibitory currents. In the present study we wished to examine the magnitude of the light-evoked excitatory and inhibitory currents.

Receptive Field Profile

The receptive field of a neuron is defined by all the sensory receptors that can influence its activity. Typically, neurons in the retina have receptive fields organized into two concentric and antagonistic regions: a smaller central excitatory region, and a larger inhibitory surround. This center-surround spatial configuration of receptive fields occurs at many levels in the visual system, including the photoreceptors (Smith and Sterling, 1990). Such organization is thought to underlie a number of visual functions including chromatic and achromatic contrast enhancement,

movement perception, and some aspects of light adaptation (Barlow and Levick, 1976; Srinivasan et al., 1982; Hare and Owen, 1990).

Bipolar cells are also organized into center and surround regions. On-bipolar cells depolarize in response to small centered stimuli, while stimuli falling in more peripheral regions of the receptive field elicit hyperpolarizations (Werblin and Dowling, 1969; Matsumoto and Naka, 1972; Kaneko, 1973; Dacey et al., 2000). The same stimuli elicit responses of the opposite sign in off-bipolar cells. The bipolar cell receptive field center arises from glutamatergic input from the photoreceptors, while the surround is believed to be generated by horizontal cell feedback onto the photoreceptors (Baylor et al., 1971; Fuortes and Simon, 1974; Marchiafava, 1978; Toyoda and Tonosaki, 1978; Attwell et al., 1983; Hare and Owen, 1990).

Size estimates for bipolar cell receptive field centers vary depending on the species. Estimates in non-mammalian retina range from around 100-200um for the center of the receptive field, while the surround region is generally several times larger (Werblin and Dowling, 1969; Kaneko, 1973; Richter and Simon, 1975; Hare and Owen, 1990). The estimates of the receptive field centers are larger than predicted from the anatomical spread of bipolar cell dendrites, and are probably the result of gap-junctional coupling between the photoreceptors, and also bipolar cell - bipolar cell coupling known to occur in non-mammalian species (Umino et al., 1994). There have been only scant reports of bipolar cell receptive field sizes in mammalian retina. The receptive field center for rod bipolar cells in cat retina was estimated to be several hundred microns (Nelson and Kolb, 1983), however the light stimulus used in that study was quite large and this is probably an overestimate. A recent study in primate cone bipolar cells has revealed receptive field centers of 40-50um, and a surround region ~10 times larger (Dacey et al., 2000). That study, however, did not report the receptive field size of rod bipolar cells. One goal of the present study was to measure the extent of the center and surround regions of the receptive fields of the three classes of bipolar cells in mouse retina.

Noise Characteristics

Reliable transmission of information requires that the signal be significantly larger than the background noise level of a system. However, biological systems are inherently noisy, and there are several sources which may contribute to noise in bipolar cell responses. First of all, the stimulus itself can be noisy due to the stochastic arrival of photons at low intensities. The photoreceptor transduction cascade also contributes noise to synaptic transmission due to spontaneous isomerization of the photopigment, and to variations in the lifetimes of multiple intermediates. At the photoreceptor-bipolar cell synapse, the stochastic release of neurotransmitter from the photoreceptor terminals will appear as variance in the bipolar cell

response, along with the noise contributed by postsynaptic mechanisms such as channel noise. In the present study, we measured the variance and mean levels of bipolar cell light response amplitudes, and derived an estimate of the size of the underlying elementary events.

Methods

Preparation

Dark-adapted mouse retinal slices were prepared following the procedures summarized in Chapter 2: General Methods. All manipulations were performed under infrared illumination.

Recordings

Whole cell voltage- and current- recordings were made from bipolar cells in the dark-adapted mouse retinal slice preparation. While in voltage-clamp, cells were held at -70mV. In current-clamp, the holding current was set to 0pA. Bipolar cells were selected by the shape of their cell soma, and by their position in the retina. During the recording, cells were filled with Lucifer Yellow (0.5%), visualized after the recording, and identified morphologically.

Stimulus

The retina was stimulated with all three guns from the computer screen light source (i.e. white light). The maximum achromatic light intensity of the screen was measured to be 47cd/m^2 (red: 21.2 cd/m^2, green:16.2cd/m^2, blue: 9.6 cd/m^2). This corresponded to a light intensity at the focal plane of the preparation of 45 lumens/m^2. All stimuli were ganzfeld and illuminated a 500μm section of the retina, except for the stimulus used in the receptive field measurements. In those experiments, a bar of light 20μm wide was used to stimulate a small section of the retina.

Solutions

Ames solution was used as the extracellular solution. There were two intracellular solutions (summarized in Table 2.1, in General Methods).

Results

Characteristic light responses

Characteristic responses to light flashes (top trace in each panel) and light steps (bottom trace in each panel) of the three classes of bipolar cells are shown in Figure 4.1. Rod (Figure 4.1A) and on-cone bipolar cells (Figure 4.1B) respond to light with inward (depolarizing) currents, while off-cone bipolar cells (Figure 4.1C) respond with outward (hyperpolarizing) currents. The rod- and the off-cone bipolar cells both displayed substantial baseline noise in darkness, which was suppressed by saturating light intensities. The noise characteristics of bipolar cells will be discussed in a later section.

Two flash responses from a rod bipolar cell are overlaid (Figure 4.1A) to show that the rising phases of the responses overlap, despite substantial noise in the baseline current, and in the decay phase of the response. Thus the timing of the light flash is reliably recorded. All three cell types display an overshoot at the offset of the response, although in the rod bipolar cell the overshoot is frequently small or not apparent. The overshoot may be due to horizontal cell influence.

Two kinetic parameters were measured across the three classes of bipolar cells, and are summarized in Table 4.1. The rise-time was calculated by fitting a sigmoid function to the rising phase of a saturating light response. The rise time was defined as the time taken for the sigmoid function to rise from 10% to 90% of the maximum response amplitude. The response latency to saturating intensities was calculated by measuring the time between the onset of the light flash and the time when the bipolar cell response reached 10% of the maximum response amplitude. The timing of the light stimulus was recorded by a photodiode which responded to a small square of light in the top left hand corner of the screen (see General Methods). This small square of light flashed simultaneously with the stimulus. Since the screen was scanned every 13.3ms (75Hz), the time between light onset at the photodiode, and light onset in the center of the screen was approximately 6.7ms (i.e. the time taken to scan the top half of the screen). In the present analysis, 6.7ms was subtracted from the measured response latency for each cell, in order to compensate for the delay introduced by the timing of the light stimulus.

There were no significant differences in the rise times, or response latencies between the three classes of bipolar cells. This was unexpected because kinetic differences between the on- and off- bipolar cells have been demonstrated in other species (Copenhagen et al., 1983) and it is well-established that the kinetics of the rods and cones differ (Schneeweis and Schnapf, 1995). It is possible that since the bipolar cell responses were evoked by applying saturating stimuli,

kinetic differences are not as apparent as they would be had the light response kinetics been measured across multiple, non-saturating intensities.

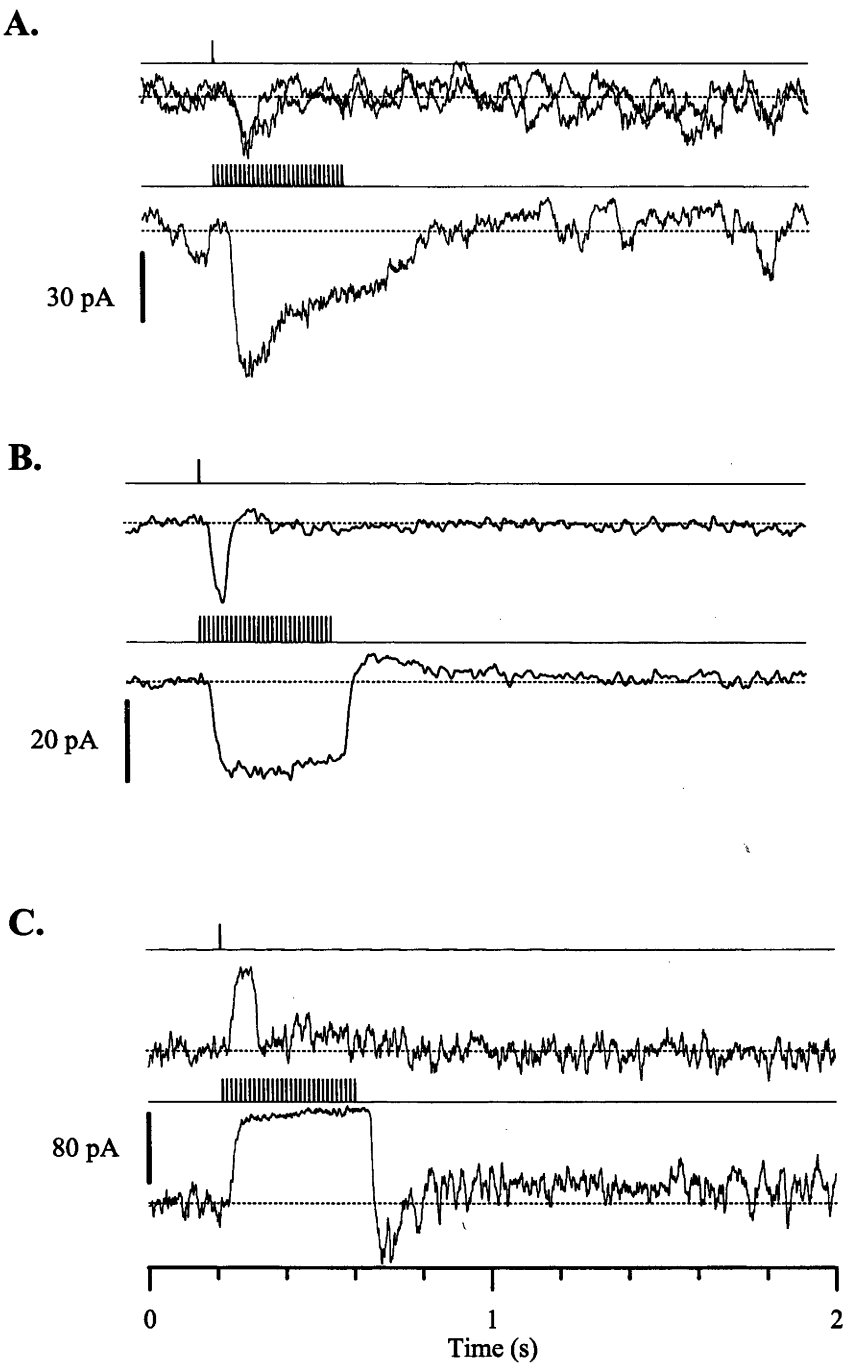

Figure 4.1 Characteristic light responses from (A) a rod bipolar cell, (B) an on-cone bipolar cell, and (C) an off-cone bipolar cell to 1ms flashes (top trace in each panel) and 390ms steps (bottom trace in each pane) of light. Notice that despite substantial noise in the baseline current of the rod bipolar cell (A) the rising phases of the two flash response overlie; thus the timing of the light flash is precisely registered. Light stimulus timing indicated by stimulus monitor above traces. Light intensities used were (A) flash: 0.1 lumen/m^2; step 0.35 lumen/ m^2, (B,C) 14.4 lumen/ m^2. Cells were held at –70mV.

Rod Bipolar Cells	28 ± 12ms (n=6)	43 ± 9ms (n=6)
On-Cone Bipolar Cells	29 ± 13ms (n=10)	54 ± 16ms (n=10)
Off-cone Bipolar Cells	24 ± 9 ms (n=10)	47 ± 13ms (n=10)

Table 4.1 Light response kinetics of the three classes of bipolar cells.

Current-voltage relation of light response

The current-voltage relation of the light evoked current was measured by stepping the bipolar cell to a series of different voltages, and flashing a light at each voltage. The light-evoked currents from a rod bipolar cell (Figure 4.2A) and an on-cone bipolar cell (Figure 4.2C) are inward at negative potentials, and outward at positive potentials. The average current-voltage relation was generated by measuring the peak response amplitude at each voltage for five rod bipolar cells (Figure 4.2B) and four on-cone bipolar cells (Figure 4.2D).

The average current-voltage relation for both the rod and on-cone bipolar cells was fit to a line with the following equation:

$$R = G(V_m - V_{rev}) \qquad \textbf{...equation 4.1}$$

where R is the response amplitude (pA), G is the conductance (S), V_m is the membrane voltage (mV), and V_{rev} is the reversal potential (mV). The average current-voltage relation is linear, and reverse close to 0mV (the expected reversal potential for a non-specific cation current).

The current-voltage relation for an off bipolar cell was measured for both light increments (Figure 4.3A) and light decrements (Figure 4.3C). For light increments, the cell was held in darkness and a light was flashed onto the retina for 400ms. The average current-voltage relation from five off-bipolar cells for light increments (Figure 4.3B) is similar to that of the on-cone bipolar cells, in that it is linear and reverses around 0mV. However, the IV relation has a negative slope due to the opposite response polarity of the off-cone bipolar cell.

In order to measure the current-voltage relation of the light-evoked current for light decrements (Figure 4.3D), the retina was exposed to a steady background light which was turned off for 400ms (shown by black bar above traces). The off bipolar cell responded to the light decrement

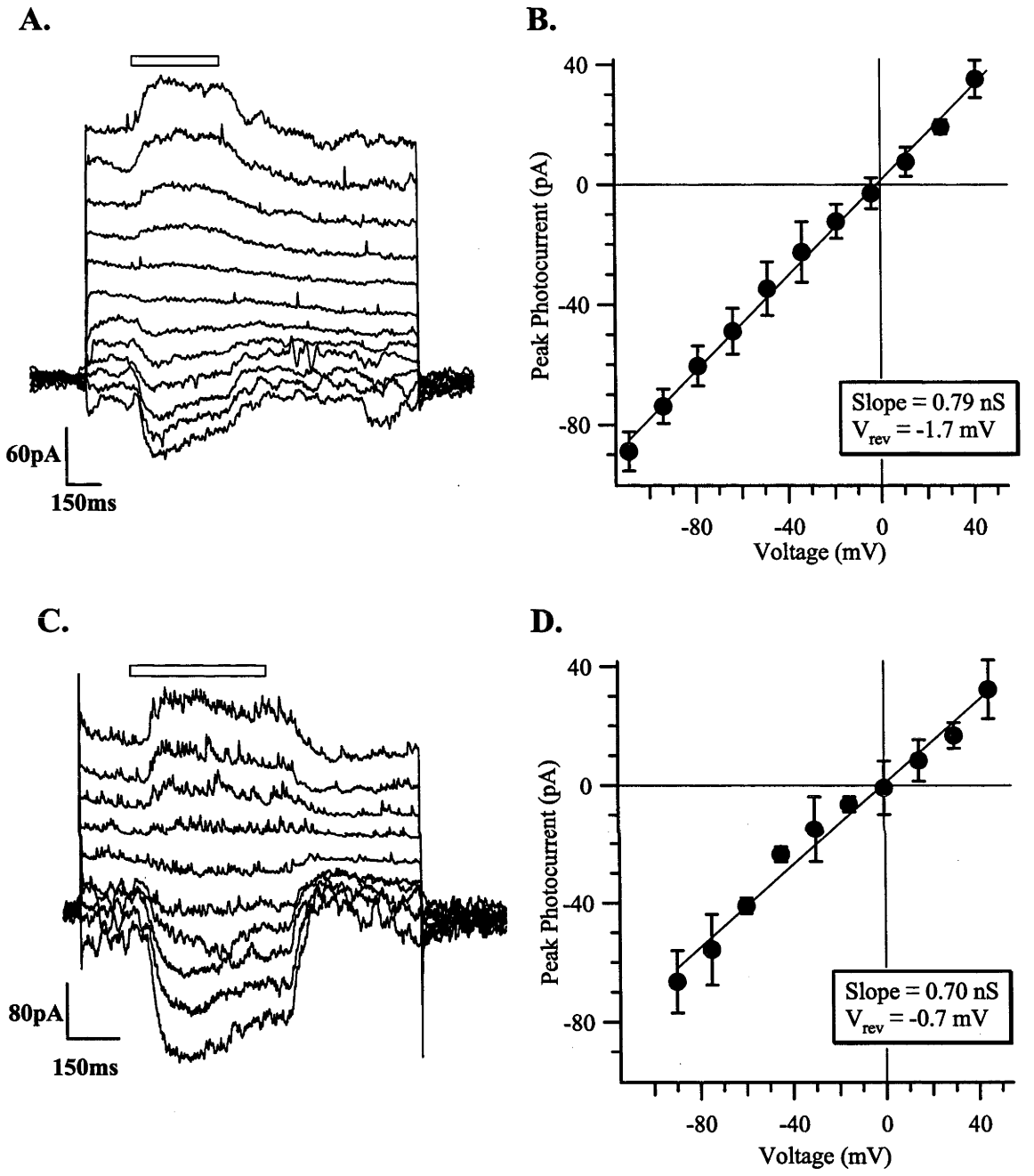

Figure 4.2 Current-voltage relation of light-evoked currents in On-bipolar cells. (A) Recordings from a rod bipolar cell. Light intensity 0.043 lumens/m^2. (B) The average normalized current-voltage relation from 5 rod bipolar cells was fit to equation 4.1 (solid line). (C) Recordings from an on-cone bipolar cell (light intensity 45 lumens/m^2). (D) The average normalized current-voltage relation from 4 on-cone bipolar cells was fit to equation 4.1 (solid line). Error bars show one standard deviation.

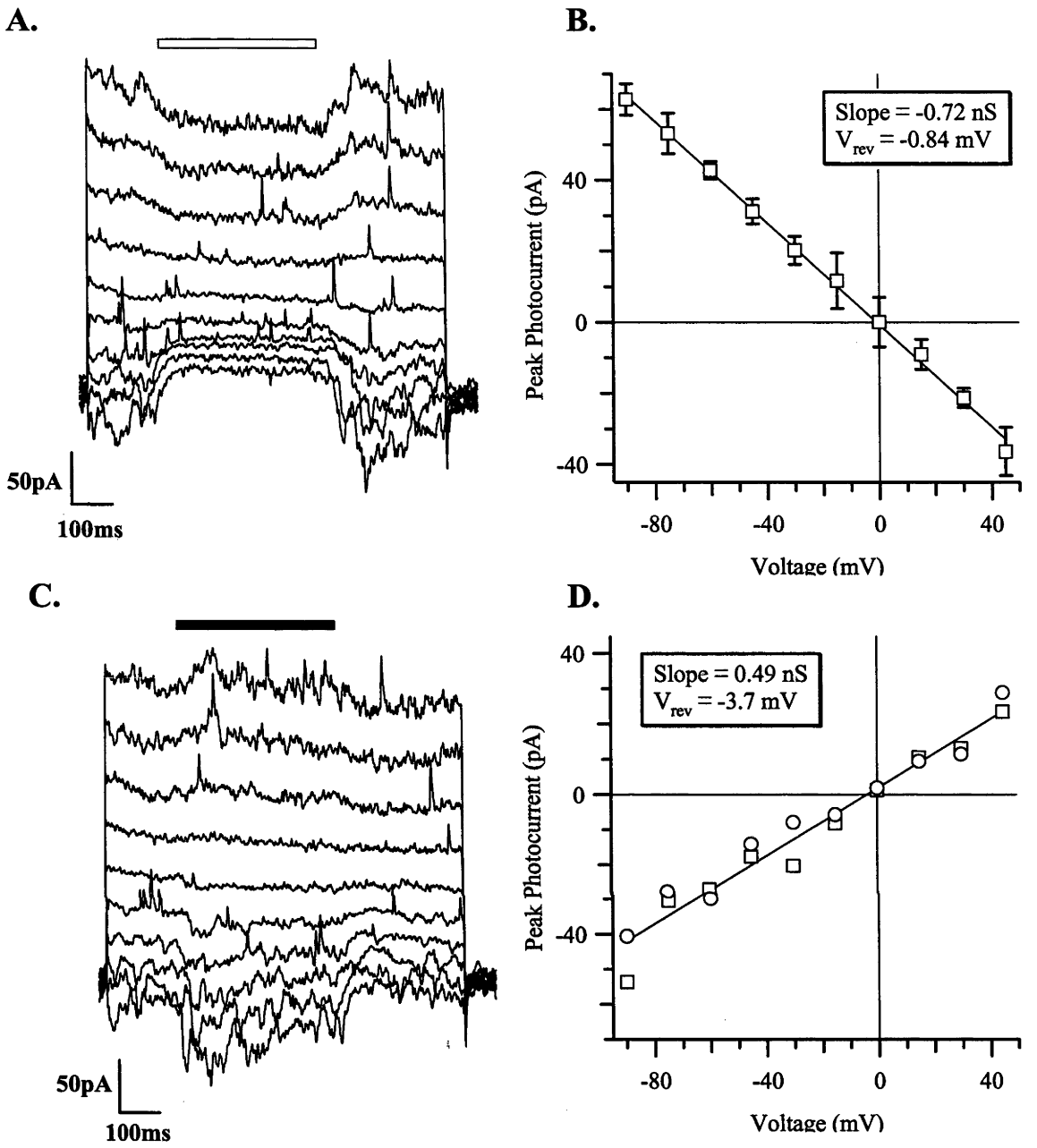

Figure 4.3 Current-voltage relation of off-cone bipolar cells. Current recordings from the same off-cone bipolar cell to (A) light increments (intensity 45 lumens/ m^2)and (C) light decrements (shown by black bar above traces). In C, the off-cone bipolar cell was exposed to a steady background light (8.56 lumens/m^2) which was then turned off. (B) Average normalized current-voltage relation for 5 off-cone bipolar cells in response to light increments (includes cell shown in A). (D) The average current-voltage relation of off-cone bipolar cell responses to light decrements from the off-cone bipolar cell shown in A/C. Two runs in the same cell. Solid lines in B and D are equation 4.1.

with an inward current at negative potentials, and an outward current at positive potentials. The average current-voltage relation for two runs in the same cell is linear and reverses around 0mV.

Inhibitory input onto off-bipolar cells was occasionally recorded (Figure 4.4A). In this off-cone bipolar cell, there were a number of fast events, in addition to the sustained glutamatergic current. It can be seen from the recordings that the fast events reverse (highlighted by the blue trace) at a potential more negative than the reversal of the glutamatergic current (highlighted by the red trace). The current-voltage relation of the sustained light-evoked current was measured at the two time points between the bursts of inhibitory input (shown by the arrows; Figure 4.4A), and plotted against membrane voltage (Figure 4.4B). The sustained current reversed around 0mV, similar to that in the previous figure, indicating that it arises from the glutamatergic input from the photoreceptors.

The fast events increased in frequency during the light step (see recordings in Figure 4.4A), and the time course of these events is shown in detail in Figure 4.4C. In order to calculate the reversal potential for these events, the integral of the current during the light step (shown by brackets under traces in A) was measured at each voltage (Figure 4.4D). The fast events reversed around -52mV, close to the chloride reversal potential. These are probably the glycinergic inputs from the AII amacrine cells, however, we were not able to apply strychnine to this cell to confirm that they are glycinergic currents. Events with this time course were blocked by the application of 1μM strychnine in another off cone bipolar cell (data not shown), although in that cell the glycinergic inputs were not light-driven. However, the kinetics are similar to glycinergic inputs in other systems (Twyman and Macdonald, 1991), providing indirect evidence for their identification as glycinergic inputs. The present results are the first direct demonstration of mixed, light-evoked input onto an off-cone bipolar cell.

Light-evoked inhibitory input was also occasionally apparent in rod bipolar cell recordings (Figure 4.5A). In this cell, light evoked a sustained inward current at potentials negative to -65mV, while at voltages positive to -65mV light evoked a sustained outward current. The sustained currents are probably GABAergic although we did not apply any pharmacological agents to this cell. However, it is known that rod bipolar cells express $GABA_C$, $GABA_A$, and glycine receptors (see Introduction). The current-voltage relation for this cell is shown in Figure 4.5B. It is linear and reverses around -59mV. These inhibitory currents must reflect sustained amacrine cell input in the IPL.

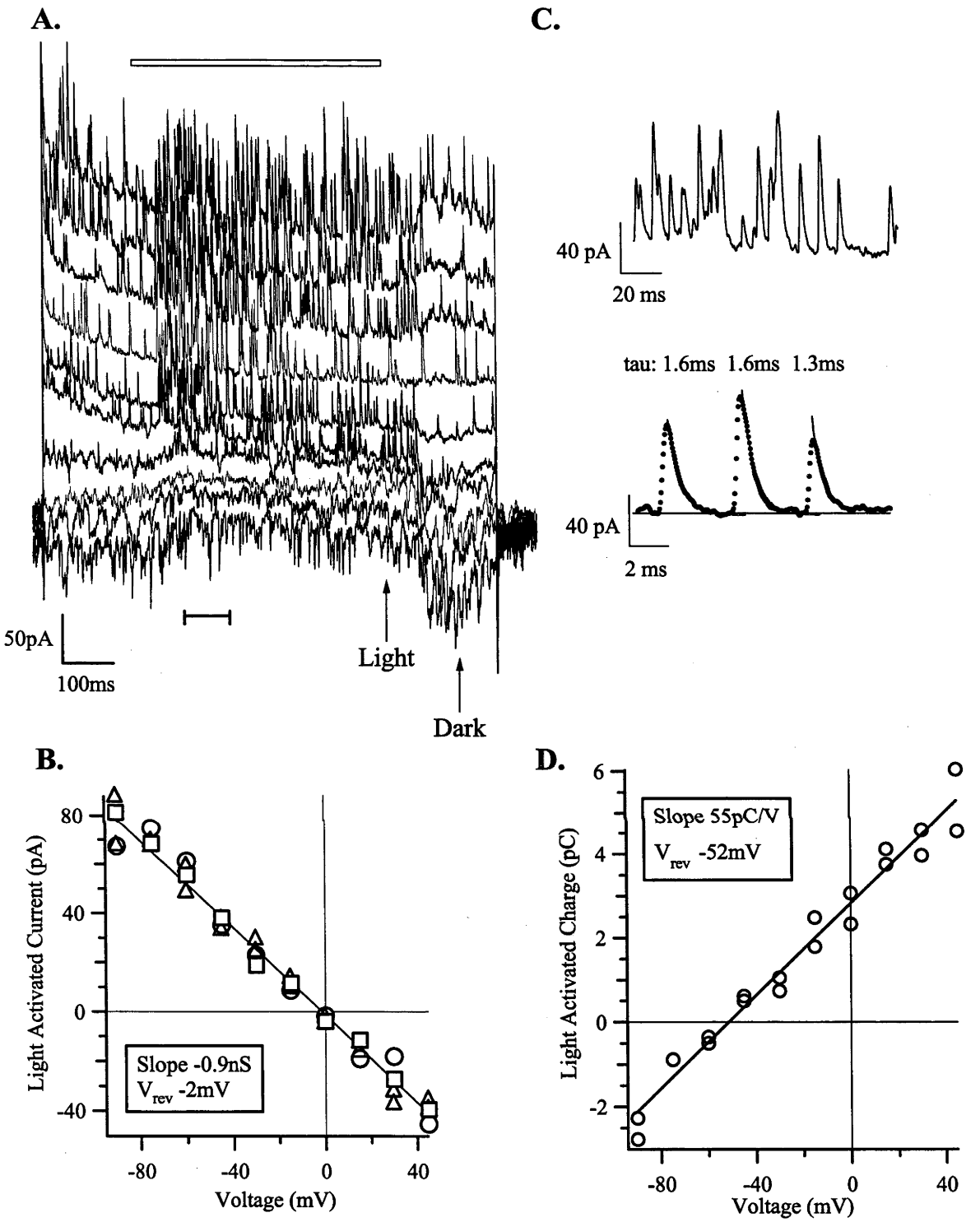

Figure 4.4 Light-evoked inhibitory input onto an off-cone bipolar cell. (A) Current recordings from an off-cone bipolar cell at a series of voltages (-90mV to +45mV in 15mV steps). Two components of the light response can be seen: a sustained glutamatergic input reversing close to 0mV, and fast inhibitory events reversing close to –60mV (blue trace:-60mV holding potential; red trace: 0mV holding potential). Light intensity: 45 Lumens/m^2.(B) Response amplitude of the glutamatergic light-evoked current plotted as a function of voltage. The line is equation 4.1. Measurements were made at the time points indicated by the arrows below the traces, during the brief intervals between bursts of inhibitory input (C) Detail of the inhibitory events. (D) The integral of the fast events were measured over the time period indicated by the brackets under the traces in A, while the baseline was estimated at the intervals between the fast events. The intregral was plotted against voltage (solid line is equation 4.1). The relation is linear, and reverses at –52mV, close to the calculated chloride equilibrium potential.

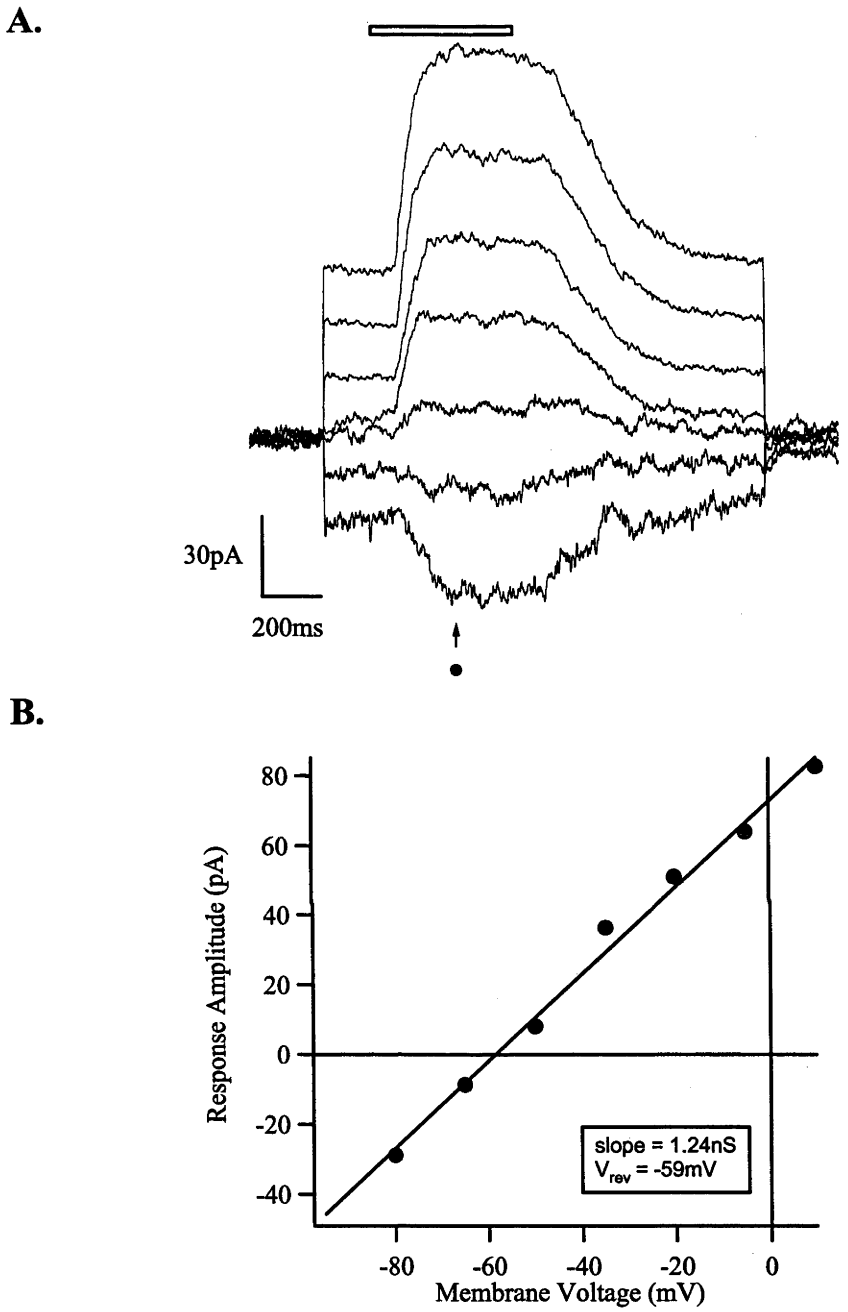

Figure 4.5 Light-evoked inhibitory input onto a rod bipolar cell. (A) Current recordings from a rod bipolar cell at a series of voltages. Membrane voltage stepped from –80mV to +20mV in 15mV steps. 490ms light step, 0.008 lumens/m^2. (B) Response amplitude of light evoked current plotted as a function of voltage. The line is equation 4.1. The current voltage relation is linear, with a reversal potential of –59mV, close to the calculated reversal potential for chloride (see text).

Receptive field profile

The bipolar cell receptive field profile was measured by stepping a 20um-wide vertically oriented bar along the retina at different positions, and measuring the bipolar cell light response at each position. The receptive field center was defined as the area within which a luminance increment causes an inward current in on-bipolar cells, and an outward current in off-bipolar cells. A response amplitude larger than 10% of the maximum was selected as the criterion response.

Multiple two-second recordings from a rod bipolar cell are displayed side by side according to the position of the light stimulus (Figure 4.6A). The light-evoked inward current was largest when the light stimulus was positioned directly over the bipolar cell (bar position 0). As the light stimulus was stepped away from the bipolar cell in 20μm steps, the light responses got smaller and finally disappeared.

The peak response amplitudes were measured, and plotted against bar position (Figure 4.6B). The data points were fit to a gaussian function:

$$R = R_{\max} e^{\frac{-(x-x_o)^2}{(w/2)^2}} \qquad \textbf{...equation 4.2}$$

where R is the peak response amplitude (pA), R_{max} is the maximum response amplitude (positive or negative), x_o is the center of the receptive field, and w is the width of the receptive field (μm) at $1/e$.

The receptive field width was calculated by measuring the width of the gaussian function at 10% of the peak response amplitude. This calculation yielded a receptive field width 67μm for the cell shown in A, and an average width of 67 ± 13μm for 6 rod bipolar cells (includes cell shown in A).

The same light stimulus protocol was applied to an on-cone bipolar cell (Figure 4.6C) and an off-cone bipolar cell (Figure 4.6E), yielding receptive field sizes of 37μm (Figure 4.6D) and 40μm (Figure 4.6F) respectively. The average receptive field profile for 5 on-cone bipolar cells was 43 ± 7μm. We recorded the receptive field profile from only one off-cone bipolar cell. There was no evidence for an inhibitory surround in any of the bipolar cells recorded from. It is possible that much of the surround is missing due to the slicing procedure. Therefore, these estimates are interpreted as the receptive field centers.

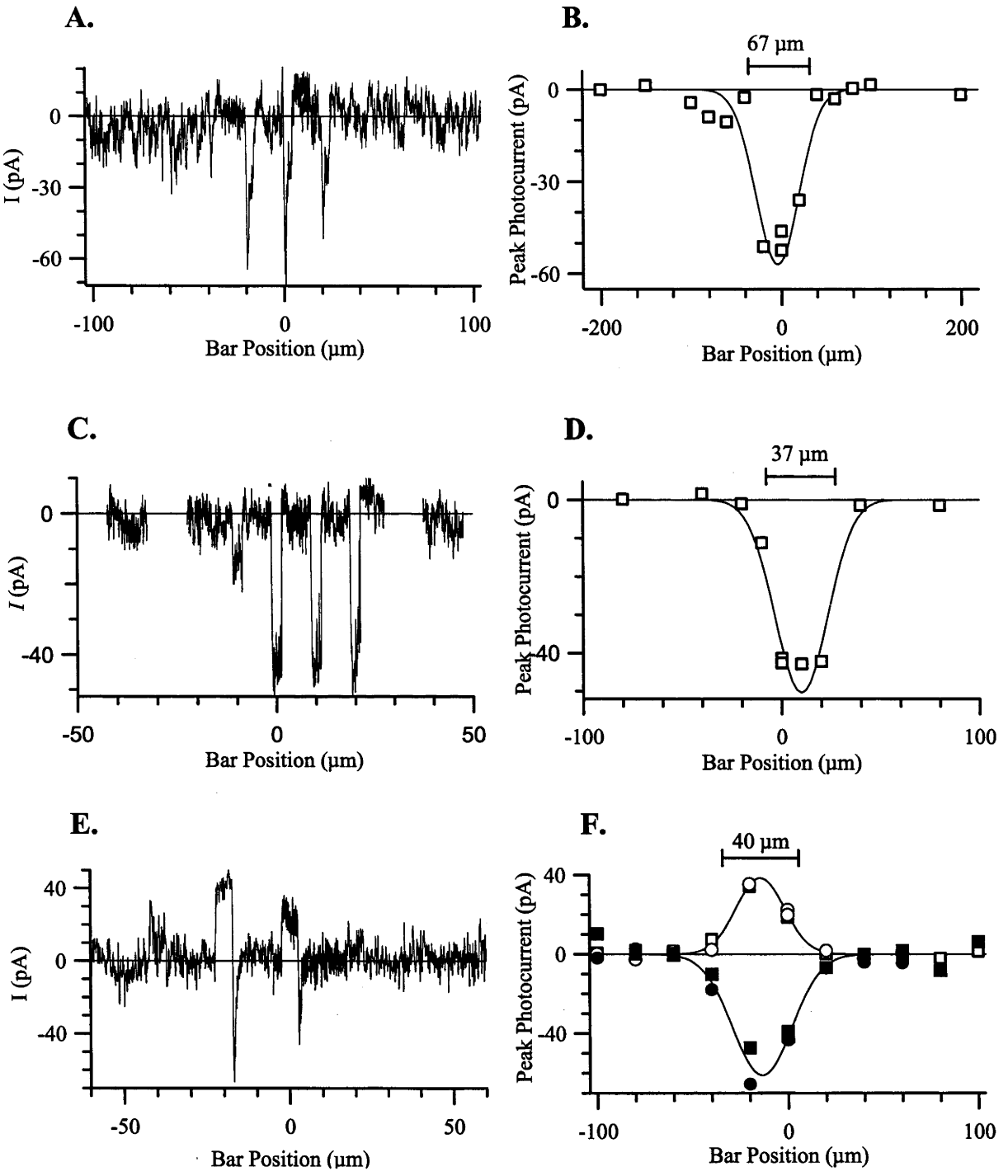

Figure 4.6 Receptive field profiles of the three classes of bipolar cells. Current recordings from (A) a rod bipolar (C) an on-cone bipolar (E) and an off-cone bipolar cell to a 20µm wide bar flashed at different positions along the retinal slice. The bar position is expressed in terms of distance in µm from the bipolar cell soma. Light response amplitudes are plotted against bar position for a (B) rod bipolar cell (D) an on-cone bipolar cell, (F) and an off-cone bipolar cell. The solid lines in B,D, and F are gaussian functions (equation 4.2) with coefficients (B) R_{max} = -57pA, x_o = -4.1µm , w = 67.2µm ; (D) R_{max} –50pA, x_o = 10 µm, w = 37 µm; (F) (closed symbols) R_{max} = -58pA, x_o = -14 µm, w = 40 µm; (open symbols) R_{max} 39pA, x_o = -13 µm, w = 36 µm.

Intensity-response relation

Light-evoked current (Figure 4.7A) and voltage (Figure 4.7C) recordings were made from the same rod bipolar cell to ganzfeld light steps of increasing intensity. At the dimmest intensities, the light step elicited no response (top three traces in 4.7A). As the light intensity was increased, the inward current became larger, and once the rod bipolar cell light response amplitude exceeded ~40% of the maximal response amplitude, it consisted of a large transient inward current followed by a smaller plateau current. This can be seen more clearly when the rod bipolar cell light responses are overlaid (Figure 4.7B). In the next chapter, we will show that this reduction in the rod bipolar cell response amplitude, which we have termed inactivation, is mediated by a rise in intracellular calcium.

In addition to the inactivation of the light response at higher intensities, the time to peak decreased, probably due to the decrease in the time to peak of the photoreceptor responses at high intensities (Schneeweis and Schnapf, 1995). The rising phase of the light response is identical in both the photocurrent and the photovoltage (Figure 4.7D), although the inactivation is less apparent in the photovoltage. This may reflect a change in the ionic driving force due to the change in voltage.

The average peak response amplitude for 6 rod bipolar cells was plotted against light intensity (Figure 4.8A) and was fit to a saturation function:

$$R = R_{\max} \frac{L^h}{L^h + L_{1/2}{}^h} \qquad \textbf{...equation 4.3}$$

where R is the peak response amplitude (pA), L is the light intensity (lumens/m^2), $L_{1/2}$ is the light intensity (lumens/m^2) that elicits a half-maximal response, h is the Hill coefficient, and R_{max} is the maximum response amplitude (pA). The average rod bipolar cell intensity-response relation of the photocurrent (n= 5; Figure 4.8A) could be fit by equation 4.3 with a Hill coefficient of 1.1 and half-maximal activation at 0.07 lumens/m^2 (summarized in Table 4.2). The average intensity-response relation of the photovoltage from 5 rod bipolar cell was also fit to equation 4.3 with a Hill coefficient of 1.46, and a half-saturating intensity of 0.027 lumens/m^2.

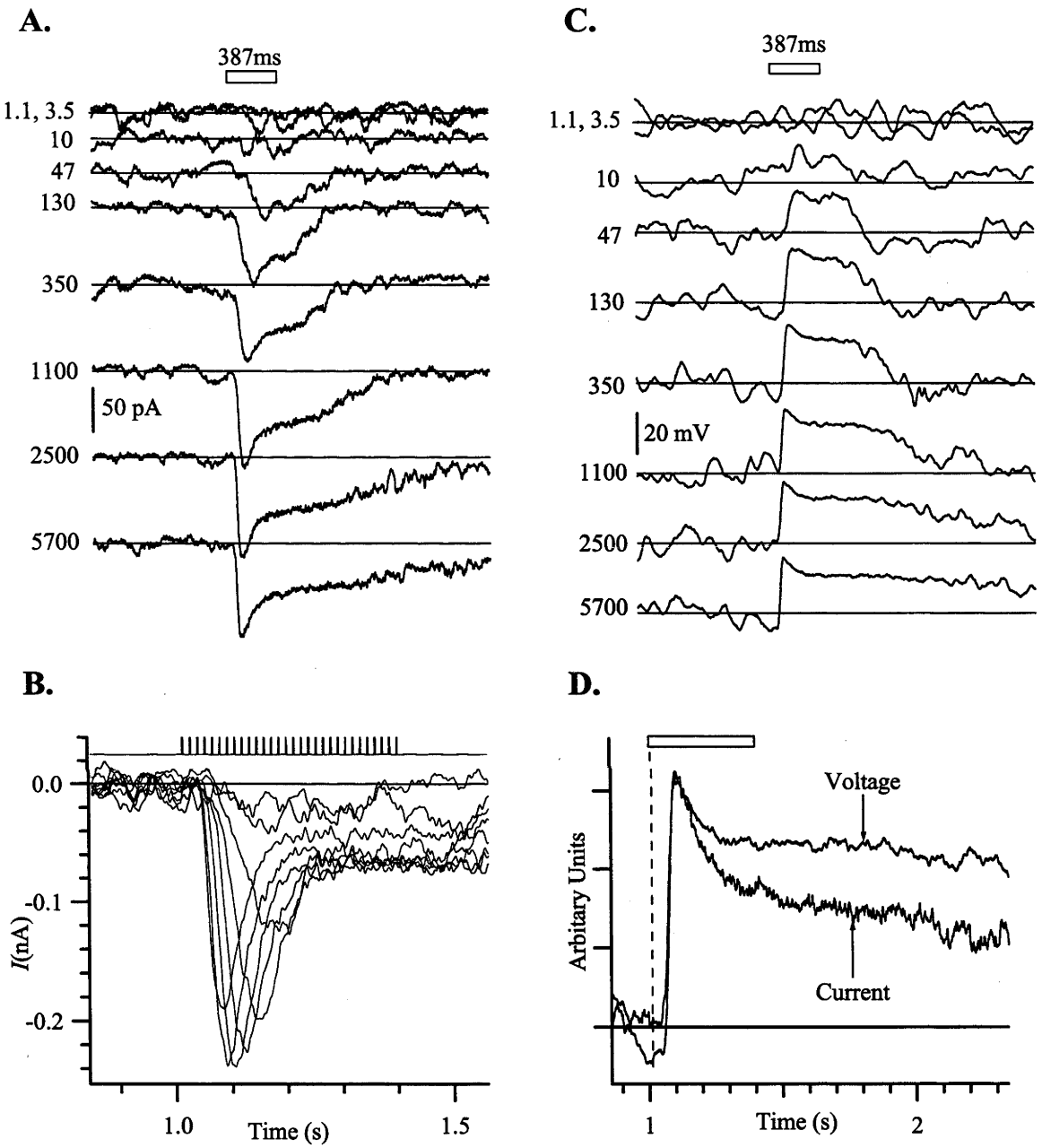

Figure 4.7 Intensity response relation of rod bipolar cells. (A) Light-evoked currents, and (C) voltages from the same rod bipolar cell. Light intensities (x 10^{-3} lumens/m^2) listed to the left of each trace. (B) Intensity responses from a rod bipolar cell overlaid. (D) The bottom trace in A was inverted, and aligned with the bottom trace in B in order to compare the response waveforms in current-clamp and voltage-clamp. Responses were scaled to arbitrary units so that the rising phases of the responses overlapped. While the rising phases are identical, inactivation was less pronounced in current-clamp mode.

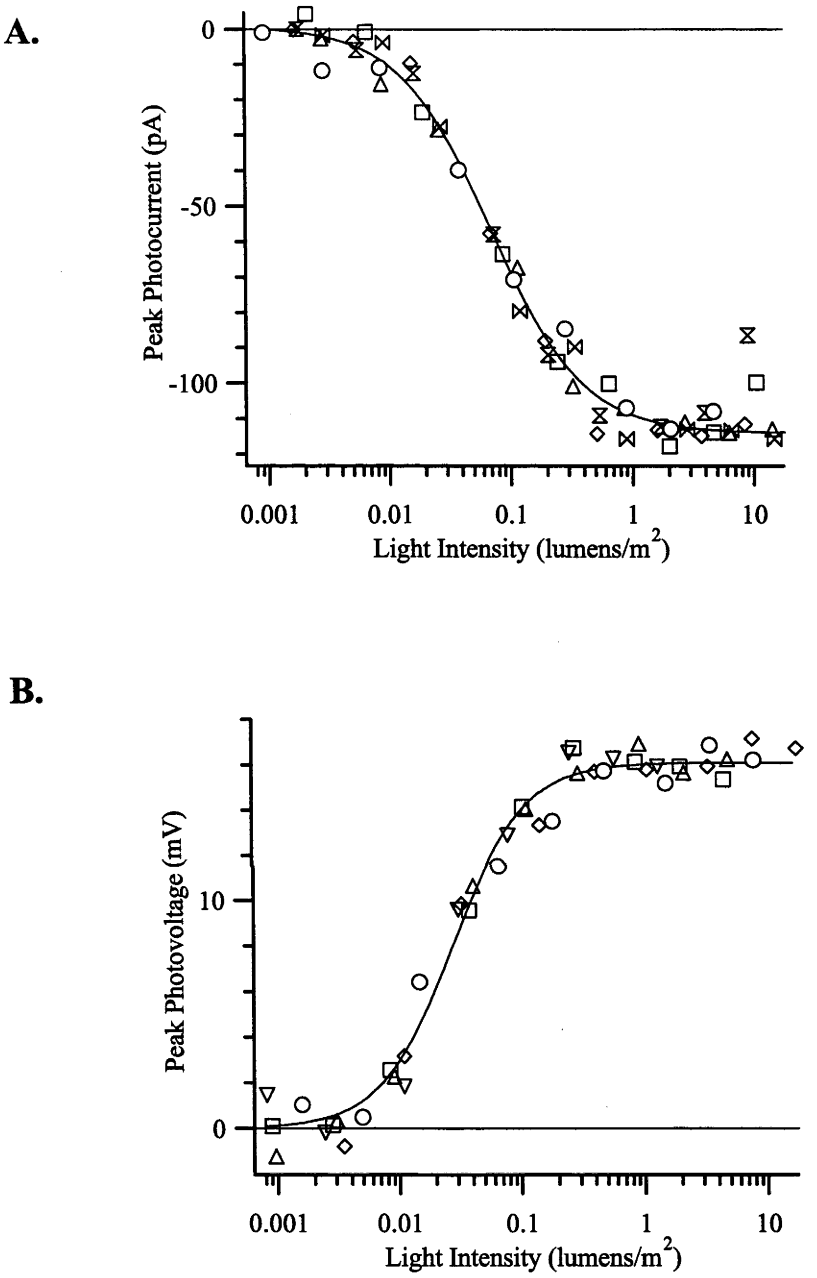

Figure 4.8 Average rod bipolar cell intensity-response relations. (A) Intensity-response relation of the photocurrents for 6 rod bipolar cells (symbols). The solid line is a saturation function (equation 4.3) with a Hill coefficient of 1.1 and a half saturating intensity of 0.07 lumens/m^2 (coefficients summarized in Table 4.2). (B) Intensity-response relation of the rod bipolar cell photovoltage for 5 rod bipolar cells (symbols). The solid line is equation 4.3 with a Hill coefficient of 1.46 and half saturating intensity of 0.027 lumens/ m^2. The rod bipolar cell shown in Figure 4.7A and C is indicated by O in both graphs. Otherwise, the symbols repeated in the above graphs do not correspond to the same cells.

	Rod Bipolar (n=6)	On-Cone Bipolar (n=3)	Off-Cone Bipolar (n=3)
Hill Coefficient	1.1	(1.1) 2.25	(1.1) 1.59
Half Saturating Intensity (lumens/m^2)	0.07	(0.035) 1.49	(0.01) 1.11

Table 4.2. Coefficients of the average photocurrent intensity-response relation. For the cone bipolar cells, the intensity-response relations were fit to the sum of two equations (equation 4.3). The coefficients corresponding to the rod component of the intensity-response curve are in parentheses.

The intensity-response relation of on-cone bipolar cell photocurrents (Figure 4.9A) and the photovoltages (Figure 4.9C) were measured using the same protocol as before, but with light intensities 2 log units higher. Saturating intensities elicited a sustained response with a suppression of the baseline noise (bottom two traces in Figure 4.9A, and top two traces in Figure 4.9B), while responses to intermediate intensities were characterized by an increase in variance. This variance increase is more apparent in the photocurrent (middle traces Figure 4.9A) than in the photovoltage (Figure 4.9B). A slight overshoot is present at the offset of the light response, and is also more apparent in the photocurrent than the photovoltage.

Peak response amplitudes were measured for five on-cone bipolar cells and plotted against light intensity (Figure 4.9C). Three of the on-cone bipolar cells displayed a prominent rod-component (open symbols), while in the other two cells a rod component was not apparent (close symbols). The intensity-response relation from the cells which displayed rod input were fit to the sum of two saturation functions (equation 4.3: coefficients summarize in Table 4.2). The intensity-response relation for the two cells which did not display rod input were not included in the fit, but are only plotted for comparison. During fitting, the Hill coefficient for the rod component of the intensity-response relation was held to 1.1, while the Hill coefficient for the cone component was free to vary. The Hill coefficient of the cone component of the intensity-response relation is much higher (2.25) than the Hill coefficient seen in rod bipolar cells (1.1). The half saturating intensity for the on-cone bipolar cell is shifted 1.7 log units to higher intensities than the rod bipolar cell. This is in agreement with the intensity-response relations from mammalian rod and cone photoreceptors, which also show a separation of 1.7 log units (Penn and Hagins, 1972; Baylor et al., 1984; Schneeweis and Schnapf, 1995).

The intensity-response relation of the photovoltage (Figure 4.9D) also contains both a rod and cone component (n=1). While the rod component response is small, it is clearly above the baseline (open symbols). The solid line is the sum of two saturation functions (equation 4.3) with Hill coefficients of 1.1 and 2.28, and half saturating intensities of 0.035 and 2.9 lumens/m^2 (a difference of ~1.9 log units), reflecting the rod and cone components, respectively. These values are very similar to those reported for the photocurrent (see Table 4.2). The magnitude of the rod component was ~30% of the peak response amplitude of the on-cone bipolar cell, both in the photocurrent and the photovoltage.

Current recordings from two different off-cone bipolar cells both exhibit rod and cone components (Figure 4.10A and C). In the off-cone bipolar cell shown in Figure 4.10A, the rod component is only apparent during low intensity light steps (top three traces). The cell shown in Figure 4.10C however, shows rod input during the dim light steps as well as a prominent rod tail following high intensity light steps. The average intensity-response relation for three off-cone bipolar cells (including cell shown in Figure 4.10A) is fit to the sum of two saturation functions (equation 4.3; Figure 4.10B), with Hill coefficients of 1.1, and 1.59, and half saturating intensities of 0.01 and 1.11 for the rod and cone components respectively. The rod and cone components of the intensity-response relation for the off-cone bipolar cell are separated by 2 log units, slightly larger than the 1.7 log unit separation expected for rod and cone input (Schneeweis and Schnapf, 1995). The average magnitude of the rod component is approximately 10% of the peak off-cone bipolar cell response amplitude.

The intensity-response relation of the cell shown in Figure 4.10C is plotted separately (Figure 4.10D) since it had a much larger rod component than the other off bipolar cell. The intensity-response relation is fit to the sum of two saturation functions (equation 4.3) with Hill coefficients of 1 and 2.4, and half saturating intensities of 0.008 lumens/m^2 and 2.48 lumens/m^2 for the rod and cone components respectively. The rod and cone components of the intensity-response relation for the off-cone bipolar cell are separated by 2.5 log units. The magnitude of the rod component in this cell was approximately 44% of the peak response amplitude,considerably larger than the off-cone bipolar cells described in Figure 4.10B.

The half saturating intensities for the rod components in the off cone bipolar cells are lower than those for the on-cone bipolar cells. It is possible that as experimental and dissection techniques were improved, the sensitivity of the rod system also improved. The off-cone bipolar cells reported in this section were recorded from many months later than the rod and on-cone bipolar cells reported in this same section. Therefore, we interpret the decrease in the half-saturating intensity for the rod input in the off-cone bipolar cell recordings as an indication of improved dark-adaptation. This is supported by the finding that intensity response relations of rod bipolar

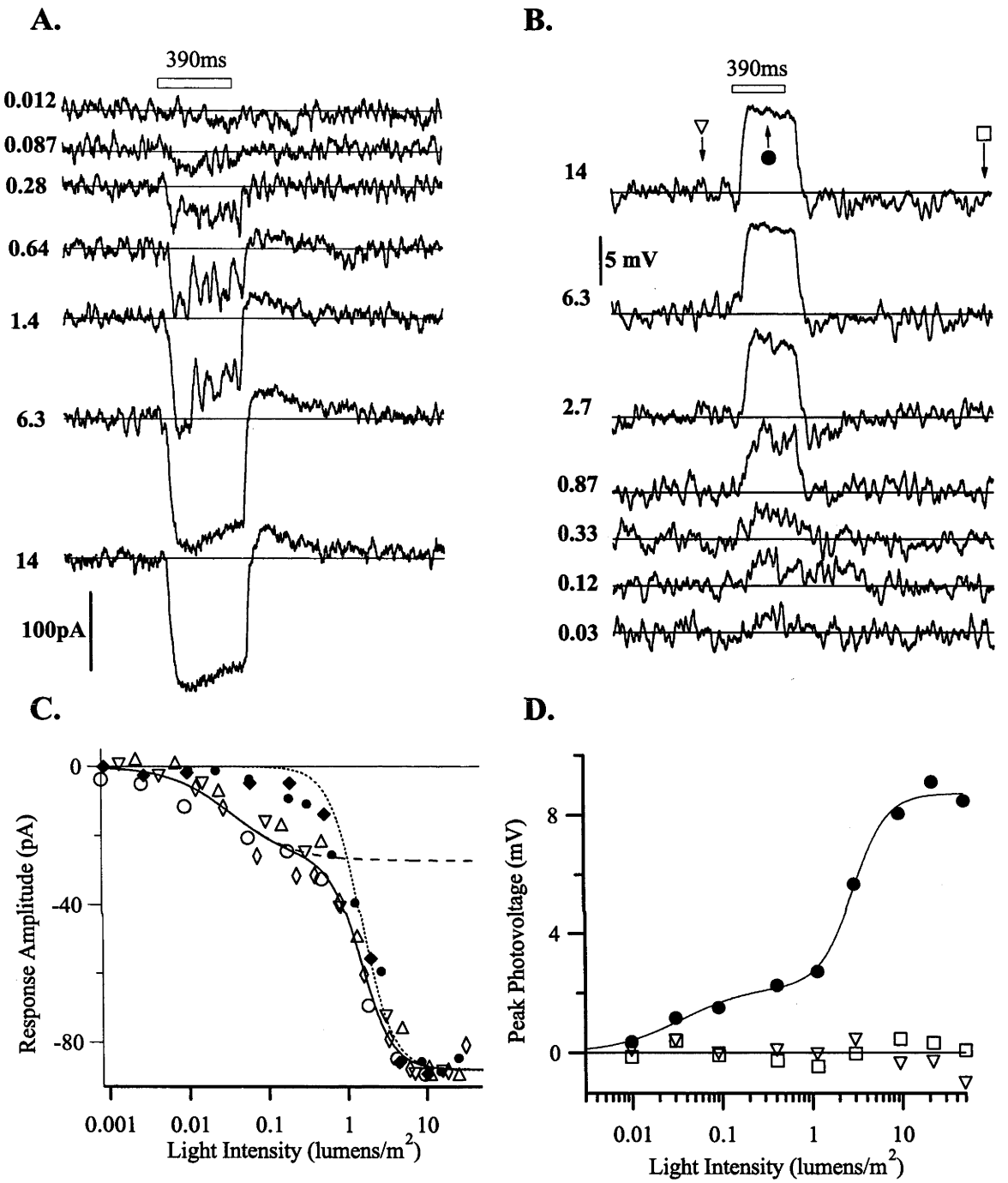

Figure 4.9 Intensity-response relation of on-cone bipolar cells. (A) Current and (B) voltage recordings from two different on-cone bipolar cells to light steps of increasing intensity. Light intensities (lumens/m^2) listed on the left. (C) Normalized intensity-response relation for 5 on-cone bipolar cells (symbols), including cell shown in A (designated by △). Three of the on-cone bipolar cells showed significant rod input (open symbols) and the average intensity-response relation of these three cells was fit by the sum (solid line) of two saturation functions (broken lines; equation 4.3) with a Hill coefficient of 1.1 and a half saturating intensity of 0.035 lumens/m^2 for the rod component (dashed line), and a Hill coefficient of 2.25 and a half saturating intensity of 1.49 lumens/ m^2 for the cone component (dotted line; coefficients summarized in Table 4.2). (D) Intensity-response relation of the photovoltage of the on-cone bipolar cell shown in B. Measurements taken at the time points indicated by the arrows. The solid line is the sum of two saturation functions (equation 4.3) with a Hill coefficient of 1.1 and a half saturating intensity of 0.035 lumens/ m^2 for the rod component, and a Hill coefficient of 2.28, and a half saturating intensity of 2.9 lumens/ m^2 for the cone component.

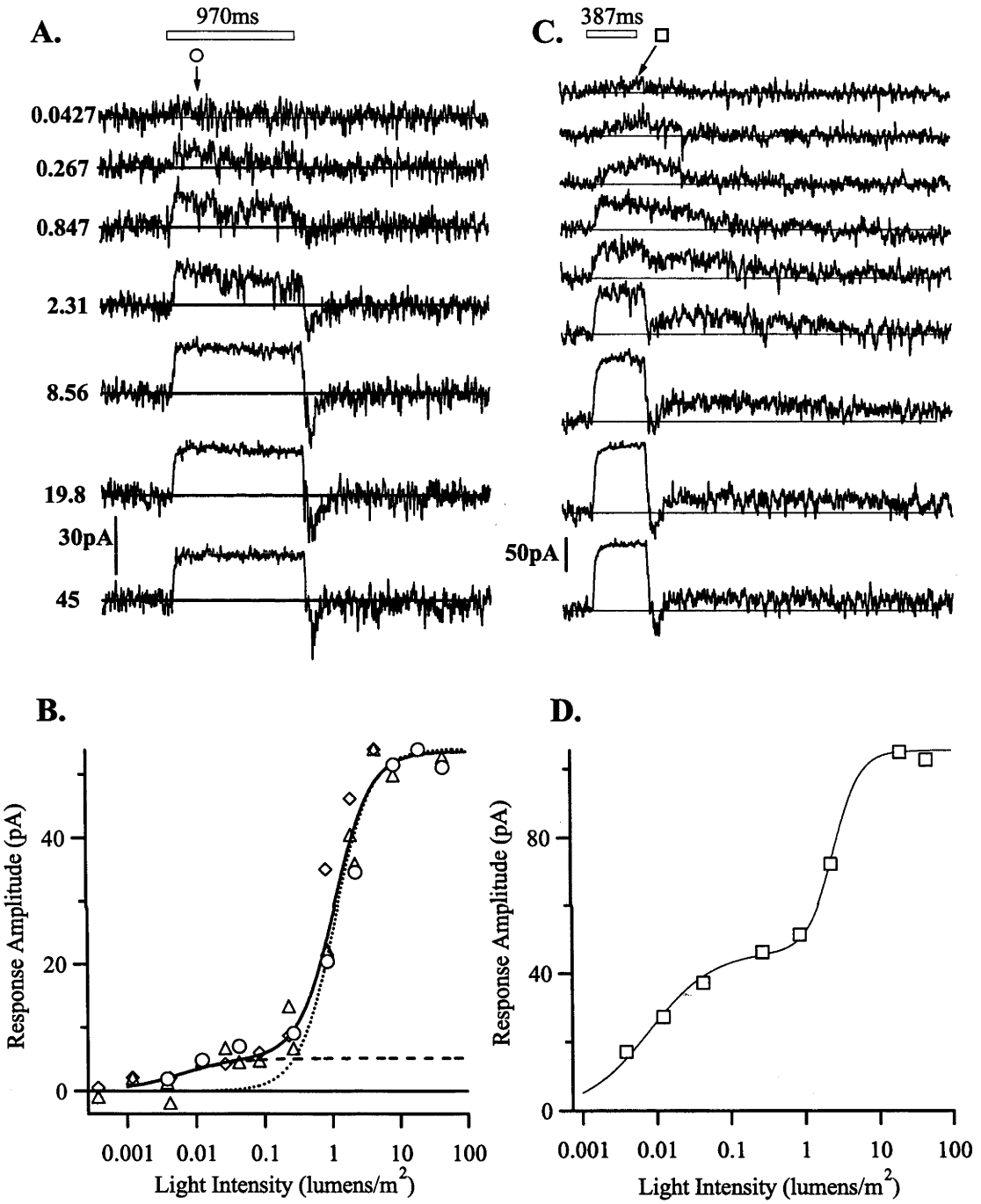

Figure 4.10 Intensity-response relation of off-cone bipolar cells. (A,C) Current recordings from two different off-cone bipolar cells to light steps of increasing intensity. Light intensities (lumens/m^2) listed to left of traces in A. (B) The normalized intensity-response relation for three off-cone bipolar cells (symbols; the cell in A is indicated by ○; The cell shown in C is not included). The intensity-response relation was well-fit by the sum (solid line) of two saturation functions (broken lines; equation 4.3) with a Hill coefficient of 1.1 and a half saturating intensity of 0.01 lumens/m^2 for the rod component (dashed line), and a Hill coefficient of 1.59 and a half saturating intensity of 1.11 lumens/ m^2 for the cone component (dotted line; coefficients summarized in Table 4.2). (D) The intensity-response relation of the cell shown in C had an unusually large rod component, and is plotted separately. The solid line is the sum of two saturation functions (equation 4.3) with Hill coefficient of 1 and a half saturating intensity of 0.008 lumens/ m^2 for the rod component, and a Hill coefficient of 2.4 and a half saturating intensity of 2.48 lumens/ m^2 for the cone component.

cells recorded around the same time (such as those reported in Chapter 5) also had lower half saturating intensities than the rod bipolar cells reported in this chapter.

Noise characteristics of on-bipolar cells

All three classes of bipolar cells showed a characteristic increase and decrease in current variance as the light intensity was stepped from darkness to saturating intensities. In this section, the variance of on-bipolar cells was analyzed in order to obtain estimates of the amplitudes of the underlying events. We have speculated about the sources of noise contributing to the variance.

Analysis of variance has commonly been used to investigate the mechanisms underlying synaptic transmission. From quantitative analysis of the statistical fluctuations in synaptic transmission one can infer key parameters - such as the number of synapses, the unitary event size, and the release probability. Variance analysis, also refered to as quantal analysis, was orignally developed on and applied to synaptic transmission at the neuromuscular junction (del Castillo and Katz, 1954; Miyamoto, 1975; Clamann et al., 1989), but since has been applied widely to central synapses (Bekkers and Stevens, 1990; Malinow and Tsien, 1990).

The simplest form of variance analysis is to assume a uniform probability of presynaptic neurotransmitter release P_r and a uniform postsynaptic event size i across synapses. If it is assumed that most of the fluctuations in the postsynaptic current arise from the stochastic release of synaptic vesicles, the change in variance can be described by a binomial function:

$$\sigma^2 = \sigma_{base} + i(\bar{I}) - \frac{1}{N}(\bar{I})^2 \qquad (N>0) \qquad \textbf{...equation 4.4}$$

where $\bar{I}$ is the mean current (pA), σ_{base} is the baseline variance (pA^2), i is the unitary event size (pA), and N is the total number of synapses. In the present analysis, it is assumed that the unitary event i is invariant for all synapses, and therefore all of the variance is attributed to fluctuations in the release of neurotransmiter.

While most of the variance seen in the present study is attributed to the stochastic nature of transmitter release, some of the variance may be due to the stochastic nature of channel activation. Channel noise would appear as variation in the unitary event size i. Variation in the unitary event size can be allowed for by replacing the term i with $i_{mean}/(1+CV^2)$, where CV_i is the coefficient of variation of the unitary event amplitude, and i_{mean} is a weighted average which emphasizes dendrites with larger postsynaptic amplitudes (Clements and Silver 2000). In central synapses, the term $i_{mean}/(1+CV^2)$ often represents a small correction factor of 5-15% (Clements and Silver, 2000).

Variance analysis applied to on-cone bipolar cells

A change in variance as the light intensity is changed can be seen in the current recordings from the on-cone bipolar cell shown in Figure 4.11A (see also traces in Figure 4.9A). Both the variance and the peak current were normalized. The maximum current for each cell was normalized to the mean value (for this group of cells -80pA) and the variance for each cell was scaled by the same factor. The normalized variance for 4 on-cone bipolar cells was then plotted against the normalized net current (Figure 4.11B) and fit to equation 4.4. This yielded i of -3.3pA, and N of 24.

The variance associated with the mGluR6-gated channel was examined by de la Villa et.al., (1995) via whole-cell recordings in isolated cat on-bipolar cells (which includes rod bipolar cells, and on-cone bipolar cells). Noise analysis was performed by bath applying multiple concentrations of glutamate onto the bipolar cells, and recording the resulting current. The responses saturated at 100uM glutamate. Since the bipolar cells were isolated, synaptic noise was eliminated, leaving channel noise as the main source of variance. Noise analysis yielded an estimate of the single channel conductance of 12.5pS, and a maximum open probability for the mGluR6-gated channels of 96% (de la Villa et al., 1995). A similar estimate of 11pS was reported for on-bipolar cells in the axolotl (Attwell et al., 1987). Since the study by de la Villa et.al. (1995) was performed on mammalian bipolar cells, the value of 12.5pS will be used as the estimate for the single channel conductance of the mGluR6-gated channels in the present study.

Assuming a reversal potential of 0mV, a single-channel chord conductance of 12.5pS would equate to a single channel current at -50mV of -0.6pA. A maximum average response amplitude of -80pA (see Figure 4.11B) would require the activation of a minimum of 128 channels if the probability of channel opening was 100%. This is very close to the 125 channels estimated in cat on-bipolar cells (de la Villa et al., 1995). If the mGluR6-gated channels on mouse bipolar cells were equally distributed among 24 active sites, there would be ~5 channels per site.

We interpret the coefficients in equation 4.4 as describing synaptic noise, as opposed to channel noise since channel noise could only account for 18% of the total variance with the following reasoning. If one assumes that in darkness glutamate release from the photoreceptors saturates the receptors and the open probability of the channels appoaches zero, and in the light the maximum open probability of the channels approaches 100% (de la Villa et al., 1995) when glutamate release from the photoreceptors is completely suppressed, then the maximal channel noise will occur when 50% of the channels are open. In other words the maximal current variance will occur when the mean current, $\bar{I}$, is half of the maximal current. For the four on-cone bipolar cells plotted in Figure 4.11B, the average maximal current was -80pA. Thus, the

magnitude of the channel noise will be at a maximum when the mean current $\bar{I}$ is -40pA. Using equation 4.4, when $\bar{I}$ is -40pA, i is -0.6pA (at -50mV) and N is 128, the maximum variance which could be produced by channel noise is -11.5pA^2, which is only 18% of the maximal variance obtained for on-cone bipolar cells of 64pA^2 (Figure 4.11B). Thus, most of the variance must result from other synaptic sources. If the open probability is very low ($P_o << 1$) even at saturation (i.e. if P_o never reached 50%), then the variance contributed by the channels will increase monotonically while the synaptic noise increases, and then decreases. However under those conditions, the overall variance contributed by channels noise will be lower than if P_o reached 50%.

Variance analysis applied to rod bipolar cells

The rod bipolar cell also displayed a characteristic increase and then decrease in variance as the light intensity was increased (Figure 4.12A). The variance was measured for seven rod bipolar cells and plotted against mean current (Figure 4.12B). The change in conductance (inactivation) which occurs at higher light intensities (see bottom four traces in 4.12B) suggests either that the unitary event size i is non-uniform, or that the number of sites N is non-uniform. Therefore, it was inappropriate to fit a parabola to the change in variance. Instead, a line was fit to the responses at low light intensities before inactivation takes place. This revealed an elementary event size of -3.5pA, very similar to that of the on-cone bipolar cell.

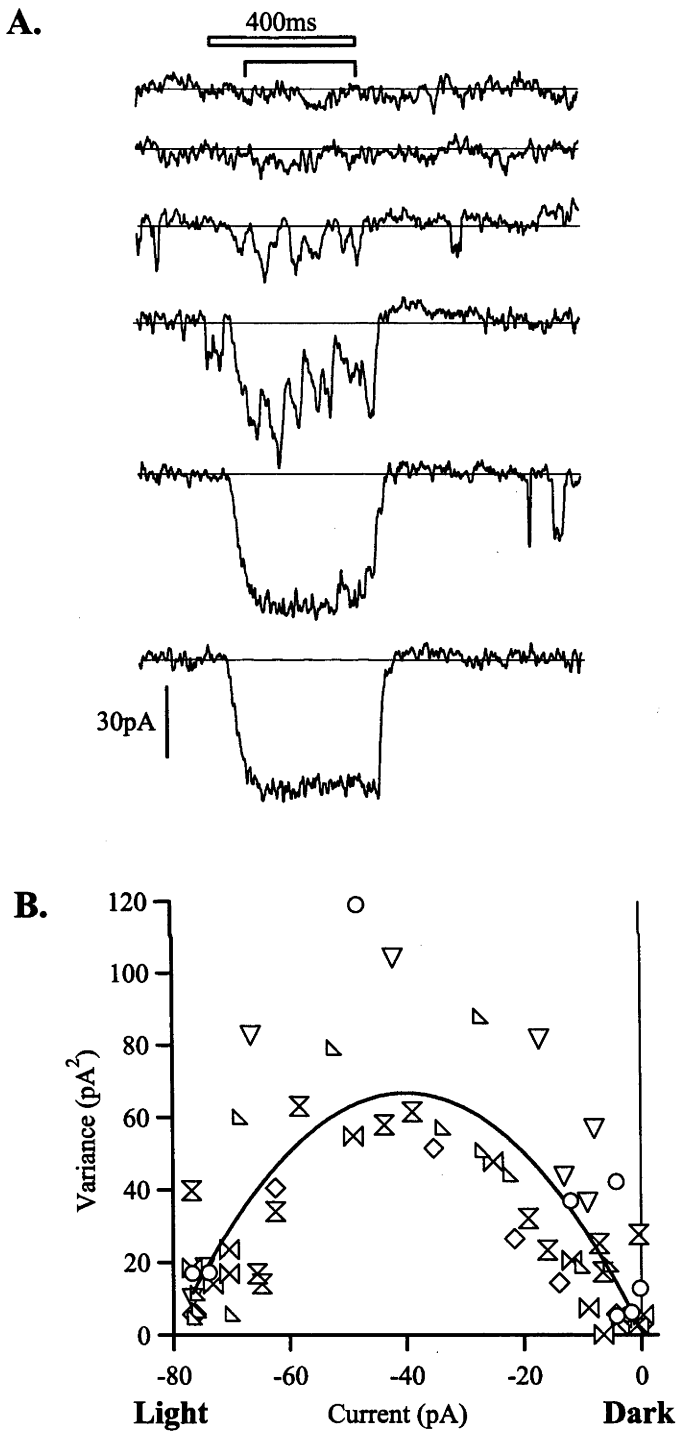

Figure 4.11 Intensity dependence of current variance. (A) Current recordings from an on-cone bipolar cell to light steps of increasing intensity (from top to bottom, in lumens/m^2: 3.86e-3, 0.043, 0.267, 0.847, 8.56, 19.8, 45). The variance was measured over the section indicated by the brackets above the traces. (B) Normalized current-variance relation for 4 on-cone bipolar cells (symbols; cell shown in A indicated by O). The solid line is a parabola (equation 4.4) with coefficients $\sigma_{base} = 1.09\text{pA}^2$, $i = -3.28\text{pA}$, and $N = 24$.

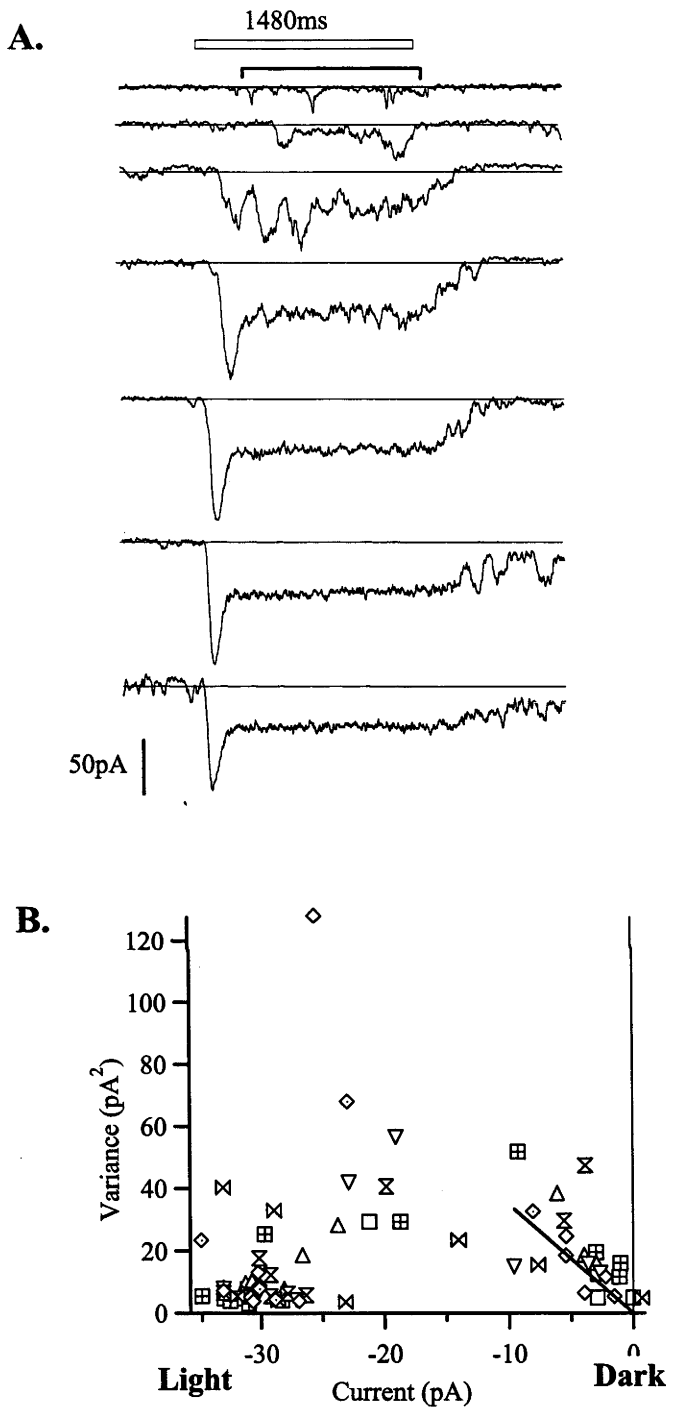

Figure 4.12 Rod bipolar cell current responses display an intensity dependent increase in variance. (A) Current recordings from a rod bipolar cell to light steps of increasing intensity. Light intensities (in lumens/m^2) from top to bottom: 3.86e-5, 0.00043, 0.00267, 0.00847, 0.0856, 0.198, 0.45). The variance was measured over the plateau region of the light response as indicated by brackets above the traces. (B) Normalized current-variance relations for 7 rod bipolar cells (symbols; two current-variance relations were measured for the cell shown in A, and are designated by the symbol O). The solid line is fit in IGOR, with a slope of –3.5pA.

Discussion

Characteristic light responses and kinetics

While morphological subtypes of bipolar cells may have distinct physiological functions, in terms of light response properties, the bipolar cells fell into three main classes: on-cone bipolar, off-cone bipolar, and rod bipolar cells. However, since there are so many subtypes of cone bipolar cells, it was not possible to record from sufficient numbers from each class to exclude functional diversity arising at the first synapse. Indeed, such a result has been suggested for the subtypes of off-cone bipolar cells in the ground squirrel retina, which express different populations of ionotropic glutamate receptors (DeVries, 2000). This has the effect of creating temporal channels in the off-cone bipolar cell pathway (DeVries, 2000).

Instead, functional diversity among cone bipolar cell subtypes may arise at the output stage, i.e. the axon terminal. Since cone bipolar cell subtypes stratify in different layers in the IPL, it is likely they receive input from distinct populations of inhibitory amacrine cells, which are thought to shape the output signals of bipolar cells (Euler and Masland, 2000). Furthermore, the axons of cone bipolar cell subtypes probably reach different postsynaptic ganglion and amacrine cells. In addition to differential connectivity, the subtypes of on- and off-cone bipolar cells have varying repertoires of GABA receptor types. For instance, the responses to the neurotransmitter GABA in some cone bipolar cell subtypes are dominated by $GABA_C$ receptors, whereas in other subtypes $GABA_A$ dominates the response (Euler and Wässle, 1998). Any functional diversity arising from amacrine cell inputs would have been missed in the present experiments due to the lack of light-driven inhibitory input onto bipolar cells.

Similar to recordings made in cat cone bipolar cells (Nelson and Kolb, 1983), cone bipolar cells in the mouse retina (Figure 4.1B, and C) responded to saturating intensities with a sustained response, except in the case of very long light steps, such as the off-cone bipolar cell shown in Figure 4.13A. In that cell the sustained response eventually sagged down to a new current level (τ=700ms), which may reflect adaptation at the first synapse, and may be caused by renewed release of neurotransmitter from the photoreceptors. This is in contrast to a report by (Euler and Masland, 2000) which showed transient, as well as sustained light responses of cone bipolar cells in response to light steps of 400ms. In the present study we found that sub-saturating intensities evoked an initial transient response followed by a sag in some cone bipolar cells, but the responses in all cone bipolar cells became sustained at high enough intensities (i.e. 1.5-2 log units above the cone bipolar cell threshold). Dacey (2000) has shown that cone bipolar cells do indeed have transient and sustained responses depending upon the spatial profile of the stimulus.

By strongly activating the surround region, sustained response of cone bipolar cells could turn into transient responses, presumably due to the activation of inhibitory input. Inhibitory input was largely absent from the present study, which may explain the lack of transient responses.

There were no significant differences between the 10-90% rise times, or the response latencies in the three classes of bipolar cells (summarized in Table 4.1). This was contrary to expectations since kinetic differences between on- and off-bipolar cells in several non-mammalian retina have been reported (Marchiafava and Torre, 1978; Frumkes and Miller, 1979; Ashmore and Falk, 1980; Shiells and Falk, 1994). However, the present results suggest that the signal transduction cascade of the rod- and the on-cone bipolar cells doesn't introduce significant delays to the light response compared to the ionotropic mechanism used by the off bipolar cells.

At least part of the response latency (summarized in Table 4.1) between the onset of the light stimulus and the onset of the light response (~45-50ms for all three bipolar cell classes) can be accounted for by the photoreceptor response kinetics. Direct recordings from photoreceptors were not possible in the present experiments, but in primate retina the time to peak for saturating intensities in the rods is around 35ms, while the time to peak of the cone photoresponse is much faster, ranging from 35ms to 10ms (Schneeweis and Schnapf, 1995). However, it is unlikely that the light intensities used in the present experiments were sufficient to saturate the cones, so the time to peak of the cone photoresponses was probably toward the slower end (i.e. ~35ms). The response latency values reported for the bipolar cells in the present study are close to the estimated response kinetics of the photoreceptors, suggesting that the photoreceptor kinetics in large part determine the response latency of the bipolar cells.

Current-voltage relation

The average current-voltage relation of the light-evoked current reversed at 0mV for all three bipolar cell classes. Since the calculated chloride reversal potential is -67mV, inhibitory input would be expected to shift the reversal potential of the light-evoked current toward negative potentials. A reversal close to 0mV, the calculated reversal potential for a non-specific cation channel, suggests the light evoked currents are almost exclusively glutamatergic. While it is accepted that rod and on-cone bipolar cells both operate through mGluR6, ionotropic glutamate receptors have been localized to on-bipolar cell dendrites in mammals (Morigiwa and Vardi, 1999). Light evoked cation currents passing through ionotropic glutamate receptors would also reverse close to 0mV, but would be opposite in polarity to those gated by mGluR6, and would result in an "off" response. We found no evidence for light-evoked currents through ionotropic glutamate channels in rod or on-conebipolar cells.

The absence of inhibitory input is surprising given that rod and cone bipolar cells have been shown to receive numerous contacts from amacrine cells along their axon terminal systems (McGuire et al., 1984; Chun et al., 1993). Inhibitory synapses from the amacrine cell network are thought to generate the ganglion cell "surround", a fundamental feature of retinal receptive field organization. There are a number of possibilities that might explain an absence of inhibitory input onto bipolar cells. First, since most inhibitory contacts occur on the bipolar cell axon terminals, inadvertently cutting off the axon during the slicing procedure would remove such inputs. This is consistent with results published by Euler and Masland (2000), where the absence of light-driven inhibitory inputs was strongly correlated with the absence of the bipolar cell axon terminal, which in some cells was inadvertantly cut off during slicing. However, all of the cells reported in this chapter were visualized with LY, and all had intact axon terminals. Therefore, this hypothesis fails to explain the lack of inhibitory input onto bipolar cells.

Another possibility is that amacrine cell function is somehow compromised in the slice, or that perhaps they have lost their photoreceptor input. However, numerous amacrine cell recordings were made during the present study and many of them responded to light. In addition, observation of spontaneous inhibitory events on bipolar cells (for instance in the off-bipolar cell shown in Figure 4.4A) suggested that amacrine cell synapses onto bipolar cell axon terminals were still intact and functional. Such spontaneous events were also seen in rod bipolar cells (data not shown), particularly at positive voltages, which was also an observation made by Hartveit (1996). In addition, in some instances it was possible to evoke inhibitory inputs onto bipolar cells with light (Figures 4.4 and 4.5). Thus the amacrine cells made functional synapses onto the bipolar cells, but in large part amacrine cell input was not light driven.

Since amacrine cells are thought to be responsible for the generating the inhibitory surround of ganglion cells, it is conceivable that due to the dark-adapted state of the retina, the sensitivity of the surround mechanism was reduced. In support of this, recordings from ganglion cells in the cat retina have shown that decreases in luminance reduce the influence of the antagonistic surround (Enroth-Cugell and Shapley, 1972; Barlow and Levick, 1976; Raynauld et al., 1979), and in some ganglion cells no evidence was found for an inhibitory surround once the retina was dark-adapted (Barlow and Levick, 1976). Furthermore, if the surround region is normally quite large (on the order of several hundred microns) much of it may be cut away during the slicing procedure. It is interesting that Euler and Masland (2000) routinely found inhibitory input onto rod bipolar cells. It is possible that the experimental conditions were slightly different in their study, and the retina was in a more light-adapted state.

Receptive field size

The receptive field diameter found for rod bipolar cells in the present study (67μm) is about three times larger than the predicted anatomical dendritic spread of rod bipolar cells of 15-20μm (Freed et al., 1987; Euler and Wässle, 1995). A similar result was also found by Dacey et al. (2000) in primate cone bipolar cells. The larger physiological receptive field could be due to signal spread both among photoreceptors and among bipolar cells. In mammalian retina, there is anatomical and physiological evidence for direct rod-cone coupling (Nelson, 1977; Smith et al., 1986; Schneeweis and Schnapf, 1995), and anatomical evidence for cone-cone coupling (Raviola and Gilula, 1973; Tsukamoto et al., 1992), and bipolar-bipolar cell coupling (Kolb, 1979; Dacey et al., 2000). Thus the physiological receptive field of mouse bipolar cells may be larger than the anatomical receptive field due to some lateral signal spread in the photoreceptors and/or the bipolar cells, although it is much smaller than the electrical signal spread reported in non-mammalian retina (Wong-Riley, 1974; Fain, 1975; Detwiler et al., 1980; Saito and Kujiraoka, 1988; Hare and Owen, 1990). Both intraretinal light scatter, and blurring of the light stimulus have been eliminated as possible explanations for in the increased physiological receptive field.

The receptive field sizes measured for the cone bipolar cells in the mouse (37μm for on-cone bipolar cells, and 40μm for off-cone bipolar cells) is similar to the receptive field size (~42um) measured in primate midgit cone bipolar cells at ~10mm eccentricity (Dacey et al., 2000). The diffuse cone bipolar cells measured in primate had receptive field centers of ~92μm at the same eccentricity (Dacey et al., 2000), although such large receptive fields were not seen in mouse. If cone bipolar cells contact all cones within reach, a dendritic spread of 40μm would put cone bipolar cells in the mouse retina in contact with 8-12 cones (calculated from Jeon and Masland, 1995), similar to the number of cone contacted by cone bipolar cells in squirrel (DeVries and Schwartz, 1999).

It is likely that bipolar cells in the mouse retina also have receptive fields organized into an excitatory center, and an inhibitory surround region. However, if the surround region of the bipolar cell receptive field is on the order of several hundred μm's as it is in tiger salamander and primate retina (Hare and Owen, 1990; Dacey et al., 2000), then much it may be cut away during the slicing procedure. Furthermore, our stimulus may not have sufficiently stimulated any remaining surround. Ashmore and Falk (1980) also failed to demonstrate a surround in the receptive field profiles of bipolar cells in dogfish retina, presumably due to the higher sensitivity of rod bipolar cells compared to the horizontal cells which are thought to mediate the surround. A similar result was reported in primate cone bipolar cells, which required a strong annulus over a large region of the retina in order to evoke a surround response (Dacey et al., 2000).

The receptive field size of the cone bipolar cells may limit the visual accuity of the mouse visual system. A receptive field size of 40um will cover ~1.5 degrees of visual angle in the mouse retina (~3mm in diameter). Thus the highest predicted spatial frequency the cone bipolar cells could resolve is ~0.3 cycles per degree. This is consistent with behavioral studies which indicate that the highest frequency that the mouse visual system can resolve is <0.5 cycles/degree. This result also indicates that at least one class of ganglion cells preserves the spatial accuity of the cone bipolar cells.

If the dendritic spread of rod bipolar cells in the mouse retina was 20μm as it is in rat, this would put them in putative contact with 110 rods (calculated from the cell densities published by Jeon et.al., 1998). If rod bipolar cells in the mouse retina have a coverage factor similar to that found in rabbit retina (2.5-3.5 Young and Vaney, 1991), and in cat retina (3.5-4.7 Freed et al., 1987), then they would contact around 37 rods. This is close to the convergence of rods onto rod bipolar cells estimated from electron microscopic studies of 25 rods per rod bipolar cell (E. Strettoi, personal communication). However, the large physiological receptive field size of 67μm suggests rod bipolar cells receive input from around 750 (calculated from the cell densities published by Jeon et.al., 1998) perhaps via gap junctional coupling in the OPL.

Intensity-response relation

In the present study, the intensity-response relation of the rod bipolar cells could be well fit by the Hill equation (equation 4.3). The intensity response relation for mammalian rods photovoltage can also be well-fit with equation 4.3 with a Hill coefficient of 1 (Normann and Werblin, 1974; Schneeweis and Schnapf, 1995), and an operating range of approximately 2 log units under dark-adapted conditions (Schneeweis and Schnapf, 1995). Our results are largely in agreement with results published by Euler and Masland (2000), who also found the intensity-response relation of the rod bipolar cell photovoltage could be well-fit by equation 4.3, although they reported a lower Hill coefficient (Hill=1.07). In the present study, the photovoltage was slightly steeper (Hill coefficient 1.45; Figure 4.8B) than that of the photocurrent (Hill coefficient 1.1; Figure 4.8A), although it is unclear whether the difference is significant. Euler and Masland (2000) did not report intensity-response relations for the photocurrent, so it is unclear whether they would have also found a shallower relation for the photocurrent. This relationship is the opposite to that of the rod photoreceptors, where the intensity-response relation of the photo*current* is steeper than the photovoltage.

These studies are in contrast with a study in dogfish retina where only about half of the fifty eight rod bipolar cells recorded from had intensity-response relations which could be fit by equation

4.3 (Ashmore and Falk, 1980). The other rod bipolar cells exhibited substantial variation in their absolute thresholds, and the intensities sufficient to elicit half-saturating responses. Many rod bipolar cells had shallower intensity-response relations than that predicted from equation 4.3, and it was necessary to introduce a scaling factor. It is unclear what underlies this difference.. Dogfish rod bipolar cells also responded over a much larger range of light intensities (4-5 log units) than the rod bipolar cells in the present study (~2 log units), perhaps reflecting greater convergence onto rod bipolar cells in dogfish retina.

The cone bipolar cell intensity response relations reflected both rod and cone input (Figures 4.9 and 4.10). The rod input could arise via two pathways: Rods feed directly onto cones, which then relay the signal to cone bipolar cells (Kolb, 1977; Nelson, 1977; Smith et al., 1986; Schneeweis and Schnapf, 1995). Alternatively, rod signals also reach the cone bipolar cells through the rod bipolar cell-AII amacrine cell pathway. At this stage it is unclear from which pathway the rod signal in the cone bipolar cell arises. Rod signals arising from either pathway would be expected to evoke an inward current in on-cone bipolar cells, since in the first instance the signal is relayed through the glutamatergic photoreceptor synapse, and in the second instance the signal arises from gap junctions with the depolarizing AII amacrine cell. In the case of the on-cone bipolar cell, it would be difficult to separate the two rod pathways pharmacologically, since blocking transmission through the rod bipolar cell-AII amacrine cell pathway by saturating the rod synapse with the mGluR6 agonist 2-amino-4-phosphonobutyric acid (AP-4), would also pre-empt transmission across the cone synapse since cone bipolar cells also signal through mGluR6. However, since AII amacrine cells express inotropic glutamate receptors (Qin and Pourcho, 1999), direct rod to cone input onto cone bipolar cells could be examined by blocking rod bipolar cell input onto AII amacrine cells via application of ionotropic glutamate receptor antagonists. Furthermore, rod signals arising from the two pathways may have different noise characteristics, which could be used to distinguish between rod pathways.

Direct rod to off-cone bipolar cell input could be also be examined pharmacologically If the rod input onto off-cone bipolar cells arises from the AII pathway, the rod input would disappear both in the presence of AP-4 (which saturates the rod to rod bipolar cell synapse), and in the presence of strychnine (which would block transmission to the off-cone bipolar cell from the AII amacrine cell). Persistence of the rod signal in the off-cone bipolar cell in the presence of one or both of these pharmacological agents would suggest that at least some of the rod signal arises from the presynaptic (rod to cone) pathway. Such a result would be consistent with the off-cone bipolar cell contacting the rods directly, as recently reported in mouse retina (Soucy et al., 1998).

Noise characteristics of on-bipolar cells

It is argued that the dominant noise source in the variance-mean analysis of the on-bipolar cells was synaptic noise because channel noise is not large enough to account for the variance. Therefore, the coefficients obtained for equation 4.4 were interpreted as follows: there are N independent sources of input, the activation of one of these sources results in a response of amplitude *i* in the postsynaptic cell, and that the post-synaptic responses sum linearly. Following these assumptions, the unitary event *i* can be interpreted as the response amplitude of the event which occurs following the activation of a single synapse, and *N* can be interpreted as the total number of synapses.

Following these assumptions, the noise analysis of both the on-cone bipolar cell resulted in an estimates of -3.5pA for the unitary event size (*i*), and an estimate of 24 synapses (*N*). If cone bipolar cells contact ~8-12 cones in mouse like they do in squirrel (DeVries and Schwartz, 1999), this implies that cone bipolar cells make multiple contacts with the same cone. This organization is common in the midget system of the primate retina, where a single midget bipolar cell may contact the same cone 15-20 times (Calkins et al., 1996). While the mouse retina lacks a midget systems, it is possible that some cone bipolar cells do make multiple contacts with the same cone.

While there are multiple noise sources which could contribute to the variance measured in the present study, the dominant noise source is probably vesicular noise. Vesicular noise could create such variance in the following way: in darkness synaptic vesicle exocytosis from the cone pedicle is maximal, and all (or most) of the channels at each bipolar cell synapse will be closed, and the variance will be at a minimum. As the light intensity approaches saturation, release from the photoreceptors will cease and the concentration of glutamate at each synapse will fall to a minimum. Under these conditions, all (or most) of the channels at each synapse will be open, and the variance will again be at a minimum. Thus variance will be at a minimum at the extremes of the bipolar cell operating range, i.e. when the synapses are exposed to maximal glutamate release (and all of the channels at each synapse are closed), and when none of the synapses are exposed to glutamate (and all of the channels at each synapse are open). At intermediate light intensities, the glutamate release from the cone pedicles will occur at a rate such that at any given time the channels at only half of the synapses are open, while the channels at the remaining synapses are closed. At this intensity, the mean response amplitude will be half of the maximum response amplitude, and the variance will also be at a maximum.

Analysis of variance of the rod bipolar cell light response to dim flashes also resulted in a unitary event size of -3.5pA, very similar to the on-cone bipolar cells. An average peak response amplitude of -100pA thus equate to the activation of 28 synapses. This is close to the number of

rod bipolar synapses estimated from anatomical studies of around 25 (Strettoi, personal communication), suggesting that the rod bipolar cells contact each rod only once. In addition to vesicular noise, the rod bipolar cell will also be susceptible to quantal noise due to the stochastic capture of photons by the rod photoreceptors. In the cat retina, at very low light intensities which stimulated only the rod system, "physiological" noise and quantal noise contributed equally to the variability in ganglion cell responses (Levick et al., 1983). Other noise sources may also contribute to the variance of both the on-cone and rod bipolar cells such as channel noise, and noise in the second messenger signal transduction cascade.

Conclusion

The results of the present study establishes the mouse retina as a viable model for retinal physiology. The responses recorded from bipolar cells could be grouped into the three main classes corresponding to rod bipolar cells, on-cone bipolar cells, and off-cone bipolar cells. In the present study, bipolar cells received almost exclusively glutamatergic input from the photoreceptors, with little to no light-driven inhibitory input. In future studies, it will be interesting to manipulate the experimental conditions in attempt to evoke light driven inhibitory input, for instance by recording under slightly more light adapted conditions, and by recording from thicker slices.

Although some functional diversity arises at the first synapse at least in the case of the off-cone bipolar cells (DeVries, 2000), it is likely that further functional diversity among bipolar cells arises at the output end, namely from amacrine cell input onto the axon terminals. It will be interesting in future studies to examine the light-evoked amacrine cell input onto bipolar cells in the IPL to see if such inputs are diverse among bipolar cell subtypes. It may be necessary to record under more light-adapted conditions to stimulate inhibitory circuits onto bipolar cells. Furthermore, it will be interesting in future studies to examine the surround mechanism of bipolar cells originating in the OPL. Such a study may require recording from bipolar cells in whole mount retina, which would leave the horizontal cell network intact.

Lastly, a more detailed analysis of the synaptic noise may be possible by recording from on-bipolar cells using the perforated patch technique. This will prevent the wash out of critical intracellular second messengers, allowing prolonged recording to multiple light intensities. It would also be interesting to apply saturating concentrations of AP-4 to on-bipolar cells in darkness. This would give an indication of whether the glutamate release from the photoreceptors is sufficient to saturate the post synaptic receptors in darkness. Similarly, by bath applying cobalt to completely shut off release from the photoreceptors allowing the mGluR6-

gated channels on the on-bipolar cells to open maximally. These two experiments would reveal whether the bipolar cells are operating over their entire possible range. It may also be possible to examine the noise characteristics of rod bipolar cell responses over a wider range of light intensities by including BAPTA in the recording electrode, thereby preventing inactivation (see Chapter 5).

Chapter 5

Calcium Mediated Inactivation of the Rod Bipolar Cell Light Response

Introduction

Results from the previous chapter show that one fundamental characteristic of the rod bipolar cell is a marked inactivation of the light response following saturating and semi-saturating light intensities. This transient/sustained waveform, i.e. the large transient current followed by a smaller, plateau current, has also been seen in rabbit rod bipolar cells (Dacheux and Raviola, 1986), and appears to be a specific feature of mammalian rod bipolar cell light responses. Interestingly, inactivation was never seen in on-cone bipolar cells, despite the fact that they express the same glutamate receptor (mGluR6) and presumably utilize the same signal transduction cascade. The transient-sustained waveform was also observed to be voltage-dependent, indicating that the origin of the waveform is post-synaptic. A goal of the present study was to examine the mechanism for the inactivation of the rod bipolar cell light response.

One clue as to the cause of the inactivation came from a study by Yamashita and Wässle (1991) who were the first to observe that currents through the mGluR6-gated channels were sensitive to calcium. While recording from dissociated rat bipolar cells, they found that when the mGluR6-gated channels were open for prolonged periods while exposed to a low extracellular calcium concentration, a tonic inward current developed which could no longer be turned off by glutamate. In contrast, high extracellular calcium (25mM) strongly attenuated the inward current, and bath-applied glutamate could once again turn off the current. They concluded that calcium attenuates the mGluR6-gated current, and is required for the normal gating of the channel by glutamate. Recently, two other groups made the observation that a rise in intracellular calcium concentration mediated a reduction in the mGluR6-gated current in on-bipolar cells in non-mammalian retina (Shiells and Falk, 1999; Nawy, 2000).

We were interested to determine whether the inactivation seen in the mouse rod bipolar cell light response was modulated by intracellular calcium. Therefore, we recorded light responses from rod bipolar cells using different intracellular calcium buffers. Similar to the calcium-mediated reduction in response amplitude reported by Shiells and Falk (1999) and Nawy (2000), the inactivation seen in mouse rod bipolar cells can be abolished by 10mM intracellular BAPTA, confirming that it is mediated by a rise in intracellular calcium. The current study extends these results by showing that the calcium-mediated inactivation in mouse rod bipolar cells occurs with a much faster time course than in non-mammalian retina. We have also found evidence for a voltage threshold for the process of inactivation. Lastly, we have measured the rate at which rod bipolar cells recover from calcium-mediated inactivation. As suggested by Shiells and Falk (1999), and Nawy (2000), the calcium-mediated inactivation of the rod bipolar cell light response may provide a mechanism for post-receptoral adaptation.

Methods

Preparation

All manipulations were done in darkness under infrared illumination. Whole cell current recordings were made from 37 rod bipolar cells in the dark-adapted mouse retinal slice preparation. Cells were held at -50mV. Bipolar cells were identified based upon their position in the retina, and their ellipsoid soma shape. Rod bipolar cells were distinguished from on-cone bipolar cells by their sensitivity to light, and by the presence of marked, intensity-dependent inactivation as established in the previous chapter.

Light stimulus

The retina was stimulated exclusively with the green gun of the computer monitor, which has a single peak at 540nm with a half-width of 75nm. All stimuli were ganzfeld. Two basic stimuli were used: Light flashes, and light steps. Flashes consisted of a single frame, lasting less than 1ms at any one point on the screen. Steps were created by presenting multiple frames (frame rate 75Hz; see General Methods).

Solutions

Three different intracellular solutions were used in these experiments. The major difference between the intracellular solutions was the calcium buffer used. One intracellular solution was K-based, and contained no calcium buffer. This will be referred to as the "no calcium buffer" condition. The "control" intracellular solution was cesium based, and contained 1mM EGTA. The third intracellular solution used was identical to the control intracellular solution, with 10mM BAPTA replacing 1mM EGTA. This will be referred to as the "BAPTA" condition. For a detailed list of the contents of the intracellular solutions see Table 2.1 in General Methods.

The extracellular solution used was oxygenated Ames (Sigma), heated to 35°C.

Results

Comparison of rod- and on-cone bipolar cell light responses

One of the first observations made in the course of characterizing the basic bipolar cell light response properties was that rod bipolar cell light responses rapidly inactivated in response to semi-saturating, and saturating intensities. This phenomenon can be seen clearly in Figure 5.1, which shows a characteristic light response from a rod bipolar cell (A) and an on-cone bipolar cell (B) to a saturating light step. In the rod bipolar cell, the light step caused a large inward current followed by rapid inactivation to a smaller, plateau current, whereas the response of the on-cone bipolar cell was sustained. Inactivation of the light response was seen in all rod bipolar cells, which responded to light. No inactivation of the light response was ever observed in on-cone bipolar cells.

Voltage dependence of light response waveform

The inactivation of the rod bipolar cell light response is voltage dependent. An example of this is shown in Figure 5.2A, where a saturating light step elicited a transient inward current (●) at negative potentials, which quickly decayed to a steady plateau current (○). Inactivation became less pronounced as the holding voltage was stepped closer to 0mV, and the inactivation disappeared at positive voltages. Since the rod bipolar cell light response qualitatively looks very much like that of the rod photovoltage (which also displays a prominent transient component followed by a sag in response to high intensities; (Schneeweis and Schnapf, 1995), it would be a natural first guess that the rod bipolar cell waveform reflects that of the presynaptic rods. However, rod bipolar cell response amplitudes saturate at intensities too low to produce such a sag in the rods themselves. Furthermore, the dependence of the rod bipolar cell light response inactivation on post-synaptic voltage indicates that it is a post-synaptic phenomenon.

In order to more closely examine the voltage dependence of the inactivation, the current-voltage relation of the two phases of the light-evoked current were measured: the peak response and the plateau response (Figure 5.2B). The average current-voltage relation for both the rod and on-cone bipolar cells was fit to a line with the following equation:

$$R = G(V_m - V_{rev}) \qquad \textbf{equation 5.1}$$

where R is the response amplitude (pA), G is the conductance (nS), V_m is the membrane voltage (mV), and V_{rev} is the reversal potential (mV). The average peak current-voltage relation from

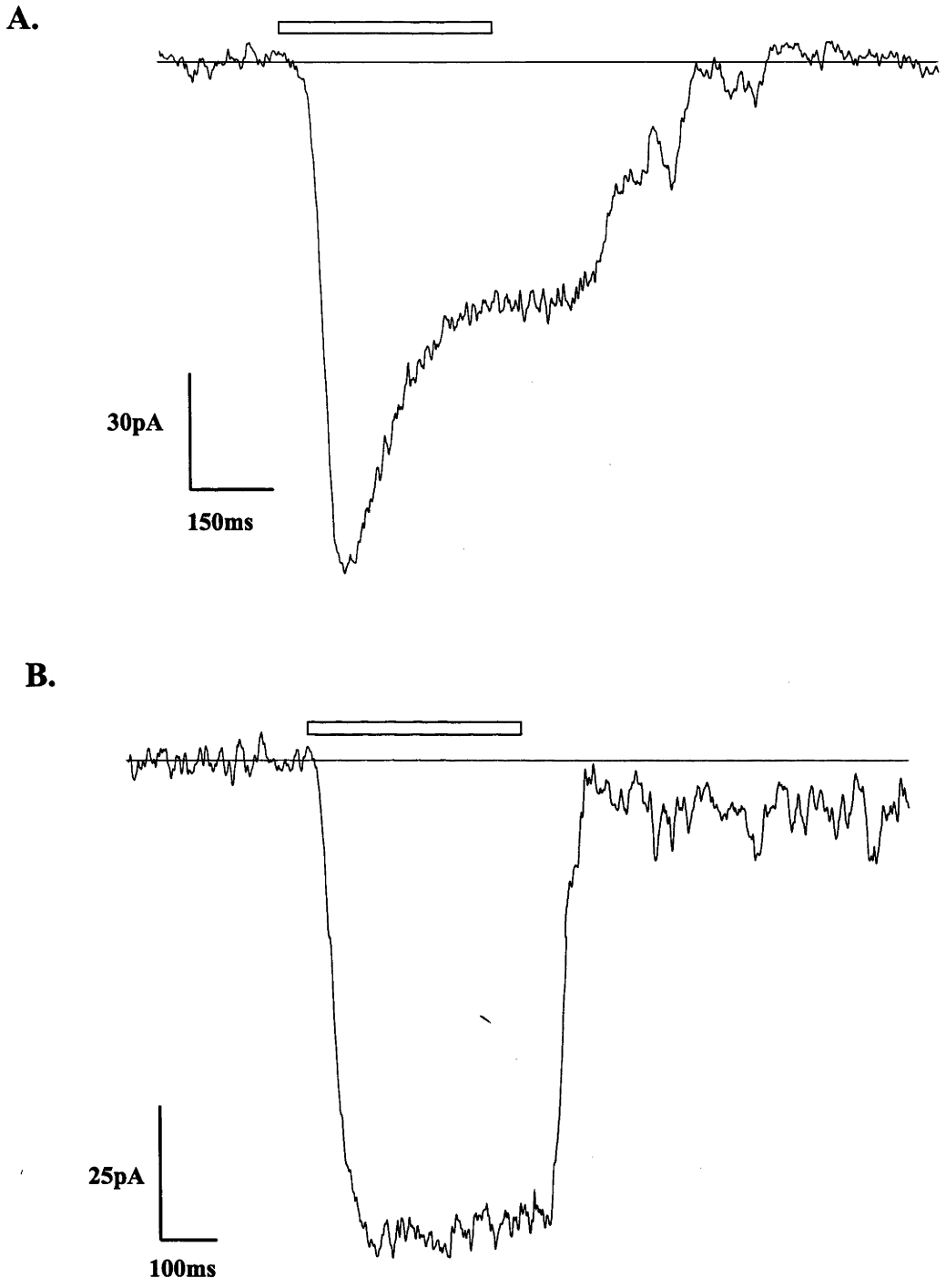

Figure 5.1. The rod bipolar cell light response is characterized by marked inactivation. Whole-cell voltage clamp responses to a 400ms saturating light step from (A) a rod bipolar cell (intensity 0.45 lumens/m^2) and (B) an on-cone bipolar cell (intensity 45 lumens /m^2) reveal this difference in response waveforms. Note the absence of inactivation in the cone bipolar cell light response. Holding potential -50mV. Timing of light stimulus shown by bar above traces.

nine rod bipolar cells is linear, with a reversal potential of +7mV, close to the 0mV reversal potential expected for non-specific cation channels.

The plateau current-voltage relation was non-linear, and was empirically fit to a second-order polynomial with the equation:

$$R = a + bV_m + cV_m^2 \qquad \textbf{equation 5.2}$$

where R is the response amplitude (pA), V_m is the membrane voltage (mV), and a, b, and c are the coefficients. For the average plateau current voltage relation a, b, and c were -5.8pA, 0.82pA/mV and 2.2pA/mV^2, respectively.

Because the plateau current-voltage relation reverses around 0mV, the expected reversal potential for a non-specific cation current, the inactivation of the rod bipolar cell light response cannot be attributed to light-evoked inhibitory input. The reversal potential for chloride in these experiments was around -60mV, thus inhibitory input would be expected to shift the current-voltage relation of the plateau light response to negative values. Therefore, some other mechanism must account for the inactivation of the rod bipolar cell light response.

We wished to determine whether voltage influenced the kinetics of the inactivation, so the inactivation phase of the light response at each voltage was fit to a single exponential function with the equation:

$$R = y_0 + R_{\max} e^{(-t/tau)} \qquad \textbf{equation 5.3}$$

where R is the response amplitude, y_0 is the final steady-state current, R_{max} is the maximal response amplitude in pA, *tau* is the time constant, and t is the time in seconds. The average inactivation time constant at negative voltages was 63 ± 6ms (range 56 to 71ms; Figure 5.2C), and was essentially voltage independent. In other words, whatever process is mediating the inactivation, post-synaptic voltage does not alter the kinetics of this process. The abrupt transition from full inactivation to no inactivation between -20mV and +20mV might be due to a voltage threshold. As noted before, there was no inactivation at positive voltages so no attempt was made to fit those responses with exponential functions.

Next, the voltage dependence of the magnitude of inactivation was examined. The magnitude of the inactivation was quantified by calculating the ratio of the plateau:peak response amplitude at each voltage (Figure 5.2D). This is achieved by dividing the average plateau-response current-voltage relation in Figure 5.2B by the average peak-response current-voltage relation. The average ratio calculated for 9 rod bipolar cells displayed a slight positive trend, rising from 0.37 at -95mV to 0.55 at -20mV (significance $p = 0.0032$ unpaired t-test). Thus the magnitude of the inactivation was slightly voltage dependent, and decreased as the membrane potential was

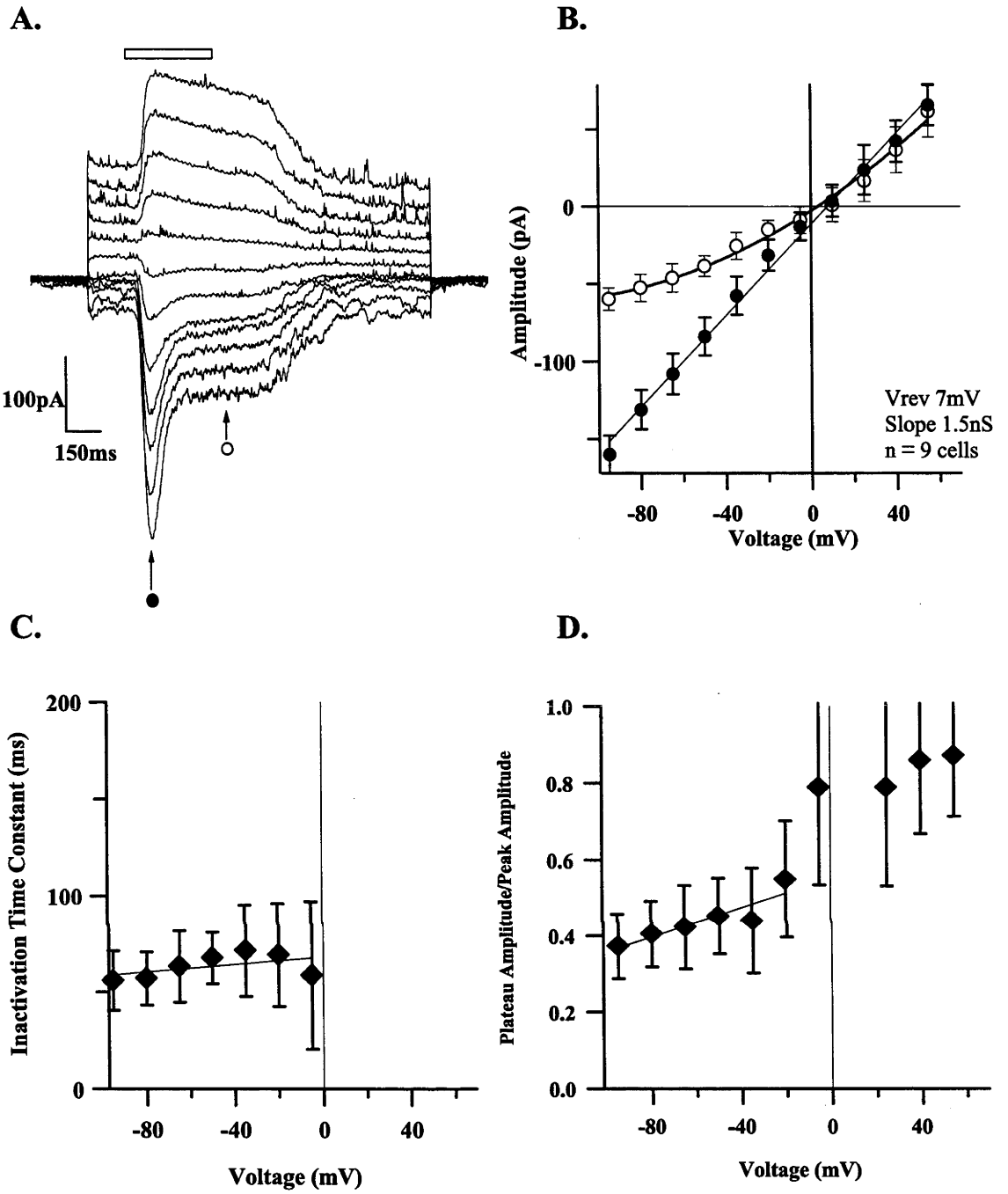

Figure 5.2. The inactivation of the rod bipolar cell light response is voltage dependent. (A) A rod bipolar cell was held at -50mV and stepped from -95 to +70 in 15mV steps. A ganzfeld 400ms light step was flashed onto the retina 200ms after each test voltage. The light intensity used was saturating for the rod bipolar cell (0.38 lumens/m^2). Inactivation is present at negative, but not at positive, potentials. (B) Average peak (●) and plateau (○) current-voltage relation from 9 rod bipolar cells (includes cell shown in A). The peak current-voltage relation was fit to a line by IGOR (equation 5.1) with a slope conductance 1.5nS and V_{rev} +7mV. The plateau current-voltage relation is fit with a second-order polynomial (equation 5.2) with the coefficients *a, b,* and *c* equal to -5.8pA, 0.82pA/mV, and 2.2pA/mV^2, respectively. (C) The average time constant of inactivation is plotted against voltage for 9 rod bipolar cells. The time constant of inactivation averaged across the negative potentials is 63±6ms. Line fit in IGOR; slope: 0.09ms/mV, y-intercept 68ms. (D) Average ratio of plateau:peak response amplitude for the same 9 rod bipolar cells. Line fit in IGOR to data points at negative potentials slope: 1.9, y-intercept: 0.55. On all graphs, error bars show 1 standard deviation.

stepped positive. There was generally some sag in the baseline current at positive potentials, possibly due to voltage dependent conductances (Kaneko and Tachibana, 1985). This may account for the plateau response amplitude being consistently less than the peak response amplitude (as in the top four traces in Figure 5.2A).

Intracellular BAPTA suppresses inactivation

Two recent studies in non-mammalian retina have shown that the mGluR6 response in on-bipolar cells is modulated by calcium (Shiells and Falk, 1999; Nawy, 2000). Therefore, the sensitivity of the inactivation of the rod bipolar cell light response to the fast calcium buffer BAPTA was examined. In most of the cells recorded from, the wash-in of the BAPTA was too rapid to track changes in the response waveform, and the suppression of the inactivation was already maximal following the first light stimulus. But in the rod bipolar cell shown in Figure 5.3A, along with four other rod bipolar cells, it was possible to observe the light response before and after the wash-in of BAPTA. The dark trace (Figure 5.3A) is a light response was recorded immediately upon breaking into the cell, while the light trace was recorded 3 seconds later. Intracellular BAPTA strongly suppressed the inactivation of the light response, demonstrating that the inactivation is mediated by a rise in intracellular calcium. Presumably the time delay between breaking into the cell and the suppression of the inactivation reflects the diffusion of BAPTA into the cell, which is expected to be rapid due to the small size of the cells.

Interestingly in some cells (n=3), in addition to the strong suppression of the inactivation, intracellular BAPTA also resulted in an increase in the peak response amplitude. In the cell shown in Figure 5.3B, the peak response amplitude increased by a factor of 1.7 following break-in. The effect of BAPTA was slower in this cell, with a maximal effect occurring after 38s. It is unclear what underlies the amplitude and temporal difference.

The idea that calcium may be responsible for the inactivation is consistent with the voltage dependence of the light response waveform. For instance, while the time course of inactivation remained constant at negative voltages, the magnitude of the inactivation displayed a slight positive trend (Figure 5.2D), which might be expected from an increased driving force on calcium at more negative potentials. In other words, at more negative potentials there will be a larger calcium influx, and thus the magnitude of the inactivation will also be larger.

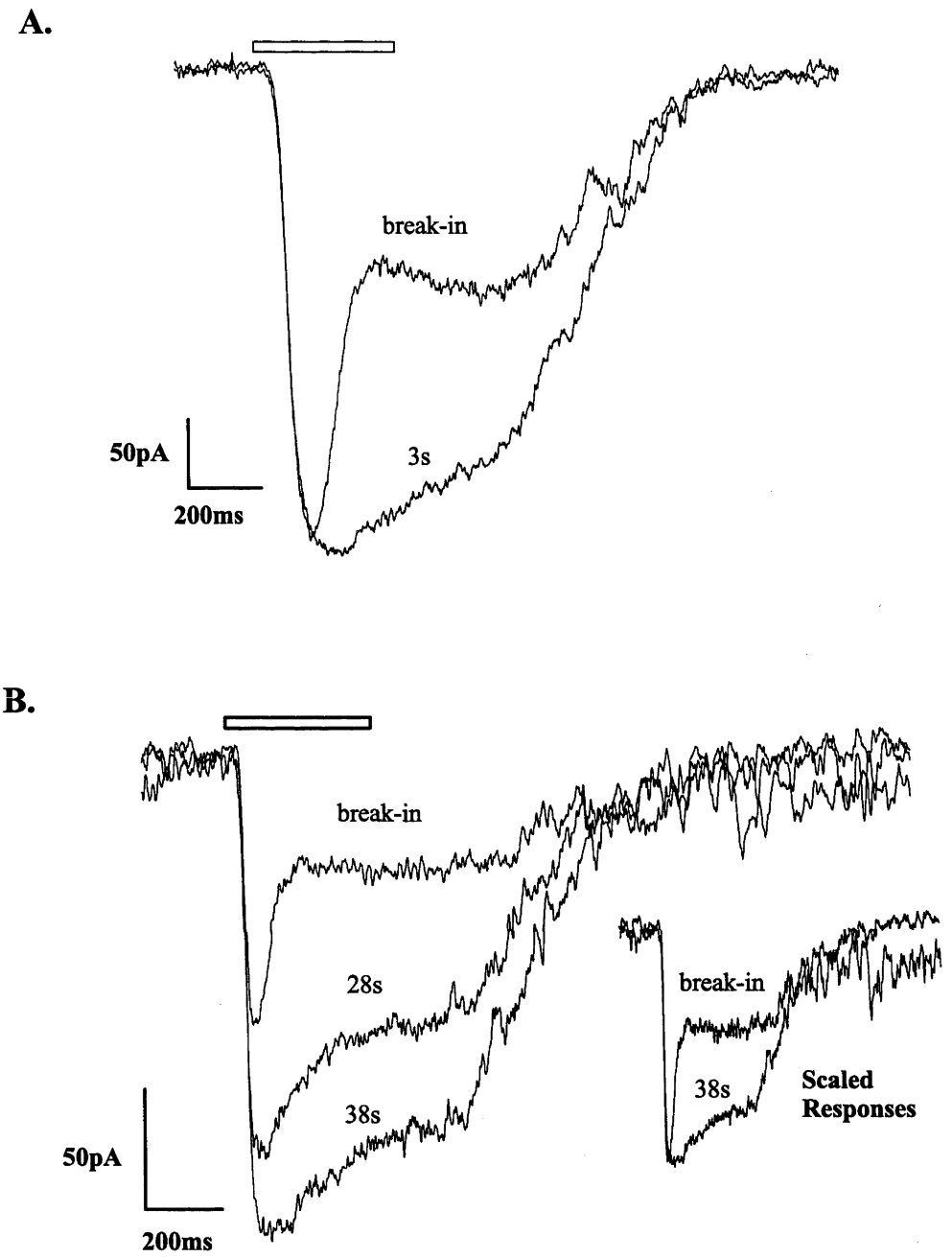

Figure 5.3. Intracellular BAPTA suppresses the inactivation of the light-evoked current. (A) Two recordings from the same rod bipolar cell immediately upon break-in, and three seconds later clearly show the suppression of the inactivation by BAPTA. (B) In some cells, intracellular BAPTA resulted in a pronounced increase in the peak response amplitude, in addition to the suppression of inactivation. Upon break-in, this rod bipolar cell had a peak response amplitude of -105pA, but 38s later the response amplitude was -198pA. There was no change in the baseline current. The inset shows the suppression of inactivation independent of the change in response amplitude. The response recorded upon break-in has been scaled in amplitude by 1.7 in order to compare the response waveforms before and after the effect of BAPTA. Holding voltage -50mV. Light stimulus 400ms saturating light step (intensity 0.38 lumens/m^2).

Intracellular BAPTA eliminated the voltage dependence of light response

If the inactivation of the rod bipolar cell light response is calcium dependent, then intracellular BAPTA should eliminate the voltage dependence of the light response waveform. This can be clearly seen from the current-voltage recordings of a rod bipolar cell with intracellular BAPTA (Figure 5.4A). The current-voltage relations were measured at the same time points as in control conditions (indicated by the symbols under the traces).

There were two obvious changes in the current-voltage relation of the light-evoked current in the presence of BAPTA. The first, and the one that was expected, was the strong suppression of the inactivation of the light response (see traces in Figure 5.4A). This resulted in the average peak (■) and the average plateau (□) current-voltage relation to be almost indistinguishable (Figure 5.4B). The second change was the inward rectification of the light-evoked current. This is even more apparent when the BAPTA current-voltage relation is compared to that of the control condition (dotted lines; replotted from Figure 5.2B).

The inward rectification of the current-voltage relation in the presence of BAPTA is an interesting result. One hypothesis which might explain such a change is that the inactivation of the light response begins during the rising phase of the light response. Thus, calcium might limit the peak response amplitude, particularly at more negative potentials where the driving force on calcium is larger. This would tend to make the peak current-voltage relation more linear. However, the effect of calcium on the peak response amplitude is variable, since sometimes intracellular BAPTA resulted in large increases in the response amplitude, while at other times there was little change (see Figure 5.3).

The time course of the flash response is also voltage dependent

Clearly, calcium-mediated inactivation modulates the response of the rod bipolar cell to light steps in a voltage dependent manner, but the flash response is also shaped by calcium-mediated inactivation. In order to examine the effect of calcium on the flash response time course, flash responses were recorded from a single rod bipolar cell at a series of different voltages (Figure 5.5A). In order to compare the flash response time course at positive and negative voltages, three flash responses (blue traces in 5.5A) at positive voltages were averaged together, inverted, and scaled in amplitude to overlie with the average of three flash responses recorded at negative potentials (dark traces in 5.5A) and are replotted in Figure 5.5B. The response to a 1ms light flash in control conditions is longer at positive potentials (half-width ~100ms) than at negative

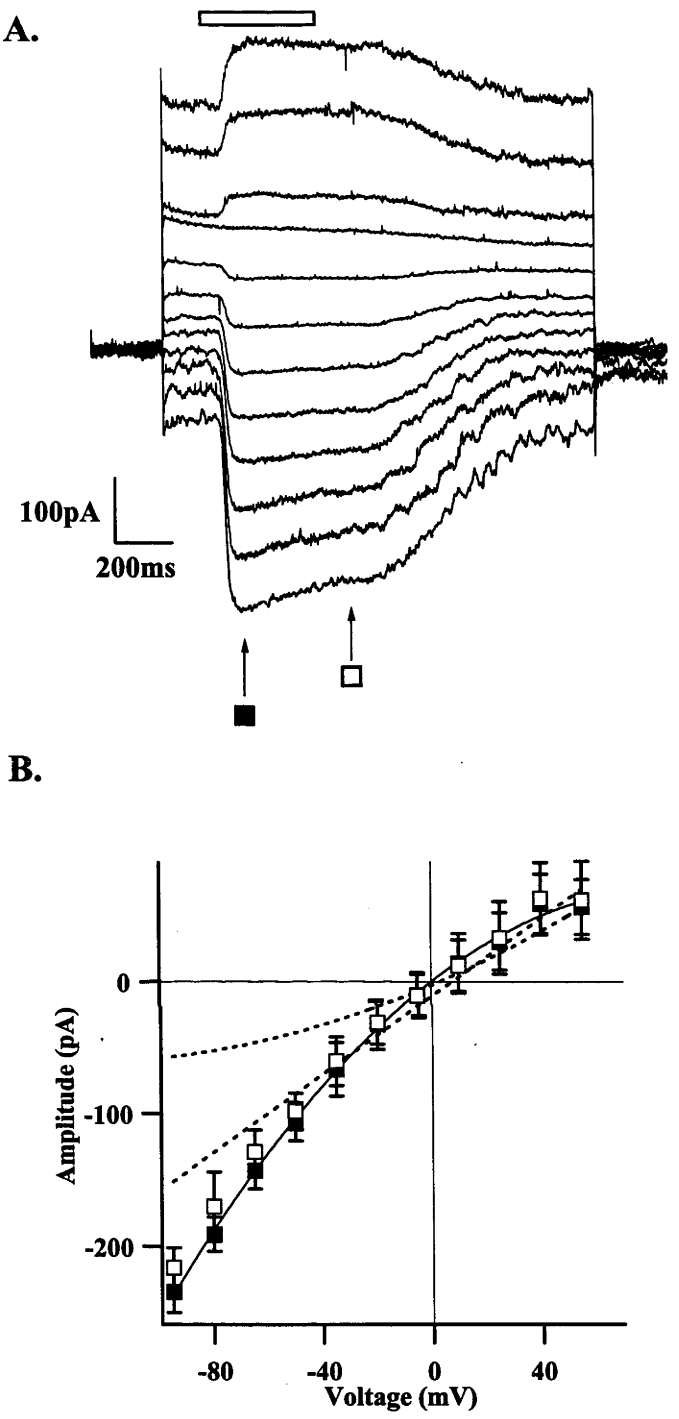

Figure 5.4. Intracellular BAPTA abolishes inactivation of rod bipolar cell light response. (A) Current-voltage relation of light-evoked current of a rod bipolar cell with 10mM intracellular BAPTA. Voltage and light protocols are the same as in Figure 5.2A. (B) The current-voltage relation was quantified in 5 cells by measuring the response amplitude at the same time points as in control conditions (Figure 5.2A. Note that the current-voltage relation in the presence of BAPTA is inwardly rectifying. The average light-evoked current at the peak and plateau time points were fit in IGOR to a second-order polynomial (equation 5.2) with coefficients *a*, *b*, and *c* equal to -0.007pA, 1.6pA/mV and -9.18pA/mV^2, respectively. The control current-voltage relation from Figure 5.2B is plotted for comparison (dotted lines).

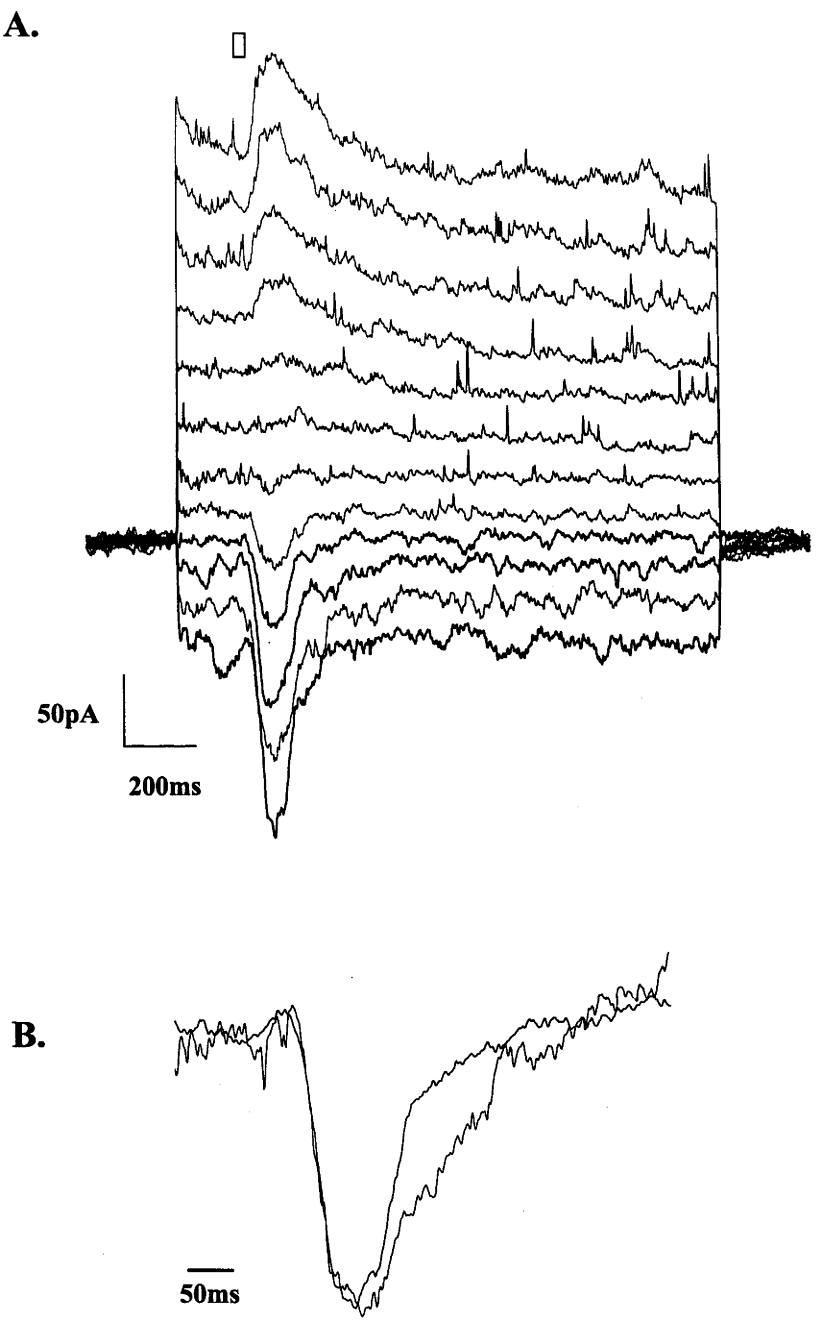

Figure 5.5 The time course of the rod bipolar cell flash response is dependent on post-synaptic voltage. (A) A rod bipolar cell was held at -50mV and stepped from -95 to +70 in 15mV steps. A ganzfeld 1ms light step was flashed onto the retina 200ms after each test voltage. The light intensity used was saturating for the rod bipolar cell (0.38 lumens/m^2). The time course of the flash response is faster at negative potentials than at positive potentials. (B) The black trace shows the average response at negative voltages (average of the three dark traces in A), and the blue trace shows the average response at positive potentials (average of the three blue traces in A). In order to compare their time courses, the average positive-voltage flash response (half width 160ms) is inverted, and scaled in amplitude to overlie with the negative-voltage flash response (half width 100ms).

potentials (half-width ~160ms). Thus the time course of the flash response is voltage-dependent, indicating that calcium-mediated inactivation modulates the flash response kinetics. This result is confirmed by the lengthening of the flash response in the presence of BAPTA (see below).

Intensity dependence of inactivation

In the quest for a possible role for the calcium-mediated inactivation of the light response, we wished to determine if the inactivation affected the response range of rod bipolar cells. In order to test this, we measured the effect of calcium on the intensity-response relation of rod bipolar cells. This was accomplished by using three different intracellular solutions: One which contained no calcium buffer, one which contained 1mM EGTA (control condition), and one which contained 10mM BAPTA (BAPTA condition; a detailed description of the intracellular solutions are listed in Table 2.1 in the General Methods).

Rod bipolar cell intensity response-relations were measured by stimulating the retina with ganzfeld light stimuli from darkness (Figure 5.6). The top panel (A) shows the responses of a rod bipolar cell to 1.5s steps of light of increasing intensity (intracellular solution: no-calcium buffer). The traces shown in Figure 5.6A look very similar to the control recordings in Figure 5.6B (intracellular solution: 1mM EGTA). Note that while the peak response increased in amplitude with increasing intensities, the light response inactivated to the same plateau current level at all intensities. In addition, once the plateau current was established it was maintained for the duration of the light, at least for steps of up to 5 seconds (see inset in Figure 5.6A).

The four lower panels show the responses to light steps and flashes of increasing intensity in control conditions (Figure 5.6B:steps and 5.6D:flashes) and in the presence of 10mM intracellular BAPTA (Figure 5.6C:steps and 5.6E:flashes). BAPTA suppressed the inactivation to steps of light at all intensities (Figure 5.6C). Inactivation of the flash response is also absent in the presence of BAPTA.. The half width of the flash response in control conditions (Figure 5.6D) was 136±25ms (n=6) but was 250±21ms (n=5) in the presence of BAPTA (Figure 5.6E; $p<0.0001$, unpaired t-test). The fact that the decay phase of the flash response is faster in the presence of calcium suggests that calcium plays an active role in turning off the rod bipolar cell light response.

The peak response amplitudes in response to steps and flashes of light of increasing intensity were plotted against light intensity, and fit to the saturation function introduced in Chapter 4 (equation 4.2). Figure 5.7A shows the average peak intensity-response relation to light steps in control, no-calcium buffer, and 10mM BAPTA conditions. The Hill coefficients and the half max values (± 1 standard deviation) are listed for each of the conditions in Table 5.1. The

difference in the Hill coefficient in the step intensity response for control and no-buffer conditions is not statistically significant. Thus the presence or absence of 1mM EGTA has little effect on the operating range of the rod bipolar cells. However in the presence of BAPTA, the step-intensity response relation is steeper (Hill = 1.96) than in control and no-buffer conditions (Hill = 1.1). The steep intensity response relation in the presence of BAPTA suggests that at least one role of calcium is to extend the response range of the cell.

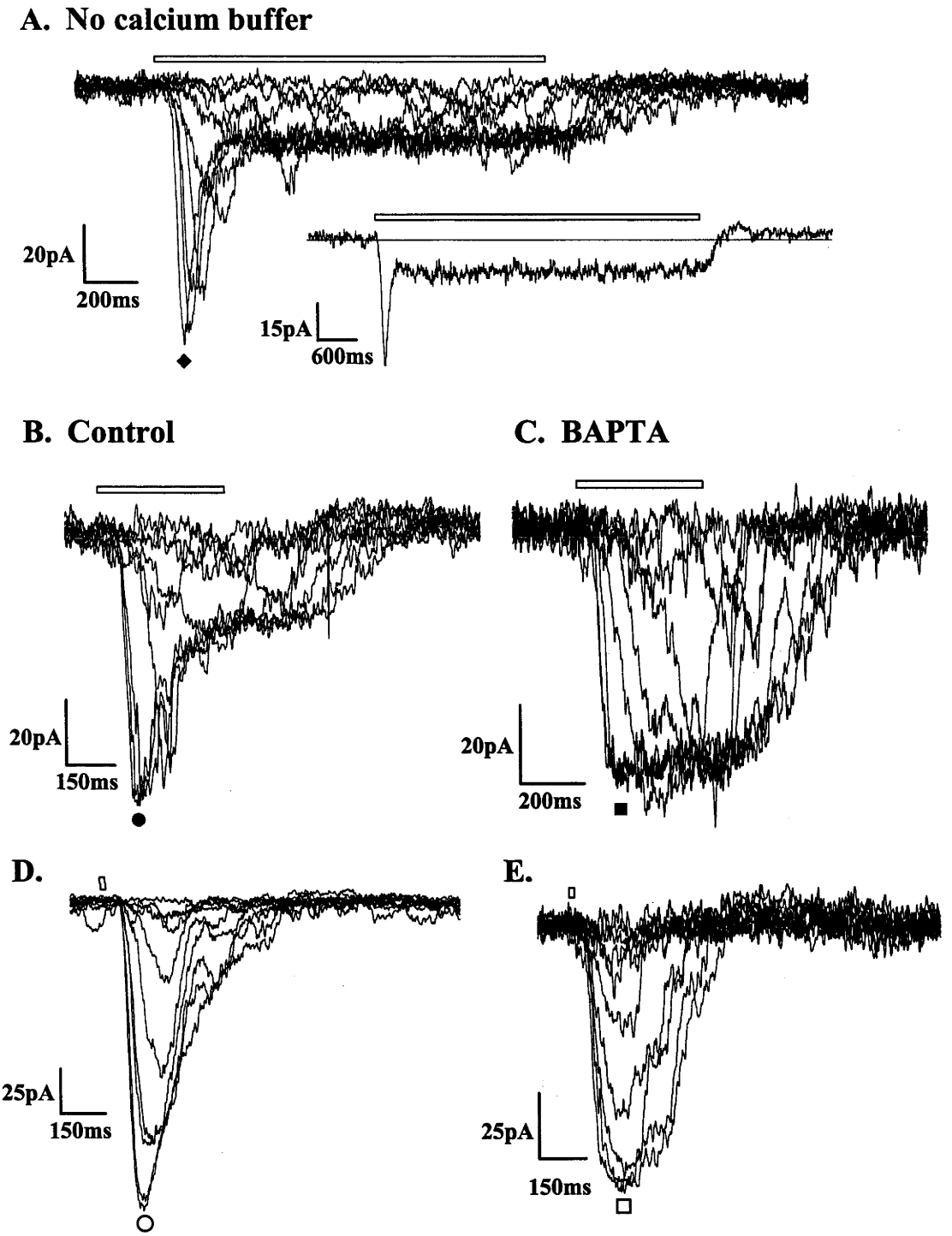

Figure 5.6. Inactivation of the light response disappears in the presence of BAPTA (A) Intensity-response recordings with no-calcium buffer in the intracellular solution. Stimulus duration 1.5 seconds. Inset shows a response from the same rod bipolar cell to a saturating light step (0.086 lumens/m^2) 5s in duration. (B) Responses to 400ms light steps, and (D) 1ms light flashes with the control intracellular solution. (C) Responses to 400ms light steps, and (E) 1ms flashes in the presence of 10mM intracellular BAPTA. Light stimulus timing shown by bars above traces. Light intensities (x10^{-3} lumens/m^2) for (A) and (B): 0.039, 0.12, 0.42, 2.6, 8, 23.9, 86, 198, 450; and for C,D, and E: 0.13, 0.28, 0.74, 2.3, 4, 8, 16, 33, 61, 120, 190, 320. The symbols under the traces are used in Figures 5.7, and 5.8.

A. Step Intensity Response

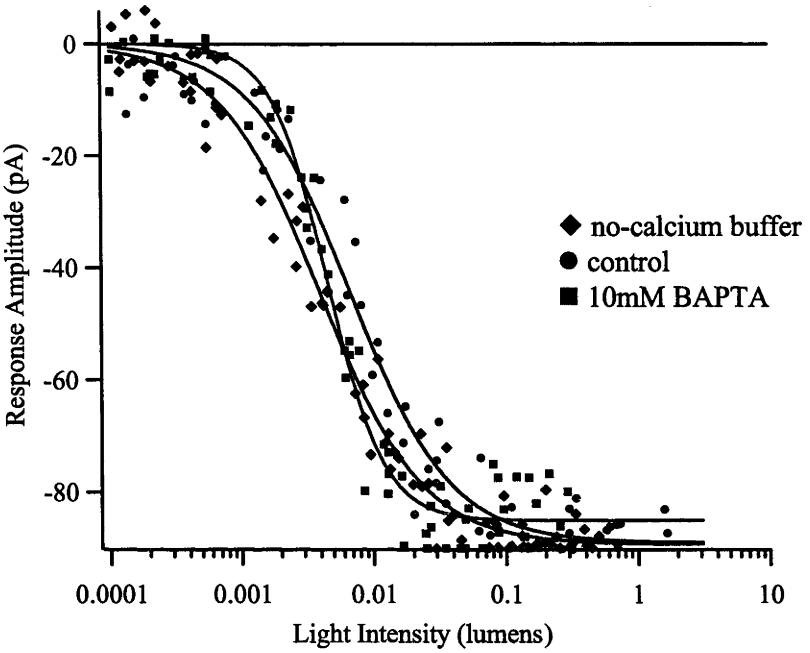

B. Flash Intensity Response

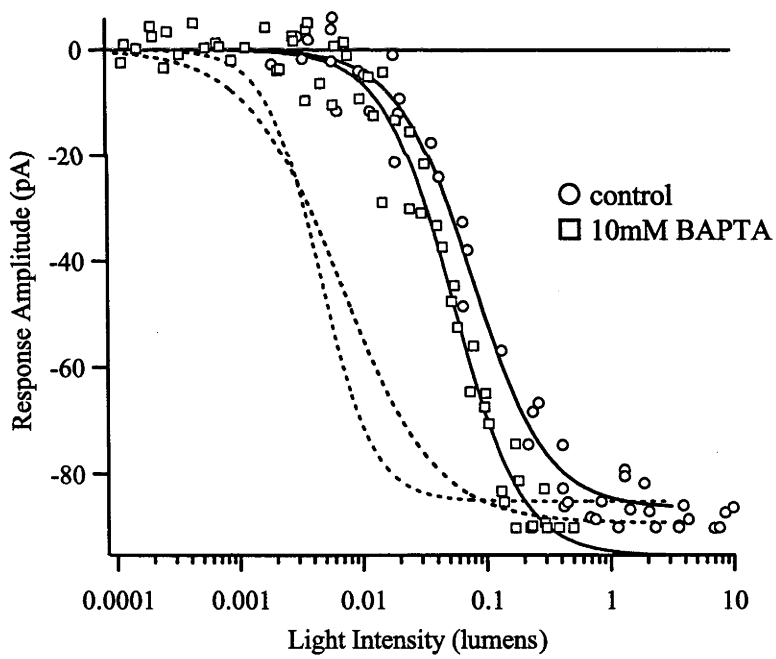

Figure 5.7 (A) Normalized intensity-response relations to light steps of increasing intensity for three conditions: (◆) no-calcium buffer (n=10) , (●) control (n=9) and (■) 10mM BAPTA (n=6). Intensity response relations are fit to saturation functions (solid lines; equation 4.2). (B) Normalized peak response amplitude in response to light flashes plotted as a function of light intensity for two conditions: (O) control (n=7) and (□) 10mM BAPTA (n=6). Solid lines show fits to saturation functions (equation 4.2). The fits from the step intensity response relations for the control and BAPTA conditions shown in (A) are plotted for comparison (dotted lines). Hill and half max values are shown in Table 5.1 in text.

Condition	Hill Coefficient	½ max Intensity (lumens/m^2)
Control Step (n=9)	1.06 ± 0.17	0.004 ± 0.001
Control Flash (n=7)	1.42 ± 0.225	0.08 ± 0.006
No-buffer Step (n=10)	1.1 ± 0.12	0.004 ± 0.0004
BAPTA Step (n=6)	1.96 ± 0.22	0.004 ± 0.0006
BAPTA Flash (n=6)	1.5 ± 0.10	0.053 ± 0.003

Table 5.1. Hill coefficients and half-saturating intensities for the step and flash intensity response relations.

The flash intensity response relations in control and BAPTA conditions are shown in Figure 5.7B (the step intensity-response functions from Figure 5.7A are plotted for comparison). There is no significant difference in the half max and Hill coefficient between the BAPTA and control conditions. However, the intensity required to elicit a half-maximal response is about one log unit lower for the step condition than for the flash condition. This is true for both the control, and the BAPTA conditions. The duration of the light steps (400ms) are on the order of the integration time of rod photoreceptors (~200ms Baylor et al., 1984). Since the step intensity response relations were measured at the peak (and not at a fixed time point), bipolar cells had a longer time to integrate at low intensities. When the intensity response relation was measured at a fixed time point, the flash and step intensity response relations were similar.

Next, we wanted to see how light intensity affected other response parameters, such as the time to peak, and the time course and magnitude of inactivation. The time to peak, defined as the time between the first frame of the light stimulus and the peak of the rod bipolar cell response, decreased with increasing light intensity in response to light steps (Figure 5.8A). In contrast, there was little variation in the time to peak in response to light flashes (Figure 5.8B). This may be explained by increased temporal integration within the photoreceptors during a light step. The photoreceptors will have more opportunities to capture photons during the continued presence of light (i.e. during a light step). This will result in variation in the timing of photon capture, particularly at low intensities when the photon flux is low. This variation in the timing of photon capture is reflected by the larger error bars surrounding the time to peak at low light

intensities (Figure 5.8A). As the light intensities increase, the time to peak of the step response will occur earlier since sufficient photons will be caught within the first few frames to saturate the rod bipolar cell response. In contrast, in the flash condition the capture of photons is time-locked by virtue of the short duration (~1ms) of the light stimulus, thus producing little variation in the time to peak independent of the light intensity (Figure 5.8B). Some of the variation that is present may be due to variability in the time course of the single photon response (Rieke and Baylor, 1998).

While the time to peak did depend on light intensity, there was little to no dependence of the time to peak on the calcium buffer used, in response to both light steps (Figure 5.8A), and flashes (Figure 5.8B). This indicates that calcium does not alter the kinetics of the rising phase of the light response.

The average time course of inactivation was independent of light intensity (Figure 5.8C) suggesting it be limited by the time course of the unitary response. The inactivation time constant was therefore averaged across all five intensities in Figure 5.8C to yield a time constant of 64±7ms (n=6) in the control condition, and 71±5ms (n=9) in the no-calcium buffer condition. This is similar to the time course of inactivation measured at different (negative) voltages (i.e. 63ms; Figure 5.2C). When inactivation occurs, its time course is markedly constant independent of both light intensity and voltage.

The magnitude of the inactivation, as measured by the ratio of the plateau current amplitude to the peak current amplitude, showed a consistent downward trend as a function of light intensity (Figure 5.8D). At the lower intensities, the amplitude of the plateau current was about 50% that of the peak, while at the highest intensities the plateau current amplitude was only about 35% of the peak. However, it is noteworthy that for each cell the light response always inactivated to the same absolute plateau current level, and the decrease in the peak/plateau ratio is due to the peak response becoming relatively larger at higher intensities (see Figure 5.6A).

Recovery from inactivation

Next, the time course of recovery from inactivation was explored by applying two saturating light flashes separated by a variable delay. When the light flashes were separated by 200ms, the response to the second light flash was very much suppressed compared to the response to the first light flash (top trace, Figure 5.9A). In subsequent stimulus trials the flashes were separated by longer delays to reveal the time course of recovery from inactivation. The response to the second flash grew larger as the delay between flashes was increased. The response to the second flash reached a steady state when the light flashes were separated by one second or more.

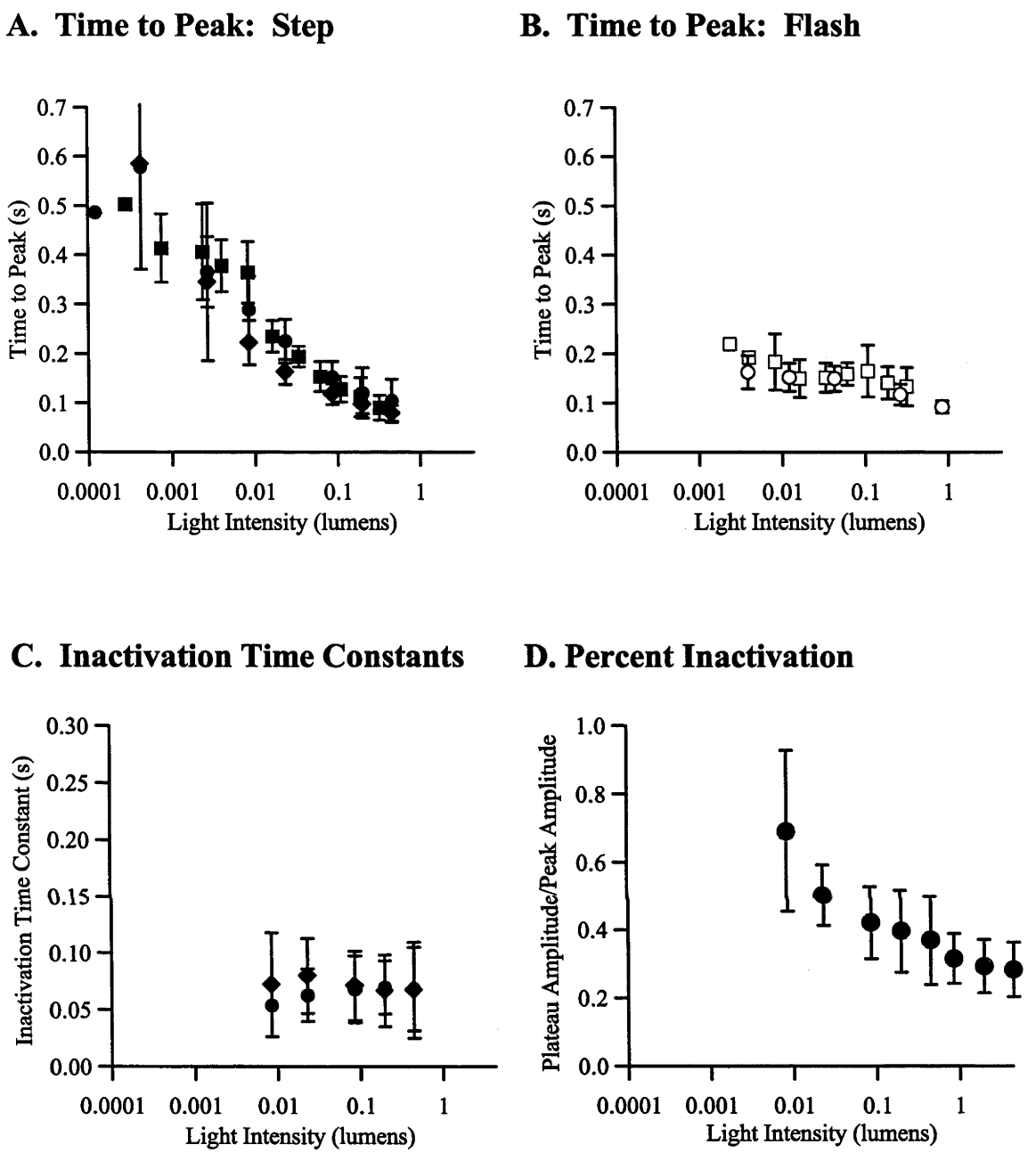

Figure 5.8 The time to peak of the light response and the magnitude of the inactivation are dependent upon light intensity, while the inactivation time course is not. (A) Average time to peak in response to light steps are plotted as a function of light intensity for the control (●), no calcium buffer (◆) and BAPTA (■) conditions (control n=7; no buffer n=8; BAPTA n=5). (B) Average time to peak in response to flashes for control (○) and BAPTA(□)conditions. (C) Average inactivation time constant plotted against light intensity for the control (●)(64 ± 7ms; n=6) and no-calcium buffer (◆) (71±5ms; n=9) conditions. (D) Ratio of plateau:peak response amplitude plotted against light intensity (control and no-calcium buffer data pooled; n=15). Error bars on all graphs show one standard deviation.

The identical experiment was performed in the presence of BAPTA (Figure 5.9B). In the first stimulus trial (200ms delay) the peak current attained in response to the second light flash was very close in amplitude to that of the first flash response. This result demonstrates that the suppression of the second flash response in control conditions is not due to an inability of the photoreceptors to drive the glutamate concentration in the synaptic cleft, but is due to a rise in post-synaptic calcium. The rise in intracellular calcium concentration is suppressed by intracellular BAPTA, allowing the cell to respond to the second flash. Subsequent stimulus trials show that the response amplitude to the second flash in the presence of BAPTA is invariant, independent of the delay between flashes.

Recovery from inactivation was quantified by measuring the response amplitude of the second flash response as a proportion of the first. Figure 5.9C shows the average ratio of second flash response amplitude to first flash amplitude for five control cells, and five BAPTA cells. The time course of recovery of the light response from inactivation was fit to equation 5.3, which yielded a time constant of 240ms.

In both the control and BAPTA conditions, the second flash response was consistently slightly smaller than the first flash response, even when there was a 2 second delay between the first and second flash. This may be explained by some adaptation occurring in the rod photoreceptors to these intensities.

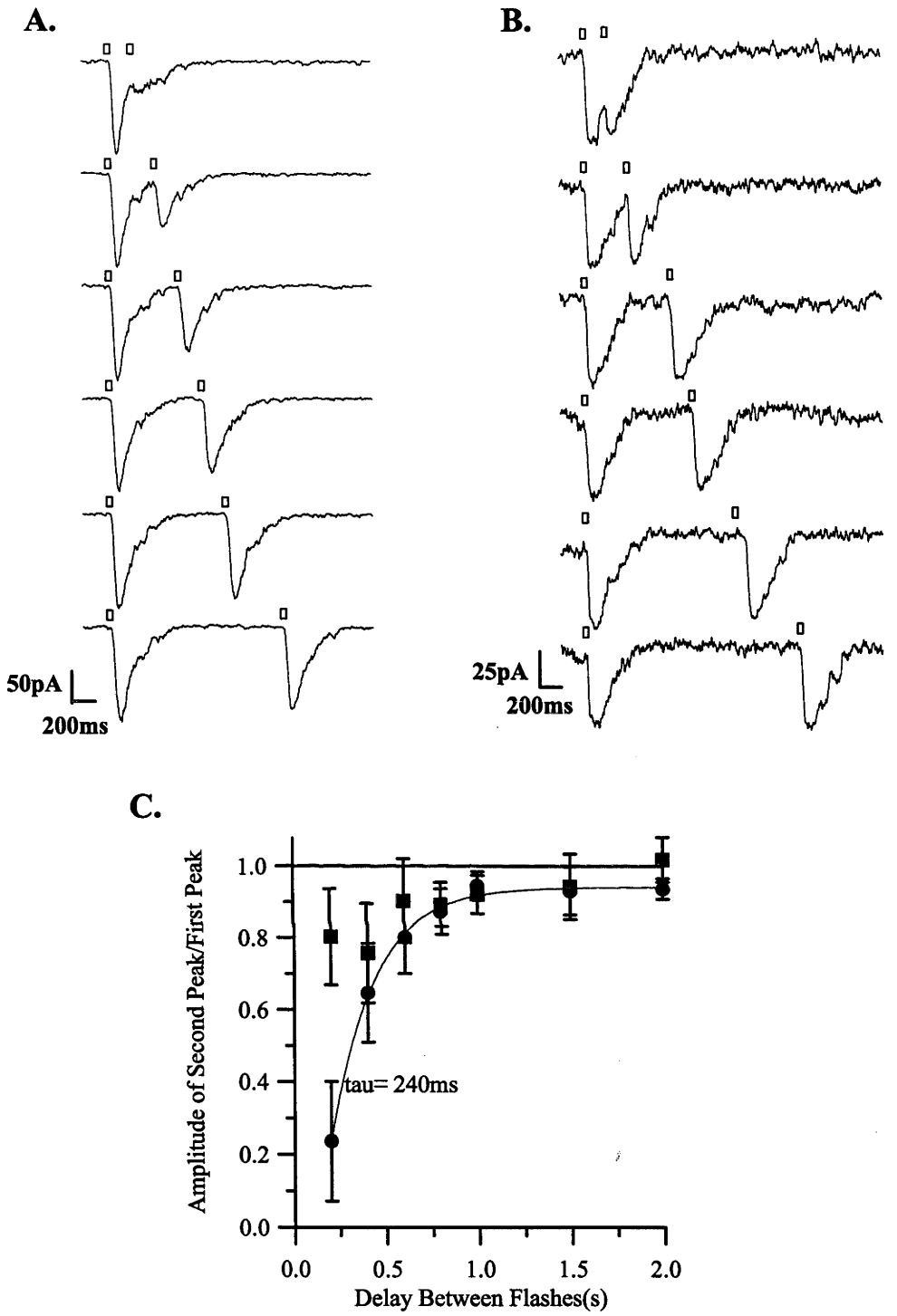

Figure 5.9 Recovery from inactivation follows an exponential time course. (A) Recordings from a rod bipolar cell to a pair of saturating flashes separated by a variable delay. Delay (in ms) between flashes (from top to bottom): 200, 400, 600, 800, 1000, 1500. 2000 (last trace not shown) (B) Recordings from a rod bipolar cell using similar light-stimulus protocol, but with intracellular BAPTA. Delay (in ms) between flashes (from top to bottom): 200, 400, 600, 1000, 1500, 2000 (C) Average ratio of the second flash response amplitude:first response amplitude plotted against the delay between flashes for control (●) (n=3) and BAPTA (■) (n=4) conditions. Solid line through control data points shows the fit to an exponential function with $\tau = 240$ms (equation 5.3). Error bars show one standard deviation.

Discussion

Results from the present study show that a characteristic feature of the rod bipolar cell is a large, transient light response which quickly inactivates to a smaller, plateau response. The origin of this waveform is post-synaptic, since manipulation of the post-synaptic voltage determines whether or not inactivation occurs. Furthermore, the inactivation is blocked by buffering post-synaptic calcium, confirming that it is mediated by a rise in post-synaptic calcium.

The transient-sustained waveform is apparent in both rod bipolar cell voltage- and current-recordings (see Figure 4.7). A similar transient/sustained response waveform is observed in the photovoltages of rods, but not in the photocurrent. The waveform in the photoreceptors has been attributed to the presence of voltage-dependent conductances in the inner segment (Baylor et al., 1971; Bader et al., 1979; Barnes, 1994; Schneeweis and Schnapf, 1995). Thus, while the photovoltage response waveforms look qualitatively similar in the photoreceptors and in the rod bipolar cells, the underlying mechanism producing the waveforms are distinct.

Yamashita and Wässle (1991) first made the observation that the mGluR6 response was sensitive to calcium. Two other groups have recently published results also showing that calcium modulates the mGluR6 response. Shiells and Falk (1999), observed a calcium-mediated desensitization of the on-bipolar cell light response in dogfish, which they suggested might provide a mechanism for light-adaptation in the rod bipolar cell. A subsequent study by Nawy (2000) showed that following the removal of bath applied glutamate (analogous to stimulating the photoreceptors with light), time dependent "run-down" of the response occurred, reducing the glutamate response to around 30% of the maximal response amplitude. This is in close agreement with the results of the present study which show that the plateau phase of the light response is between 30-40% of the peak response amplitude at -50mV (see Figures 5.2D, and 5.8D). The "run down" observed by Nawy (2000) was found to be voltage dependent, an observation also made in the present study, and was strongly attenuated by intracellular BAPTA.

While the calcium-mediated inactivation in mouse rod bipolar cells shares many of the properties of the calcium-mediated inactivation occurring in non-mammalian retina, there is a large discrepancy in the kinetics. The "desensitization", or "run-down" occurring in the bipolar cells of salamander and dogfish was one to two orders of magnitude slower than the inactivation observed in the present experiments, with time constants of 1-6 seconds (Shiells and Falk, 1999; Nawy, 2000). It is possible that calcium mediates a process with two components: one with a time constant ~60ms (see Figure 5.2C) and the other occurring over several seconds. However, the recordings from the non-mammalian bipolar cells showed no evidence for a fast component,

and mouse rod bipolar cells also showed no sign of a "slow" inactivation. Even in response to a five second light step, which is one to five time constants of "slow" inactivation process reported by (Shiells and Falk, 1999; Nawy, 2000), rod bipolar cells in the present study show no indication of a slower inactivation process. Furthermore, the current amplitude following both the "slow" and "fast" inactivation reached the same end-point, i.e. ~30% of the peak amplitude, suggesting both of the processes had reached completion. It seems more likely that calcium mediates two different processes in mammalian and non-mammalian bipolar cells, which have similar effects of reducing the response amplitude. The disparity in the kinetics seems too large to be accounted for by a difference in recording temperature.

Voltage dependence of inactivation

While the inactivation of the light response is mediated by an increase in the calcium concentration, the origin of the voltage dependence of the inactivation (see Figure 5.2) is still a puzzle. A natural first guess might be that the calcium-mediated inactivation occurs at negative voltages due to the electrical driving force on calcium, which would result in substantial calcium influx at negative voltages. However, this cannot entirely account for the inactivation because there is also a steep concentration gradient which would be expected to cause significant calcium influx even at positive potentials, yet inactivation does not occur at positive voltages. Thus, it is likely that calcium is required, but not sufficient, to cause inactivation. Perhaps the voltage dependence arises from voltage-dependent binding of calcium to its target, or by a voltage sensitivity of the channel in the presence of cytoplasmic calcium.

At negative voltages, there is only a weak dependence of the magnitude of inactivation on voltage. At voltages negative to -20mV the plateau response amplitude is consistently about 35-40% of the peak response amplitude (Figure 5.2D). There is a slight downward trend which is consistent with the magnitude of inactivation increasing slightly as the driving force on calcium increases. However, the inactivation disappears (or is unmeasurable) at positive voltages. This suggests that there is some voltage threshold below which inactivation will occur. The exact voltage threshold (or threshold range) for inactivation appears to lie between 0 and -20mV, but the size of the light response was small at these voltages, and it was difficult to resolve the magnitude of inactivation. It may be possible in future experiments to more closely examine the inactivation over this voltage range by including an impermeant cation, such as N-methyl-glucamine or Isethionate, in the recording electrode. This would shift the cation reversal potential more positive, allowing for better observation of the mGluR6-gated current close to 0mV.

Does calcium restrict the peak response amplitude?

One interesting issue to resolve is to determine how quickly the calcium effect takes place. Clearly, inactivation occurs rapidly with a time constant of ~65ms, but does the inactivation occur fast enough to attenuate the peak response amplitude? If it does, then it has to act within the rising phase of the light response, i.e. within ~28ms (the 10-90% rise time of rod bipolar cell light response; see Table 4.1). If the inactivation process beings as soon as the mGluR6-gated channels open, and it takes about 30ms (i.e. half of the inactivation time constant) for the peak response amplitude to be reached, then one would expect calcium to have at least some affect on the peak response amplitude.

If the calcium effect does begin during the rising phase of the light response, such rapid kinetics might suggest a direct effect of calcium on the channel, as suggested by Yamashita and Wässle (1991). However, in some rod bipolar cells, like the one in Figure 5.3A, the wash-in of BAPTA resulted in little change in the peak response amplitude, suggesting that such a restriction of the peak current by calcium is minimal. This observation was made for three other rod bipolar cells. In contrast, there were three instances where the rod bipolar cell peak response amplitude was dramatically increased (in one case almost by a factor of two; see Figure 5.3B) following the wash-in of BAPTA, suggesting that calcium does attenuate the peak response amplitude.

The question of calcium's effect on the peak response amplitude arises in the interpretation of the intensity-response relation. The steeper Hill coefficient in the presence of BAPTA (1.96 compared to 1.06; see Table 5.1, and Figure 5.7A) implies that there is a larger gain across the photoreceptor-bipolar cell synapse when intracellular calcium is buffered by BAPTA. A change in the Hill coefficient could come about in two ways. First, the light responses in the presence of BAPTA could saturate at a lower light intensities. This is consistent with calcium playing a role in limiting the peak response amplitude at high intensities in order to prevent saturation and to extend the cell's operating range. This hypothesis is feasible, given that the intensity-response relation in the presence of BAPTA does seem to saturate at a lower intensity (Figure 5.7A). However, this effect is subtle since some of the data points from the BAPTA intensity-response relation overlap with the data points from the control and no calcium-buffer conditions.

Alternatively, a steeper Hill coefficient could arise from a higher light response threshold in the presence of BAPTA. This also may be possible since the foot of the intensity response relation in the presence of BAPTA is slightly shifted to higher intensities (see Figure 5.7A). Again, the effect is subtle since there is overlap of the data points from the three conditions around threshold. It is possible that calcium affects both ends of the rod bipolar cell operating range, with large rises in intracellular calcium concentration leading to inactivation of the mGluR6-

gated current, and small rises in calcium potentiating currents through the mGluR6-gated channels. This latter role of calcium was suggested by R.Shiells (personal communication) who has recently found that a small increase in intracellular calcium does in fact boost currents through the light-gated channels. This is consistent with the rod bipolar cell threshold response occurring at the lowest intensities when calcium buffers are excluded from the intracellular solution (black symbols, Figure 5.7A). Thus perhaps both BAPTA and EGTA can suppress the potentiation of light responses, while the inactivation can be abolished exclusively by BAPTA.

Lack of inactivation in on-cone bipolar cells

Another interesting observation made in the present experiments is the absence of calcium-mediated inactivation in on-cone bipolar cells (Figure 5.1). Since both the rod- and the on-cone bipolar cells express mGluR6, it would be natural to presume that they utilize the same signal transduction cascade. However, the results of the present experiments suggest either that the rod bipolar cells have an additional, calcium dependent step in the signal transduction cascade, such as the binding of calcium to an intermediate protein, or that cone bipolar cells express different mGluR6-gated channels. The inactivation may be an important feature of the rod bipolar cell which lends the rod pathway specific signaling properties. As was suggested by (Shiells and Falk, 1999; Nawy, 2000), one possible role for the inactivation is post-receptoral adaptation, which is known to occur somewhere in the rod pathway.

Source of calcium

Calcium has been shown to modulate multiple operations in neurons (reviewed in Berridge, 1998) such as short term potentiation and depression, gene transcription and translation, and synaptic integration within dendrites (Guthrie et al., 1991; Eilers et al., 1995; Yuste and Denk, 1995). Calcium which modulates synaptic integration might be expected to be localized to the dendrites. Calcium influx into the dendrites at glutamatergic synapses occurs through multiple pathways, including NMDA and AMPA receptors which will open in the presence of glutamate, and through voltage-gated calcium channels which will open following membrane depolarizations (Bollmann et al., 1998). Cytoplasmic calcium can also increase following synaptic activation due to calcium release from intracellular stores located in the dendrites (Eilers and Konnerth, 1997).

The most likely source of the calcium mediating the inactivation in rod bipolar cells are the mGluR6-gated channels themselves, as they have been shown to be highly permeable to calcium (Nawy, 2000). There are other sources of calcium in the rod bipolar cells, such as voltage-gated

calcium channels (Kaneko et al., 1989; de la Villa et al., 1998; Pan, 2000), and the endoplasmic reticulum (ER). Voltage-gated calcium channels may be excluded as a potential source of calcium for the inactivation for two reasons: (i) there would be little calcium influx through voltage-gated calcium channels while the rod bipolar cell is held at or negative to -50mV as in the present experiments, and (ii), calcium influx through voltage-gated channels cannot explain the dependence of the inactivation on light intensity (in a voltage-clamped cell). Furthermore, Nawy (2000) confirmed that the calcium mediated run-down cannot be explained by calcium influx through L-type channels since the run-down was not blocked by the L-type channel blocker Nifedipine.

Intracellular calcium stores have recently been shown to play an important role in calcium signaling in neurons (reviewed in Berridge, 1998; Mattson et al., 2000). Intracellular calcium stores have been shown to influence calcium dynamics in the dendrites of other neurons (Majewska et al., 2000), so it is possible that they contribute to the inactivation of the rod bipolar cell light response. However, calcium release from intracellular stores is usually mediated either by IP_3 receptors, or by ryanodine receptors (reviewed in Petersen and Cancela, 1999). Group III mGluRs (like mGluR6) are not known to operate through IP_3 making this pathway an unlikely possibility. In addition, preliminary results from the present study fail to find an effect on the shape or time course of the inactivation following application of caffeine (data not shown), which both blocks IP_3 mediated calcium release, and stimulates ryanodine receptor mediated calcium release (Ehrlich et al., 1994). While we cannot rule out a role for calcium-mediated calcium release from intracellular stores, an original source of calcium is still required to evoke release in the first place. Thus, it is most parsimonious to conclude that the calcium evoking inactivation enters through the mGluR6-gated channels when they open in response to light.

Molecular mechanisms of inactivation

The model we propose is as follows: In darkness, glutamate binds to the mGluR6 receptor which keeps the channels closed. In the light, glutamate unbinds from the mGluR6 and the channels open. The calcium entering through the mGluR6-gated channels, binds to a target protein and inactivates the channels, thereby reducing the light evoked conductance (Figure 5.10).

At this stage, it is unclear what the molecular mechanism is for calcium-mediated inactivation. The current through any channel can be described by the following equation:

$$I = NiP_o \qquad \textbf{equation 5.4}$$

where I is the current amplitude, N equals the number of channels, i is the single channel current, and P_o is the open probability of the channel. A change in any of these variables could account

for the inactivation seen in the rod bipolar cell light response. For instance after channel opening, calcium could directly block or bind to the channel (or to a calcium binding protein which then blocks/binds to the channel) to prevent the channel from re-opening after it has closed. This would effectively reduce the number of channels (N) available for activation. Alternatively, the calcium could reduce the single channel conductance (g) by only partially blocking the channel, or by causing a conformational change in the channel. Or the calcium could reduce the mean-open time of the channels (P_o) perhaps by stabilizing the closed state of the channel (or by destabilizing the open state). Additional experiments, such as single channel recordings or whole-cell noise analysis, will be necessary to determine which parameters are altered in the presence of calcium.

Two studies suggest that the phosphorylation of either a target protein, or the mGluR6-gated channel itself, is required for the calcium mediated modulation of the mGluR6-gated current. A study by (Walters et al., 1998) revealed that the current through the mGluR6-gated channels in tiger salamander bipolar cells is suppressed when the activity of a type II calcium/calmodulin-dependent kinase (CaMKII) is blocked. According to Walters et. al., (1998), calcium binds to calmodulin, and the calcium/calmodulin complex activates CaMKII, which then potentiates the current though the mGluR6-gated channel (by phosphorylating an unknown target). However, the opposite finding was made in dogfish on-bipolar cells where desensitization was prevented by inhibiting CaMKII (i.e. the activation of CaMKII induces desensitization, rather than potentiating the current)(Shiells and Falk, 2000). It is possible that experimental conditions underlie this difference, since the experiments by Walters et.al, (1998) were performed under light adapted conditions, where as the study in Dogfish was under dark-adapted conditions.

Another possible target for calcium is protein kinase C (PKC) which is highly expressed in rod bipolar cells. Shiells and Falk (1999) have found that inhibiting PKC (and thereby preventing the phosphorylation of an unidentified target) prevented the desensitization of the light response in dogfish on-bipolar cells (Shiells and Falk, 1999). In other words, inhibiting PKC had an effect similar to including BAPTA in the recording electrode. Thus perhaps there are two targets for calcium, PKC and CamKII, each which initiate separate signalling pathways. For instance, under dark adapted conditions low concentations of calcium might activate the "PKC pathway" which ultimately protects the rod bipolar cell from inactivation. In contrast, at higher light intensities calcium influx through the mGluR6-gated channels activate the "CamKII pathway" causing inactivation. Further experiments will be required to fully elucidate the molecular mechanism of the inactivation.

Model of dendritic calcium accumulation

Similar to the findings of Shiells and Falk (1999) and Nawy (2000), the inactivation of the rod bipolar cell light response was abolished by BAPTA, but not by EGTA. While direct comparison of the BAPTA and EGTA data in the present experiments may be confounded by a concentration difference (10mM intracellular BAPTA was used, versus only 1mM EGTA), in the study by Nawy (2000), both calcium buffers were used at 10mM with similar results. The effects of different intracellular calcium buffers may reveal clues about the calcium dynamics required to control inactivation. While BAPTA and EGTA buffer calcium to the same level at large distances from the source (>400nm) the rapid binding kinetics of BAPTA (on-rate 160 times faster than EGTA, Naraghi and Neher, 1997) allow it to significantly buffer calcium as close as 30nm from the source. In contrast, EGTA produces only small, linear calcium gradients between 100-400nm (Naraghi and Neher, 1997). The suppression of the inactivation by BAPTA, but not by EGTA, suggests that the inactivation may be due to rapid localized calcium accumulation, as opposed to changes in global calcium concentration. Such a rise in intracellular calcium may occur at the mouth of the open mGluR6-linked channels. If the channels are localized to the dendritic spines, very close to the mGluR6 receptors (Vardi et al., 2000), the rapid change in calcium concentration could be too fast for EGTA to buffer (Borst and Sakmann, 1996).

How would inactivation affect signaling in the rod pathway?

Like in other neurons, each dendritic spine in the rod bipolar cell may act as an individual calcium compartment (Guthrie et al., 1991; Muller and Connor, 1991; Yuste and Denk, 1995). In this model, each dendritic spine invaginating a rod spherule will act as its own processing unit, such that activity occurring in one dendritic spine will be independent from activity occurring in other dendritic spines. In this model, in darkness each individual rod will be releasing glutamate at a high rate onto each individual rod bipolar cell dendritic spine, and the channels on each of these spines will be closed. When a photon is caught by a rod, it will pause glutamate release, and the dendritic spine postsynaptic to the rod will be activated, i.e. the channels will open. The subsequent inward current will depolarize the rod bipolar cell, resulting in a single photon response. The influx of calcium through the mGluR6-gated channels will result in a rapid increase in calcium concentration in that spine. If a high concentration of calcium is necessary to cause inactivation, the localized increase in calcium might be sufficient to inactivate that spine, but will not affect neighboring spines. Thus, a photon caught by the same rod photoreceptor within one or two recovery time constants (τ = 240ms; see Figure 5.9) will evoke a smaller response in the rod bipolar cell, because the dendritic spine invaginating that rod photoreceptor will still be in the inactivated state. However, photons caught by other rod photoreceptors will

evoke a normal response since the dendritic spines postsynaptic to those rods are still in the naïve, un-inactivated state.

At intermediate light levels, the rods may capture more than one photon before the rod bipolar cell dendrite completely recovers from inactivation. In this situation, the rod bipolar cell dendritic spines will be cycling between the naïve and the inactivated state. Therefore, a single photon caught in the presynaptic rod will evoke a large response sometimes, and other times it will evoke a suppressed response depending on the time since that dendrite was last activated. As the light levels become progressively higher, more and more of the rod bipolar cell dendritic spines will be in the inactivated state, and will contribute only small (~30-40% of the normal amplitude, see Figure 5.8D) postsynaptic currents when a photon is caught by the presynaptic rod.

The light intensities required to produce inactivation in the rod bipolar cell are in line with what is expected from the rod system (Rao-Mirotznik et al., 1995). Since the recovery from inactivation has a time constant of 240ms, after 3 time constants (720ms) the rod bipolar cell response will be about 90% of the maximal response. Thus single photon responses will be of maximal amplitude in the rod bipolar cell when each rod captures a photon only once every 720ms, or 1.39 photons/rod/ s. Since rod bipolar cells collect from approximately 25 rods, this translates into 35 single photon events per rod bipolar cell per second (1.39 photons/rod/s times 25 rods). This is around the same light intensity that caused desensitization in dogfish on-bipolar cells, i.e.1 photon/rod bipolar cell per second (Shiells and Falk, 1999). Since photon capture is a Poisson process, at this light level some rods will capture two photons, and some will capture zero. Therefore, this light intensity may represents the boundary of the 'binary signaling region' of the rod system hypothesized by Rao-Mirotznik et al., (1995). Below this light intensity, the rods may act as photon counters, signaling one photon or none (Rao-Mirotznik et al., 1995).

Recovery from inactivation

At this stage, it is unclear what is limiting the kinetics of recovery from inactivation. The measured recovery time course may reflect, in part, the calcium dynamics in the rod bipolar cell dendrites. In the dendritic spines of hippocampal cells, the measured decay kinetics of the calcium concentration had a two components: a fast decay time constant of about 80ms, and a slower decay time constant of around 780ms (Majewska et al., 2000). A dual exponential of the decay in the calcium-activated chloride current (reflecting calcium extrusion) was also found in the cone photoreceptor terminals in Tupaia retina, with time constants of 50-80ms and 150ms (Morgans et al., 1998). In hippocampal neurons, the slow time constant was attributed to diffusional equilibrium of calcium between the spine and the dendrite, while the fast decay time

constant was partially attributed to the pumping of calcium into the smooth endoplasmic reticulum. Whether calcium pumps on the endoplasmic reticulum limit the recovery from inactivation, or whether the calcium dynamics are controlled by other calcium extrusion mechanisms, such as the plasma membrane calcium ATPase found on cone photoreceptor terminals (Morgans et al., 1998) is unknown. There are numerous other variables which could influence the recovery time constant such as the transition kinetics between channel states, or the buffering, diffusion or binding rates of other proteins involved in the signal transduction cascade. Further experiments will be necessary to elucidate the mechanisms utilized to remove calcium from the dendrites.

Conclusion

The rod bipolar cell light response strongly inactivates following stimulation by light, but no inactivation was seen in on-cone bipolar cells. Since the mGluR6-gated channel has not yet been identified, it will be interesting to see from future experiments whether the rod and on-cone bipolar cells express different channels, or whether the inactivation arises from an additional step in the rod bipolar cell signal transduction cascade.

Signal attentuation caused by an automatic gain control mechanism at a site independent from the photoreceptors has been proposed to explain adaptation of the visual system at intensities which are too low to cause adaptation in the rods (Enroth-Cugell and Shapley, 1973; Baylor et al., 1984; Tamura et al., 1991; Kraft et al., 1993). The present results suggest that the rod-rod bipolar cell synapse may be a site for post-receptoral adaptation. Indeed, inactivation of the rod bipolar cell light response occurs at light intensities which are lower than those expected to produce adaptation in the rods. Furthermore, the post-receptoral adaptation described by Enroth-Cugell and Shapley (1973) occurred within 100ms of applying an adapting light. This is similar to the time course of the inactivation of the rod bipolar cell light response (60ms).

Alternatively, or perhaps in addition to a role in post-receptoral adaptation, it is possible that the inactivation shuts down the rod bipolar cell-AII amacrine cell pathway, leaving the direct rod-to-cone pathway as the main thoroughfare for rod signals. It has already been suggested that under dark-adapted conditions the rod bipolar cell-AII amacrine cell pathway dominates as the route for rod signals, while light intensities extending into the mesopic range favor the rod-to-cone pathway (Enroth-Cugell et al., 1977; Nelson, 1977). A model developed by Smith (1986) provided a physical mechanism by which this may occur. Namely, at high scotopic, and mesopic intensities when all the rods converging onto a cone pedicle via gap junctions are active (~40 rods per cone), the collective rod signal would be efficiently conveyed to the cone pedicle.

Under these conditions, the rod signal arrives at the cone bipolar cells by way of the cone pedicle. In contrast, under low scotopic conditions the rods and cones become elecrically unconnected, and the rod signal is then transmitted to the cone bipolar cells via the rod bipolar cell-AII amacrine cell pathway (Smith et al., 1986). A difference in gain characteristics between the two pathways may also explain the attenuation of the rod signal at intensities which would not adapt the rod photoreceptors.

These two possibilities are not mutually exclusive, and it is possible that the inactivation of the rod bipolar cell reduces the gain of rod signals transmitted via the rod bipolar cell-AII amacrine cell pathway, while increased coupling between rods and cones to diverts rod signals directly into the cone pathway. It will be very interesting in future experiments to examine these possibilities by exploring the response characteristics of the rod bipolar cells exposed to steady backgrounds sufficient to induce inactivation.

References

References

Adelson, E. H. (1982). "Saturation and adaptation in the rod system." Vision Res **22**(10): 1299-312.

Albillos, A., Neher, E. and Moser, T. (2000). "R-Type Ca2+ channels are coupled to the rapid component of secretion in mouse adrenal slice chromaffin cells." J Neurosci **20**(22): 8323-30.

Alpern, M., Rushton, W. A. and Torii, S. (1970). "Signals from cones." J Physiol (Lond) **207**(2): 463-75.

Ashmore, J. F. and Copenhagen, D. R. (1980). "Different postsynaptic events in two types of retinal bipolar cell." Nature **288**(5786): 84-6.

Ashmore, J. F. and Copenhagen, D. R. (1983). "An Analysis of transmission from cones to hyperpolarizing bipolar cells in the retina of the turtle." Journal of Physiology **300**: 115-150.

Ashmore, J. F. and Falk, G. (1979). "Transmission of visual signals to bipolar cells near absolute threshold." Vision Res **19**(4): 419-23.

Ashmore, J. F. and Falk, G. (1980). "Responses of rod bipolar cells in the dark-adapted retina of the dogfish, Scyliorhinus canicula." Journal of Physiology **300**: 115-50.

Ashmore, J. F. and Falk, G. (1981). "Photon-like signals following weak rhodopsin bleaches." Nature **289**(5797): 489-91.

Attwell, D. (1986). "Ion channels and signal processing in the outer retina." Quartely Journal of Experimental Physiology **71**: 497-536.

Attwell, D., Borges, S., Wu, S. M. and Wilson, M. (1987). "Signal clipping by the rod output synapse." Nature **328**: 522-524.

Attwell, D., Mobbs, P., Tessier-Lavigne, M. and Wilson, M. (1987). "Neurotransmitter-induced currents in retinal bipolar cells of the axolotl, Ambystoma mexicanum." J Physiol **387**: 125-61.

Attwell, D., Werblin, F. S., Wilson, M. and Wu, S. M. (1983). "A sign-reversing pathway from rods to double and single cones in the retina of the tiger salamander." J Physiol (Lond) **336**: 313-33.

Augustine, G. J., Burns, M. E., DeBello, W. M., Pettit, D. L. and Schweizer, F. E. (1996). "Exocytosis: proteins and perturbations." Annu Rev Pharmacol Toxicol **36**: 659-701.

Augustine, G. J., Charlton, M. P. and Smith, S. J. (1985). "Calcium entry and transmitter release at voltage-clamped nerve terminals of squid." J Physiol (Lond) **367**: 163-81.

Bader, C. R., Macleish, P. R. and Schwartz, E. A. (1979). "A voltage-clamp study of the light response in solitary rods of the tiger salamander." J Physiol (Lond) **296**: 1-26.

Barlow, H. and Levick, W. (1965). "The mechanism of directionally selective units in rabbit's retina." Journal of Physiology **178**: 477-504.

Barlow, H. B. and Levick, W. R. (1976). "Threshold setting by the surround of cat retinal ganglion cells." Journal of Physiology **259**(3): 737-57.

Barlow, H. B., Levick, W. R. and Yoon, M. (1971). "Responses to single quanta of light in retinal ganglion cells of the cat." Vision Research **Suppl 3**: 87-101.

Barnes, S. (1994). "After transduction: response shaping and control of transmission by ion channels of the photoreceptor inner segments." Neuroscience **58**(3): 447-59.

Baylor, D. A., Fuortes, M. G. and O'Bryan, P. M. (1971). "Receptive fields of cones in the retina of the turtle." J Physiol (Lond) **214**(2): 265-94.

Baylor, D. A., Nunn, B. J. and Schnapf, J. L. (1984). "The photocurrent, noise and spectral sensitivity of rods of the monkey Macaca fascicularis." Journal of Physiology **357**: 575-607.

Bean, B. P. (1984). "Nitrendipine block of cardiac calcium channels: high-affinity binding to the inactivated state." Proc Natl Acad Sci U S A **81**(20): 6388-92.

Bech-Hansen, N. T., Naylor, M. J., Maybaum, T. A., Pearce, W. G., Koop, B., Fishman, G. A., Mets, M., Musarella, M. A. and Boycott, K. M. (1998). "Loss-of-function mutations in a calcium-channel alpha1-subunit gene in Xp11.23 cause incomplete X-linked congenital stationary night blindness." Nat Genet **19**(3): 264-7.

Bekkers, J. M. and Stevens, C. F. (1990). "Presynaptic mechanism for long-term potentiation in the hippocampus." Nature **346**(6286): 724-9.

Belgum, J. H. and Copenhagen, D. R. (1988). "Synaptic transfer of rod signals to horizontal and bipolar cells in the retina of the toad (Bufo marinus)." Journal of Physiology **396**: 225-245.

Berntson, A. and Taylor, W. R. (2000). "Response characteristics and receptive field widths of on-bipolar cells in the mouse retina." J Physiol (Lond) **524 Pt 3**: 879-89.

Berridge, M. J. (1998). "Neuronal calcium signaling." Neuron **21**(1): 13-26.

Betz, W. J. and Bewick, G. S. (1993). "Optical monitoring of transmitter release and synaptic vesicle recycling at the frog neuromuscular junction." J Physiol (Lond) **460**: 287-309.

Bito, H., Deisseroth, K. and Tsien, R. W. (1997). "Ca2+-dependent regulation in neuronal gene expression." Curr Opin Neurobiol **7**(3): 419-29.

Bloomfield, S. A. and Miller, R. F. (1986). "A functional organization of ON and OFF pathways in the rabbit retina." Journal of Neuroscience **6**(1): 1-13.

Bollmann, J. H., Helmchen, F., Borst, J. G. and Sakmann, B. (1998). "Postsynaptic Ca2+ influx mediated by three different pathways during synaptic transmission at a calyx-type synapse." J Neurosci **18**(24): 10409-19.

Borst, J. G. and Sakmann, B. (1996). "Calcium influx and transmitter release in a fast CNS synapse [see comments]." Nature **383**(6599): 431-4.

Boycott, B. B. (1988). "Horizontal cells of mammalian retinae." Neurosci Res Suppl **8**(111): S97-111.

Boycott, B. B., Hopkins, J. M. and Sperling, H. G. (1987). "Cone connections of the horizontal cells of the rhesus monkey's retina." Proc R Soc Lond B Biol Sci **229**(1257): 345-79.

Boycott, B. B. and Kolb, H. (1973). "The connections between bipolar cells and photoreceptors in the retina of the domestic cat." J Comp Neurol **148**(1): 91-114.

Boycott, B. B. and Wassle, H. (1974). "The morphological types of ganglion cells of the domestic cat's retina." J Physiol (Lond) **240**(2): 397-419.

Boycott, B. B. and Wässle, H. (1991). "Morphological classification of bipolar cells in the macaque monkey retina." European Journal of Neuroscience **3**: 1069-88.

Boynton, R. M. and Whitten, D. N. (1970). "Visual adaptation in monkey cones: recordings of late receptor potentials." Science **170**(965): 1423-6.

Brandstätter, J. H., Koulen, P. and Wässle, H. (1998). "Diversity of glutamate receptors in the mammalian retina." Vision Research **38**(10): 1385-97.

Bridges, C. D. and Quilliam, T. A. (1973). "Visual pigments of men, moles and hedgehogs." Vision Res **13**(12): 2417-21.

Burkhardt, D. A. (1977). "Responses and receptive-field organization of cones in perch retinas." Journal of Neurophysiology **40**(1): 53-62.

Burkhardt, D. A. (1993). "Synaptic feedback, depolarization, and color opponency in cone photoreceptors." Vis Neurosci **10**(6): 981-9.

Burkhardt, D. A. (1994). "Light adaptation and photopigment bleaching in cone photoreceptors in situ in the retina of the turtle." J Neurosci **14**(3 Pt 1): 1091-105.

Calderone, J. B. and Jacobs, G. H. (1995). "Regional variations in the relative sensitivity to UV light in the mouse retina." Vis Neurosci **12**(3): 463-8.

Calkins, D., Tsukamoto, Y. and Sterling, P. (1996). "Foveal cones form basal as well as invaginating junctions with diffuse ON bipolar cells." Vision Res **36**(21): 3373-81.

Carter-Dawson, L. D. and LaVail, M. M. (1979). "Rods and cones in the mouse retina. I. Structural analysis using light and electron microscopy." J Comp Neurol **188**(2): 245-62.

Carter-Dawson, L. D. and LaVail, M. M. (1979). "Rods and cones in the mouse retina. II. Autoradiographic analysis of cell generation using tritiated thymidine." J Comp Neurol **188**(2): 263-72.

Catterall, W. A. (1991). "Functional subunit structure of voltage-gated calcium channels." Science **253**(5027): 1499-500.

Catterall, W. A. (1995). "Structure and function of voltage-gated ion channels." Annu Rev Biochem **64**: 493-531.

Catterall, W. A. (1998). "Structure and function of neuronal Ca2+ channels and their role in neurotransmitter release." Cell Calcium **24**(5-6): 307-23.

Chiu, M. I., Zack, D. J., Wang, Y. and Nathans, J. (1994). "Murine and bovine blue cone pigment genes: cloning and characterization of two new members of the S family of visual pigments." Genomics **21**(2): 440-3.

Chun, M. H., Han, S. H., Chung, J. W. and Wassle, H. (1993). "Electron microscopic analysis of the rod pathway of the rat retina." J Comp Neurol **332**(4): 421-32.

Chung, Y. H., Shin, C., Park, K. H. and Cha, C. I. (2000). "Immunohistochemical study on the distribution of neuronal voltage-gated calcium channels in the rat cerebellum." Brain Res **865**(2): 278-82.

Clamann, H. P., Mathis, J. and Luscher, H. R. (1989). "Variance analysis of excitatory postsynaptic potentials in cat spinal motoneurons during posttetanic potentiation." J Neurophysiol **61**(2): 403-16.

Cleland, B. G., Dubin, M. W. and Levick, W. R. (1971). "Sustained and transient neurones in the cat's retina and lateral geniculate nucleus." Journal Of Physiology **217**(2): 473-96.

Clements, J. D. and Silver, R. A. (2000). "Unveiling synaptic plasticity: a new graphical and analytical approach." Trends Neurosci **23**(3): 105-13.

Conner, J. D. (1982). "The temporal properties of rod vision." J Physiol (Lond) **332**: 139-55.

Conner, J. D. and MacLeod, D. I. (1977). "Rod photoreceptors detect rapid flicker." Science **195**(4279): 698-9.

Copenhagen, D., Ashmore, J. and Schnapf, J. (1983). "Kinetics of synaptic transmission from photoreceptors to horizontal and bipolar cells in turtle retina." Vision Research **23**(4): 363-9.

Cribbs, L. L., Lee, J. H., Yang, J., Satin, J., Zhang, Y., Daud, A., Barclay, J., Williamson, M. P., Fox, M., Rees, M. and Perez-Reyes, E. (1998). "Cloning and characterization of alpha1H from human heart, a member of the T-type Ca2+ channel gene family." Circ Res **83**(1): 103-9.

Crognale, M. and Jacobs, G. H. (1988). "Temporal properties of the short-wavelength cone mechanism: comparison of receptor and postreceptor signals in the ground squirrel." Vision Res **28**(10): 1077-82.

Dacey, D., Packer, O. S., Diller, L., Brainard, D., Peterson, B. and Lee, B. (2000). "Center surround receptive field structure of cone bipolar cells in primate retina." Vision Res **40**(14): 1801-11.

Dacheux, R. and Raviola, E. (1986). "The rod pathway in the rabbit retina: a depolarizing bipolar and amacrine cell." Journal of Neuroscience **6**(2): 331-45.

de la Villa, P., Kurahashi, T. and Kaneko, A. (1995). "L-glutamate-induced responses and cGMP-activated channels in three subtypes of retinal bipolar cells dissociated from the cat." Journal of Neuroscience **15**(5 Pt 1): 3571-82.

de la Villa, P., Vaquero, C. F. and Kaneko, A. (1998). "Two types of calcium currents of the mouse bipolar cells recorded in the retinal slice preparation." Eur J Neurosci **10**(1): 317-23.

Deegan, J. F. d. and Jacobs, G. H. (1993). "On the identity of the cone types of the rat retina [letter]." Exp Eye Res **56**(3): 375-7.

del Castillo, J. and Katz, B. (1954). "Quantal components of the end-plate potential." Journal of Physiology **124**: 560-573.

Detwiler, P. B., Hodgkin, A. L. and McNaughton, P. A. (1980). "Temporal and spatial characteristics of the voltage response of rods in the retina of the snapping turtle." J Physiol (Lond) **300**: 213-50.

DeVries, S. H. (2000). "Bipolar cells use kainate and AMPA receptors to filter visual information into separate channels." Neuron **28**(3): 847-56.

DeVries, S. H. and Schwartz, E. A. (1999). "Kainate receptors mediate synaptic transmission between cones and 'Off' bipolar cells in a mammalian retina." Nature **397**(6715): 157-60.

Dowling, J. E. (1987). The Retina: An Approachable Part of the Brain. Cambridge, The Belknap Press of Harvard University Press.

Dowling, J. E. and Boycott, B. B. (1966). "Organization of the primate retina: electron microscopy." Proc R Soc Lond B Biol Sci **166**(2): 80-111.

Dunlap, K., Luebke, J. I. and Turner, T. J. (1995). "Exocytotic Ca2+ channels in mammalian central neurons." Trends Neurosci **18**(2): 89-98.

Dvorak, D. (1984). "Off-pathway synaptic transmission in the outer retina of the axolotl is mediated by a kainic acid-preferring receptor." Neuroscience Letters **50**(1-3): 7-11.

Ehrlich, B. E., Kaftan, E., Bezprozvannaya, S. and Bezprozvanny, I. (1994). "The pharmacology of intracellular Ca(2+)-release channels." Trends Pharmacol Sci **15**(5): 145-9.

Eilers, J., Augustine, G. J. and Konnerth, A. (1995). "Subthreshold synaptic Ca2+ signalling in fine dendrites and spines of cerebellar Purkinje neurons [see comments]." Nature **373**(6510): 155-8.

Eilers, J. and Konnerth, A. (1997). "Dendritic signal integration." Curr Opin Neurobiol **7**(3): 385-90.

Ekesten, B., Gouras, P. and Yamamoto, S. (2000). "Cone inputs to murine retinal ganglion cells." Vision Res **40**(19): 2573-7.

Ellinor, P. T., Zhang, J. F., Randall, A. D., Zhou, M., Schwarz, T. L., Tsien, R. W. and Horne, W. A. (1993). "Functional expression of a rapidly inactivating neuronal calcium channel." Nature **363**(6428): 455-8.

Enroth-Cugell, C. and Freeman, A. W. (1987). "The receptive-field spatial structure of cat retinal Y cells." Journal of Physiology **384**: 49-79.

Enroth-Cugell, C., Hertz, G. and Lennie, P. (1977). "Cone signals in the cat's retina." J Physiol **269**(2): 273-96.

Enroth-Cugell, C. and Robson, J. G. (1966). "The contrast sensitivity of retinal ganglion cells of the cat." Journal of Physiology **187**: 517-552.

Enroth-Cugell, C. and Shapley, R. M. (1972). "Cat retinal ganglion cells: correlation between size of receptive field centre and level of field adaptation." J Physiol (Lond) **225**(2): 58P-59P.

Enroth-Cugell, C. and Shapley, R. M. (1973). "Adaptation and dynamics of cat retinal ganglion cells." J Physiol (Lond) **233**(2): 271-309.

Enz, R., Brandstätter, J., Wässle, H. and Bormann, J. (1996). "Immunocytochemical localization of the GABAc receptor rho subunits in the mammalian retina." J Neurosci **16**(14): 4479-90.

Euler, T. and Masland, R. H. (2000). "Light-evoked responses of bipolar cells in a mammalian retina." J Neurophysiol **83**(4): 1817-29.

Euler, T., Schneider, H. and Wässle, H. (1996). "Glutamate responses of bipolar cells in a slice preparation of the rat retina." Journal Of Neuroscience **16**(9): 2934-44.

Euler, T. and Wässle, H. (1995). "Immunocytochemical identification of cone bipolar cells in the rat retina." J Comp Neurol **361**(3): 461-78.

Euler, T. and Wässle, H. (1998). "Different contributions of GABAA and GABAC receptors to rod and cone bipolar cells in a rat retinal slice preparation." Journal of Neurophysiology **79**(3): 1384-95.

Fain, G. L. (1975). "Interactions of rod and cone signals in the mudpuppy retina." J Physiol (Lond) **252**(3): 735-69.

Famiglietti, E. V. J. (1981). "Functional architecture of cone bipolar cells in mammalian retina." Vision Research **21**(11): 1559-63.

Famiglietti, E. V. J. and Kolb, H. (1975). "A bistratified amacrine cell and synaptic cirucitry in the inner plexiform layer of the retina." Brain Research **84**(2): 293-300.

Famiglietti, E. V. J. and Kolb, H. (1976). "Structural basis for ON-and OFF-center responses in retinal ganglion cells." Science **194**(4261): 193-5.

Freed, M., Smith, R. and Sterling, P. (1987). "Rod bipolar array in the cat retina: pattern of input from rods and GABA-accumulating amacrine cells." Journal of Comparative Neurology **266**(3): 445-55.

Frumkes, T. E. and Miller, R. F. (1979). "Pathways and polarities of synaptic interactions in the inner retina of the mudpuppy: II. Insight revealed by an analysis of latency and threshold." Brain Res **161**(1): 13-24.

Fuortes, M. G. and Simon, E. J. (1974). "Interactions leading to horizontal cell responses in the turtle retina." J Physiol (Lond) **240**(1): 177-98.

Geisler, W. S. (1983). "Mechanisms of visual sensitivity: backgrounds and early dark adaptation." Vision Res **23**(12): 1423-32.

Gillette, M. and Dacheux, R. (1995). "GABA- and glycine-activated currents in the rod bipolar cell of the rabbit retina." Journal of Neurophysiology **74**(2): 856-75.

Green, D. G., Dowling, J. E., Siegel, I. M. and Ripps, h. (1975). "Retinal mechanisms of visual adaptation in the skate." J Gen Physiol **65**(4): 483-502.

Green, D. G. and Powers, M. K. (1982). "Mechanisms of light adaptation in rat retina." Vision Res **22**(2): 209-16.

Greferath, U., Grünert, U., Müller, F. and Wässle, H. (1994). "Localization of GABAA receptors in the rabbit retina." Cell Tissue Res **276**(2): 295-307.

Grunert, U. and Martin, P. R. (1991). "Rod bipolar cells in the macaque monkey retina: immunoreactivity and connectivity." J Neurosci **11**(9): 2742-58.

Gurnett, C. A., De Waard, M. and Campbell, K. P. (1996). "Dual function of the voltage-dependent Ca2+ channel alpha 2 delta subunit in current stimulation and subunit interaction." Neuron **16**(2): 431-40.

Guthrie, P. B., Segal, M. and Kater, S. B. (1991). "Independent regulation of calcium revealed by imaging dendritic spines." Nature **354**(6348): 76-80.

Hare, W. and Owen, W. (1990). "Spatial organization of the bipolar cell's receptive field in the retina of the tiger salamander." Journal of Physiology **421**: 223-45.

Hartveit, E. (1997). "Functional organization of cone bipolar cells in the rat retina." Journal of Neurophysiology **77**(4): 1716-30.

Hayhoe, M. M., Benimoff, N. I. and Hood, D. C. (1987). "The time-course of multiplicative and subtractive adaptation process." Vision Res **27**(11): 1981-96.

Heidelberger, R., Heinemann, C., Neher, E. and Matthews, G. (1994). "Calcium dependence of the rate of exocytosis in a synaptic terminal." Nature **371**(6497): 513-5.

Heidelberger, R. and Matthews, G. (1992). "Calcium influx and calcium current in single synaptic terminals of goldfish retinal bipolar neurons." Journal of Physiology **447**: 235-256.

Hodgkin, A. L., McNaughton, P. A. and Nunn, B. J. (1985). "The ionic selectivity and calcium dependence of the light-sensitive pathway in toad rods." J Physiol **358**: 447-68.

Hood, D. C. and Finkelstein, M. A. (1986). Sensitivity to Light. Handbook of Perception and Human Performance. Toronto, John Wiley & Sons. **1, Sensory Processes and Perception.**

Hood, D. C. and Greenstein, V. (1990). "Models of the normal and abnormal rod system." Vision Res **30**(1): 51-68.

Hopkins, J. and Boycott, B. (1995). "Synapses between cones and diffuse bipolar cells of a primate retina." J Neurocytol **24**(9): 680-94.

Hopkins, J. and Boycott, B. (1997). "The cone synapses of cone bipolar cells of primate retina." J Neurocytol **26**(5): 313-25.

Hughes, T. E. (1997). "Are there ionotropic glutamate receptors on the rod bipolar cell of the mouse retina?" Visual Neuroscience **14**(1): 103-9.

Ishida, A. T., Stell, W. K. and Lightfoot, D. O. (1980). "Rod and cone inputs to bipolar cells in goldfish retina." J Comp Neurol **191**(3): 315-35.

Jacobs, G. H., Neitz, J. and Deegan, J. F. d. (1991). "Retinal receptors in rodents maximally sensitive to ultraviolet light." Nature **353**(6345): 655-6.

Jeon, C. and Masland, R. (1995). "A population of wide-field bipolar cells in the rabbit's retina." J Comp Neurol **360**(3): 403-12.

Jeon, C. J., Strettoi, E. and Masland, R. H. (1998). "The major cell populations of the mouse retina." Journal Of Neuroscience **18**(21): 8936-46.

Kamermans, M. and Spekreijse, H. (1999). "The feedback pathway from horizontal cells to cones. A mini review with a look ahead." Vision Res **39**(15): 2449-68.

Kaneko, A. (1973). "Receptive field organization of bipolar and amacrine cells in goldfish retina." Journal of Physiology **235**: 133-153.

Kaneko, A., Pinto, L. H. and Tachibana, M. (1989). "Transient calcium current of retinal bipolar cells of the mouse." J Physiol (Lond) **410**: 613-29.

Kaneko, A., Suzuki, S., Pinto, L. H. and Tachibana, M. (1991). "Membrane currents and pharmacology of retinal bipolar cells: a comparative study on goldfish and mouse." Comp Biochem Physiol C **98**(1): 115-27.

Kaneko, A. and Tachibana, M. (1985). "A voltage-clamp analysis of membrane currents in solitary bipolar cells dissociated from Carassius auratus." J Physiol **358**: 131-52.

Karschin, A. and Wässle, H. (1990). "Voltage- and transmitter-gated currents in isolated rod bipolar cells of rat retina." Journal Of Neurophysiology **63**(4): 860-76.

Kater, S. B., Mattson, M. P., Cohan, C. and Connor, J. (1988). "Calcium regulation of the neuronal growth cone." Trends Neurosci **11**(7): 315-21.

Katz, B. and Miledi, R. (1967). "The timing of calcium action during neuromuscular transmission." Journal of Physiology **189**: 535-544.

Kavalali, E. T., Zhuo, M., Bito, H. and Tsien, R. W. (1997). "Dendritic Ca2+ channels characterized by recordings from isolated hippocampal dendritic segments." Neuron **18**(4): 651-63.

Kikkawa, S., Nakagawa, M., Iwasa, T., Kaneko, A. and Tsuda, M. (1993). "GTP-binding protein couples with metabotropic glutamate receptor in bovine retinal on-bipolar cell." Biochem Biophys Res Commun **195**(1): 374-9.

Kim, H. G. and Miller, R. F. (1993). "Properties of synaptic transmission from photoreceptors to bipolar cells in the mudpuppy retina." J Neurophysiol **69**(2): 352-60.

Kolb, H. (1974). "The connections between horizontal cells and photoreceptors in the retina of the cat: electron microscopy of Golgi preparations." J Comp Neurol **155**(1): 1-14.

Kolb, H. (1977). "The organization of the outer plexiform layer in the retina of the cat: electron microscopic observations." Journal of Neurocytology **6**(2): 131-153.

Kolb, H. (1979). "The inner plexiform layer in the retina of the cat: electron microscopic observations." J Neurocytol **8**(3): 295-329.

Kolb, H. (1994). "The architecture of functional neural circuits in the vertebrate retina. The Proctor Lecture [published erratum appears in Invest Ophthalmol 1994 Sep;35(10):3576]." Invest Ophthalmol Vis Sci **35**(5): 2385-404.

Kolb, H. and Famiglietti, E. (1974). "Rod and cone pathways in the inner plexiform layer of cat retina." Science **186**(4158): 47-9.

Kolb, H. and Nelson, R. (1983). "Rod pathways in the retina of the cat." Vision Research **23**(4): 301-12.

Kolb, H., Nelson, R. and Mariani, A. (1981). "Amacrine cells, bipolar cells and ganglion cells of the cat retina: A Golgi study." Vision Research **21**: 1081-1114.

Kollmar, R., Montgomery, L. G., Fak, J., Henry, L. J. and Hudspeth, A. J. (1997). "Predominance of the alpha1D subunit in L-type voltage-gated Ca2+ channels of hair cells in the chicken's cochlea." Proc Natl Acad Sci U S A **94**(26): 14883-8.

Korn, H. and Faber, D. S. (1991). "Quantal analysis and synaptic efficacy in the CNS." Trends Neurosci **14**(10): 439-45.

Koulen, P., Malitschek, B., Kuhn, R., Bettler, B., Wassle, H. and Brandstatter, J. H. (1998). "Presynaptic and postsynaptic localization of GABA(B) receptors in neurons of the rat retina." Eur J Neurosci **10**(4): 1446-56.

Kouyama, N. and Marshak, D. W. (1992). "Bipolar cells specific for blue cones in the macaque retina." Journal Of Neuroscience **12**(4): 1233-52.

Kraft, T. W., Schneeweis, D. M. and Schnapf, J. L. (1993). "Visual transduction in human rod photoreceptors." J Physiol **464**: 747-65.

Kuffler, S. W. (1953). "Discharge Patterns and Functional Organization of Mammalian Retina." Journal of Neurophysiology **16**: 37-68.

Lamb, T. D. (1980). "Spontaneous quantal events induced in toad rods by pigment bleaching." Nature **287**(5780): 349-51.

Lamb, T. D. (1994). "Stochastic simulation of activation in the G-protein cascade of phototransduction." Biophys J **67**(4): 1439-54.

Lamb, T. D. and Pugh, E. N., Jr. (1992). "G-protein cascades: gain and kinetics." Trends Neurosci **15**(8): 291-8.

Lasansky, A. (1973). "Organization of the outer synaptic layer in the retina of the larval tiger salamander." Philos Trans R Soc Lond B Biol Sci **265**(872): 471-89.

Leskov, I. B., Klenchin, V. A., Handy, J. W., Whitlock, G. G., Govardovskii, V. I., Bownds, M. D., Lamb, T. D., Pugh, E. N., Jr. and Arshavsky, V. Y. (2000). "The gain of rod phototransduction: reconciliation of biochemical and electrophysiological measurements [In Process Citation]." Neuron **27**(3): 525-37.

Leventhal, A. G., Rodieck, R. W. and Dreher, B. (1981). "Retinal ganglion cell classes in the Old World monkey: morphology and central projections." Science **213**(4512): 1139-42.

Leventhal, A. G., Rodieck, R. W. and Dreher, B. (1985). "Central projections of cat retinal ganglion cells." J Comp Neurol **237**(2): 216-26.

Levick, W., Thibos, L., Cohn, T., Catanzaro, D. and Barlow, H. (1983). "Performance of cat retinal ganglion cells at low light levels." Journal of General Physiology **82**(3): 405-26.

Levick, W. R. (1975). "Form and function of cat retinal ganglion cells." Nature **254**(5502): 659-62.

Llinas, R., Steinberg, I. Z. and Walton, K. (1981). "Presynaptic calcium currents in squid giant synapse." Biophys J **33**(3): 289-321.

Lo, W., Molloy, R. and Hughes, T. E. (1998). "Ionotropic glutamate receptors in the retina: moving from molecules to circuits." Vision Research **38**(10): 1399-410.

Luebke, J. I., Dunlap, K. and Turner, T. J. (1993). "Multiple calcium channel types control glutamatergic synaptic transmission in the hippocampus." Neuron **11**(5): 895-902.

MacNeil, M. and Masland, R. (1998). "Extreme diversity among amacrine cells: implications for function." Neuron **20**(5): 971-82.

Maguire, G., Maple, B., Lukasiewicz, P. and Werblin, F. (1989). "γ-aminobutyric type B receptor modulation of L-type calcium channel current at bipolar cell terminals in the retina of the tiger salamander." Proceedings of the National Academy of Science (USA) **86**: 10144-10147.

Majewska, A., Brown, E., Ross, J. and Yuste, R. (2000). "Mechanisms of calcium decay kinetics in hippocampal spines: role of spine calcium pumps and calcium diffusion through the spine neck in biochemical compartmentalization." J Neurosci **20**(5): 1722-34.

Malinow, R. and Tsien, R. W. (1990). "Presynaptic enhancement shown by whole-cell recordings of long-term potentiation in hippocampal slices." Nature **346**(6280): 177-80.

Mangel, S. (1991). "Analysis of the horizontal cell contribution to the receptive field surround of ganglion cells in the rabbit retina." Journal of Physiology **442**: 211-34.

Mangel, S. and Dowling, J. (1987). "The interplexiform-horizontal cell system of the fish retina: effects of dopamine, light stimulation and time in the dark." Proceedings of the Royal Society of London. Series B: Biological Sciences **231**(1262): 91-121.

Marchiafava, P. L. (1978). "Horizontal cells influence membrane potential of bipolar cells in the retina of the turtle." Nature **275**(5676): 141-2.

Marchiafava, P. L. and Torre, V. (1978). "The responses of amacrine cells to light and intracellularly applied currents." J Physiol **276**: 83-102.

Mariani, A. P. (1984). "Bipolar cells in monkey retina selective for the cones likely to be blue-sensitive." Nature **308**(5955): 184-6.

Marks, W. B., Dobelle, W. H. and MacNichol, E. F. (1964). "Visual pigments of single primate cones." Science **143**: 1181-1183.

Masland, R. H. (1988). "Amacrine cells." Trends Neurosci **11**(9): 405-10.

Mastronarde, D. N. (1983). "Correlated firing of cat retinal ganglion cells. II. Responses of X- and Y-cells to single quantal events." Journal Of Neurophysiology **49**(2): 325-49.

Matsumoto, N. and Naka, K. I. (1972). "Identification of intracellular responses in the frog retina." Brain Res **42**(1): 59-71.

Matthews, H. R., Fain, G. L., Murphy, R. L. and Lamb, T. D. (1990). "Light adaptation in cone photoreceptors of the salamander: a role for cytoplasmic calcium." J Physiol (Lond) **420**: 447-69.

Matthews, H. R., Murphy, R. L., Fain, G. L. and Lamb, T. D. (1988). "Photoreceptor light adaptation is mediated by cytoplasmic calcium concentration." Nature **334**(6177): 67-9.

Mattson, M. P., LaFerla, F. M., Chan, S. L., Leissring, M. A., Shepel, P. N. and Geiger, J. D. (2000). "Calcium signaling in the ER: its role in neuronal plasticity and neurodegenerative disorders." Trends Neurosci **23**(5): 222-9.

McGuire, B. A., Stevens, J. K. and Sterling, P. (1984). "Microcircuitry of bipolar cells in cat retina." J Neurosci **4**(12): 2920-38.

Menini, A. (1999). "Calcium signalling and regulation in olfactory neurons." Curr Opin Neurobiol **9**(4): 419-26.

Merighi, A., Raviola, E. and Dacheux, R. (1996). "Connections of two types of flat cone bipolars in the rabbit retina." J Comp Neurol **371**(1): 164-78.

Mills, S. and Massey, S. (1995). "Differential properties of two gap junctional pathways made by AII amacrine cells [see comments]." Nature **377**(6551): 734-7.

Miyamoto, M. D. (1975). "Binomial analysis of quantal transmitter release at glycerol treated frog neuromuscular junctions." J Physiol **250**(1): 121-42.

Moreno, H., Rudy, B. and Llinas, R. (1997). "beta subunits influence the biophysical and pharmacological differences between P- and Q-type calcium currents expressed in a mammalian cell line." Proc Natl Acad Sci U S A **94**(25): 14042-7.

Morgans, C., El Far, O., Berntson, A., Wässle, H. and Taylor, W. (1998). "Calcium extrusion from mammalian photoreceptor terminals." Journal of Neuroscience **18**(7): 2467-74.

Morgans, C. W. (1999). "Calcium channel heterogeneity among cone photoreceptors in the tree shrew retina." Eur J Neurosci **11**(8): 2989-93.

Morigiwa, K. and Vardi, N. (1999). "Differential expression of ionotropic glutamate receptor subunits in the outer retina." Journal Of Comparative Neurology **405**(2): 173-84.

Moyer, J. R., Thompson, L. T., Black, J. P. and Disterhoft, J. F. (1992). "Nimodipine increases excitability of rabbit CA1 pyramidal neurons in an age- and concentration-dependent manner." J Neurophysiol **68**(6): 2100-9.

Muller, W. and Connor, J. A. (1991). "Dendritic spines as individual neuronal compartments for synaptic Ca2+ responses." Nature **354**(6348): 73-6.

Naka, K. I. and Nye, P. W. (1971). "Role of horizontal cells in organization of the catfish retinal receptive field." J Neurophysiol **34**(5): 785-801.

Naka, K. I. and Witkovsky, P. (1972). "Dogfish ganglion cell discharge resulting from extrinsic polarization of the horizontal cells." Journal of Physiology **223**(2): 449-460.

Nakajima, Y., Iwakabe, H., Akazawa, C., Nawa, H., Shigemoto, R., Mizuno, N. and Nakanishi, S. (1993). "Molecular characterization of a novel retinal metabotropic glutamate receptor mGluR6 with a high agonist selectivity for L-2-amino-4- phosphonobutyrate." J Biol Chem **268**(16): 11868-73.

Nakatani, K. and Yau, K. W. (1988). "Calcium and light adaptation in retinal rods and cones." Nature **334**(6177): 69-71.

Naraghi, M. and Neher, E. (1997). "Linearized buffered Ca2+ diffusion in microdomains and its implications for calculation of [Ca2+] at the mouth of a calcium channel." J Neurosci **17**(18): 6961-73.

Nawy, S. (1999). "The metabotropic receptor mGluR6 may signal through G(o), but not phosphodiesterase, in retinal bipolar cells." Journal Of Neuroscience **19**(8): 2938-44.

Nawy, S. (2000). "Regulation of the on bipolar cell mGluR6 pathway by Ca2+." J Neurosci **20**(12): 4471-9.

Nawy, S. and Jahr, C. E. (1990). "Suppression by glutamate of cGMP-activated conductance in retinal bipolar cells." Nature **346**(6281): 269-71.

Naylor, M. J., Rancourt, D. E. and Bech-Hansen, N. T. (2000). "Isolation and characterization of a calcium channel gene, Cacna1f, the murine orthologue of the gene for incomplete X-linked congenital stationary night blindness." Genomics **66**(3): 324-7.

Neitz, M. and Neitz, J. (2001). "The uncommon retina of the common house mouse." Trends Neurosci **24**(5): 248-249.

Nelson, R. (1977). "Cat cones have rod input: a comparison of the response properties of cones and horizontal cell bodies in the retina of the cat." J Comp Neurol **172**(1): 109-35.

Nelson, R., Famiglietti EV, J. and Kolb, H. (1978). "Intracellular staining reveals different levels of stratification for on- and off-center ganglion cells in cat retina." J Neurophysiol **41**(2): 472-83.

Nelson, R. and Kolb, H. (1983). "Synaptic patterns and response properties of bipolar and ganglion cells in the cat retina." Vision Research **23**(10): 1183-95.

Neves, G. and Lagnado, L. (1999). "The kinetics of exocytosis and endocytosis in the synaptic terminal of goldfish retinal bipolar cells." Journal Of Physiology **515 (Pt 1)**: 181-202.

Nilius, B., Hess, P., Lansman, J. B. and Tsien, R. W. (1985). "A novel type of cardiac calcium channel in ventricular cells." Nature **316**(6027): 443-6.

Normann, R. A. and Werblin, F. S. (1974). "Control of retinal sensitivity. I. Light and dark adaptation of vertebrate rods and cones." J Gen Physiol **63**(1): 37-61.

Nowycky, M. C., Fox, A. P. and Tsien, R. W. (1985). "Three types of neuronal calcium channel with different calcium agonist sensitivity." Nature **316**(6027): 440-3.

Olivera, B. M., Miljanich, G. P., Ramachandran, J. and Adams, M. E. (1994). "Calcium channel diversity and neurotransmitter release: the omega- conotoxins and omega-agatoxins." Annu Rev Biochem **63**: 823-67.

Pan, Z. H. (2000). "Differential expression of high- and two types of low-voltage-activated calcium currents in rod and cone bipolar cells of the rat retina." J Neurophysiol **83**(1): 513-27.

Pan, Z. H. and Lipton, S. A. (1995). "Multiple GABA receptor subtypes mediate inhibition of calcium influx at rat retinal bipolar cell terminals." Journal of Neuroscience **15**(4): 2668.

Peng, Y. W., Blackstone, C. D., Huganir, R. L. and Yau, K. W. (1995). "Distribution of glutamate receptor subtypes in the vertebrate retina." Neuroscience **66**(2): 483-97.

Penn, R. D. and Hagins, W. A. (1972). "Kinetics of the photocurrent of retinal rods." Biophys J **12**(8): 1073-94.

Perez-Reyes, E., Cribbs, L., Daud, A., Lacerda, A., Barclay, J., Williamson, M., Fox, M., Rees, M. and Lee, J. (1998). "Molecular characterization of a neuronal low-voltage-activated T-type calcium channel [see comments]." Nature **391**(6670): 896-900.

Petersen, O. H. and Cancela, J. M. (1999). "New Ca2+-releasing messengers: are they important in the nervous system?" Trends Neurosci **22**(11): 488-95.

Picones, A. and Korenbrot, J. I. (1992). "Permeation and interaction of monovalent cations with the cGMP-gated channel of cone photoreceptors." J Gen Physiol **100**(4): 647-73.

Picones, A. and Korenbrot, J. I. (1995). "Permeability and interaction of Ca2+ with cGMP-gated ion channels differ in retinal rod and cone photoreceptors." Biophys J **69**(1): 120-7.

Piedras-Renteria, E. S. and Tsien, R. W. (1998). "Antisense oligonucleotides against alpha1E reduce R-type calcium currents in cerebellar granule cells." Proc Natl Acad Sci U S A **95**(13): 7760-5.

Pourcho, R. G. and Goebel, D. J. (1987). "A combined Golgi and autoradiographic study of 3H-glycine-accumulating cone bipolar cells in the cat retina." J Neurosci **7**(4): 1178-88.

Protti, D. and Llano, I. (1998). "Calcium currents and calcium signaling in rod bipolar cells of rat retinal slices." Journal of Neuroscience **18**(10): 3715-24.

Protti, D. A., Flores-Herr, N. and von Gersdorff, H. (2000). "Light evokes Ca2+ spikes in the axon terminal of a retinal bipolar cell." Neuron **25**(1): 215-27.

Pugh, E. N., Jr., Nikonov, S. and Lamb, T. D. (1999). "Molecular mechanisms of vertebrate photoreceptor light adaptation." Curr Opin Neurobiol **9**(4): 410-8.

Qin, P. and Pourcho, R. G. (1999). "Localization of AMPA-selective glutamate receptor subunits in the cat retina: a light- and electron-microscopic study." Visual Neuroscience **16**(1): 169-77.

Rao, R., Buchsbaum, G. and Sterling, P. (1994). "Rate of quantal transmitter release at the mammalian rod synapse." Biophysical Journal **67**(1): 57-63.

Rao-Mirotznik, R., Harkins, A. B., Buchsbaum, G. and Sterling, P. (1995). "Mammalian rod terminal: architecture of a binary synapse." Neuron **14**(3): 561-9.

Raviola, E. and Gilula, N. B. (1973). "Gap junctions between photoreceptor cells in the vertebrate retina." Proc Natl Acad Sci U S A **70**(6): 1677-81.

Raynauld, J. P., Laviolette, J. R. and Wagner, H. J. (1979). "Goldfish retina: a correlate between cone activity and morphology of the horizontal cell in clone pedicules." Science **204**(4400): 1436-8.

Regehr, W. G. and Mintz, I. M. (1994). "Participation of multiple calcium channel types in transmission at single climbing fiber to Purkinje cell synapses." Neuron **12**(3): 605-13.

Richter, A. and Simon, E. J. (1975). "Properties of centre-hyperpolarizing, red-sensitive bipolar cells in the turtle retina." J Physiol **248**(02): 317-34.

Rieke, F. and Baylor, D. A. (1998). "Origin of reproducibility in the responses of retinal rods to single photons." Biophys J **75**(4): 1836-57.

Rieke, F. and Baylor, D. A. (1998). "Single-photon detection by rod cells of the retina." Reviews of Modern Physics **70**(3): 1027-1036.

Rieke, F. and Schwartz, E. (1994). "A cGMP-gated current can control exocytosis at cone synapses." Neuron **13**(4): 863-73.

Rouze, N. C. and Schwartz, E. A. (1998). "Continuous and transient vesicle cycling at a ribbon synapse." Journal Of Neuroscience **18**(21): 8614-24.

Rowe, M. and Cox, J. (1993). "Spatial receptive-field structure of cat retinal W cells." Vis Neurosci **10**(4): 765-79.

Saito, H. A. (1983). "Morphology of physiologically identified X-, Y-, and W-type retinal ganglion cells of the cat." J Comp Neurol **221**(3): 279-88.

Saito, T. and Kaneko, A. (1983). "Ionic mechanisms underlying the responses of off-center bipolar cells in the carp retina. I. Studies on responses evoked by light." J Gen Physiol **81**(4): 589-601.

Saito, T. and Kujiraoka, T. (1988). "Characteristics of bipolar-bipolar coupling in the carp retina." Journal Of General Physiology **91**(2): 275-87.

Sakitt, B. (1972). "Counting every quantum." J Physiol (Lond) **223**(1): 131-50.

Sandell, J., Masland, R., Raviola, E. and Dacheux, R. (1989). "Connections of indoleamine-accumulating cells in the rabbit retina." J Comp Neurol **283**(2): 303-13.

Scheller, R. H. (1995). "Membrane trafficking in the presynaptic nerve terminal." Neuron **14**(5): 893-7.

Schneeweis, D. and Schnapf, J. (1995). "Photovoltage of rods and cones in the macaque retina." Science **268**: 1053-1056.

Schneeweis, D. M. and Schnapf, J. L. (1999). "The photovoltage of macaque cone photoreceptors: adaptation, noise, and kinetics." J Neurosci **19**(4): 1203-16.

Schultz, K., Goldman, D. J., Ohtsuka, T., Hirano, J., Barton, L. and Stell, W. K. (1997). "Identification and localization of an immunoreactive AMPA-type glutamate receptor subunit (GluR4) with respect to identified photoreceptor synapses in the outer plexiform layer of goldfish retina." Journal Of Neurocytology **26**(10): 651-66.

Shapley, R. and Enroth-Cugell, C. (1985). "Visual adaptation and retinal gain controls." Progress in Retinal Research **3**: 263-346.

Shen, W. and Slaughter, M. M. (1999). "Metabotropic GABA receptors facilitate L-type and inhibit N-type calcium channels in single salamander retinal neurons." J Physiol (Lond) **516**(Pt 3): 711-8.

Shiells, R. A. and Falk, G. (1990). "Glutamate receptors of rod bipolar cells are linked to a cyclic GMP cascade via a G-protein." Proceedings Of The Royal Society Of London. Series B: Biological Sciences **242**(1304): 91-4.

Shiells, R. A. and Falk, G. (1992). "Properties of the cGMP-activated channel of retinal on-bipolar cells." Proceedings Of The Royal Society Of London. Series B: Biological Sciences **247**(1318): 21-5.

Shiells, R. A. and Falk, G. (1994). "Responses of rod bipolar cells isolated from dogfish retinal slices to concentration-jumps of glutamate." Visual Neuroscience **11**(6): 1175-83.

Shiells, R. A. and Falk, G. (1999). "Calcium activation of protein kinase C (PKC) initiates light adaptation in dogfish retinal ON-bipolar cells." Journal of Physiology **515P.**: 34P.

Shiells, R. A. and Falk, G. (1999). "A rise in intracellular Ca2+ underlies light adaptation in dogfish retinal 'on' bipolar cells." J Physiol (Lond) **514 (Pt 2)**: 343-50.

Shiells, R. A. and Falk, G. (2000). "Activation of Ca2+-calmodulin kinase II induces desensitization by background light in dogfish retinal 'on' bipolar cells." J Physiol **528**(Pt 2): 327-338.

Simon, E. J., Lamb, T. D. and Hodgkin, A. L. (1975). "Spontaneous voltage fluctuations in retinal cones and bipolar cells." Nature **256**(5519): 661-2.

Sinex, D., Burdette, L. and Pearlman, A. (1979). "A psychophysical investigation of spatial vision in the normal and reeler mutant mouse." Vision Research **19**(8): 853-7.

Singer, D., Biel, M., Lotan, I., Flockerzi, V., Hofmann, F. and Dascal, N. (1991). "The roles of the subunits in the function of the calcium channel." Science **253**(5027): 1553-7.

Slaughter, M. M. and Miller, R. F. (1981). "2-amino-4-phosphonobutyric acid: a new pharmacological tool for retina research." Science **211**(4478): 182-5.

Smith, R. and Sterling, P. (1990). "Cone receptive field in cat retina computed from microcircuitry." Visual Neuroscience **5**(5): 453-61.

Smith, R. G., Freed, M. A. and Sterling, P. (1986). "Microcircuitry of the dark-adapted cat retina: functional architecture of the rod-cone network." Journal of Neuroscience **6**(12): 3505-3517.

Soucy, E., Wang, Y., Nirenberg, S., Nathans, J. and Meister, M. (1998). "A novel signaling pathway from rod photoreceptors to ganglion cells in mammalian retina." Neuron **21**(3): 481-93.

Sparks, D. L. (1988). "Neural cartography: sensory and motor maps in the superior colliculus." Brain Behav Evol **31**(1): 49-56.

Srinivasan, M. V., Laughlin, S. B. and Dubs, A. (1982). "Predictive coding: a fresh view of inhibition in the retina." Proc R Soc Lond B Biol Sci **216**(1205): 427-59.

Stea, A., Dubel, S. J., Pragnell, M., Leonard, J. P., Campbell, K. P. and Snutch, T. P. (1993). "A beta-subunit normalizes the electrophysiological properties of a cloned N-type Ca2+ channel alpha 1-subunit." Neuropharmacology **32**(11): 1103-16.

Sterling, P. (1990). Retina. The Synaptic Organization of the Brain. G. M. Shepherd. New York, Oxford University Press: 170-213.

Sterling, P. (1998). ""Knocking out" a neural circuit." Neuron **21**(4): 643-4.

Sterling, P., Freed, M. A. and Smith, R. G. (1988). "Architecture of rod and cone circuits to the on-beta ganglion cell." J Neurosci **8**(2): 623-42.

Sterling, P. and Harkins, A. B. (1990). "Ultrastructure of the cone pedicle in cat retina." Invest Ophthalmol Vis Sci **31**: 177.

Sterling, P. and Lampson, L. A. (1986). "Molecular specificity of defined types of amacrine synapse in cat retina." J Neurosci **6**(5): 1314-24.

Stone, J. and Hoffmann, K. (1972). "Very slow-conducting ganglion cells in the cat's retina: a major, new functional type?" Brain Research **43**(2): 610-6.

Strettoi, E., Dacheux, R. and Raviola, E. (1990). "Synaptic connections of rod bipolar cells in the inner plexiform layer of the rabbit retina." J Comp Neurol **295**(3): 449-66.

Strettoi, E., Dacheux, R. and Raviola, E. (1994). "Cone bipolar cells as interneurons in the rod pathway of the rabbit retina." Journal of Comparative Neurology **347**(1): 139-49.

Strom, T. M., Nyakatura, G., Apfelstedt-Sylla, E., Hellebrand, H., Lorenz, B., Weber, B. H., Wutz, K., Gutwillinger, N., Ruther, K., Drescher, B., Sauer, C., Zrenner, E., Meitinger, T., Rosenthal, A. and Meindl, A. (1998). "An L-type calcium-channel gene mutated in incomplete X-linked congenital stationary night blindness." Nat Genet **19**(3): 260-3.

Su, Z. L., Jiang, S. C., Gu, R. and Yang, W. P. (1995). "Two types of calcium channels in bullfrog saccular hair cells." Hear Res **87**(1-2): 62-8.

Sudhof, T. C. (1995). "The synaptic vesicle cycle: a cascade of protein-protein interactions." Nature **375**(6533): 645-53.

Sun, H., Macke, J. P. and Nathans, J. (1997). "Mechanisms of spectral tuning in the mouse green cone pigment." Proc Natl Acad Sci U S A **94**(16): 8860-5.

Suzuki, S., Tachibana, M. and Kaneko, A. (1990). "Effects of glycine and GABA on isolated bipolar cells of the mouse retina." J Physiol (Lond) **421**: 645-62.

Szel, A., Rohlich, P., Caffe, A. R., Juliusson, B., Aguirre, G. and Van Veen, T. (1992). "Unique topographic separation of two spectral classes of cones in the mouse retina." J Comp Neurol **325**(3): 327-42.

Szel, A., Rohlich, P. and Van Veen, T. (1993). "Short-wave sensitive cones in the rodent retinas [letter]." Exp Eye Res **57**(4): 503-5.

Tachibana, M. and Okada, T. (1991). "Release of endogenous excitatory amino acids from ON-type bipolar cells isolated from the goldfish retina." Journal of Neuroscience **11**(7): 2199-2208.

Tachibana, M., Okada, T., Arimura, T., Kobayashi, K. and Piccolino, M. (1993). "Dihydropyridine-sensitive calcium current mediates neurotransmitter release from bipolar cells of the goldfish retina." Journal of Neuroscience **13**(7): 2898-909.

Tamura, T., Nakatani, K. and Yau, K. W. (1991). "Calcium feedback and sensitivity regulation in primate rods." J Gen Physiol **98**(1): 95-130.

Taylor, W. and Morgans, C. (1998). "Localization and properties of voltage-gated calcium channels in cone photoreceptors of Tupaia belangeri." Vis Neurosci **15**(3): 541-52.

Toyoda, J. and Tonosaki, K. (1978). "Effect of polarisation of horizontal cells on the on-centre bipolar cell of carp retina." Nature **276**(5686): 399-400.

Tsien, R. W., Lipscombe, D., Madison, D. V., Bley, K. R. and Fox, A. P. (1988). "Multiple types of neuronal calcium channels and their selective modulation." Trends Neurosci **11**(10): 431-8.

Tsukamoto, Y., Masarachia, P., Schein, S. J. and Sterling, P. (1992). "Gap junctions between the pedicles of macaque foveal cones." Vision Res **32**(10): 1809-15.

Twyman, R. E. and Macdonald, R. L. (1991). "Kinetic properties of the glycine receptor main- and sub-conductance states of mouse spinal cord neurones in culture." J Physiol **435**: 303-31.

Umino, O., Maehara, M., Hidaka, S., Kita, S. and Hashimoto, Y. (1994). "The network properties of bipolar-bipolar cell coupling in the retina of teleost fishes." Visual Neuroscience **11**(3): 533-48.

Vaney, D. I., Gynther, I. C. and Young, H. M. (1991). "Rod-signal interneurons in the rabbit retina: 2. AII amacrine cells." J Comp Neurol **310**(2): 154-69.

Vardi, N. (1998). "Alpha subunit of Go localizes in the dendritic tips of ON bipolar cells." Journal Of Comparative Neurology **395**(1): 43-52.

Vardi, N., Duvoisin, R., Wu, G. and Sterling, P. (2000). "Localization of mGluR6 to dendrites of ON bipolar cells in primate retina." J Comp Neurol **423**(3): 402-12.

Vardi, N., Matesic, D. F., Manning, D. R., Liebman, P. A. and Sterling, P. (1993). "Identification of a G-protein in depolarizing rod bipolar cells." Visual Neuroscience **10**(3): 473-8.

Vardi, N. and Morigiwa, K. (1997). "ON cone bipolar cells in rat express the metabotropic receptor mGluR6." Visual Neuroscience **14**(4): 789-94.

Vaughn, J. E., Famiglietti, E. V. J., Barber, R. P., Saito, K., Roberts, E. and Ribak, C. E. (1981). "GABAergic amacrine cells in rat retina: immunocytochemical identification and synaptic connectivity." Journal Of Comparative Neurology **197**(1): 113-27.

Verweij, J., Kamermans, M. and Spekreijse, H. (1996). "Horizontal cells feed back to cones by shifting the cone calcium- current activation range." Vision Res **36**(24): 3943-53.

Victor, J. D. (1988). "The dynamics of the cat retinal Y cell subunit." J Physiol **405**: 289-320.

von Gersdorff, H. and Matthews, G. (1994). "Dynamics of synaptic vesicle fusion and membrane retrieval in synaptic terminals." Nature **367**(6465): 735-9.

von Gersdorff, H., Vardi, E., Matthews, G. and Sterling, P. (1996). "Evidence that vesicles on the synaptic ribbon of retinal bipolar neurons can be rapidly released." Neuron **16**(6): 1221-7.

Walters, R., Kramer, R. and Nawy, S. (1998). "Regulation of cGMP-dependent current in On bipolar cells by calcium/calmodulin-dependent kinase." Vis Neurosci **15**(2): 257-61.

Wang, G., Dayanithi, G., Newcomb, R. and Lemos, J. R. (1999). "An R-type Ca(2+) current in neurohypophysial terminals preferentially regulates oxytocin secretion." J Neurosci **19**(21): 9235-41.

Wassle, H. and Boycott, B. B. (1991). "Functional architecture of the mammalian retina." Physiol Rev **71**(2): 447-80.

Wassle, H., Grunert, U., Cook, N. J. and Molday, R. S. (1992). "The cGMP-gated channel of rod outer segments is not localized in bipolar cells of the mammalian retina." Neurosci Lett **134**(2): 199-202.

Werblin, F. S. and Dowling, J. E. (1969). "Organization of the retina of the mudpuppy, Necturus maculosus. II. Intracellular recording." Journal Of Neurophysiology **32**(3): 339-55.

Westenbroek, R. E., Sakurai, T., Elliott, E. M., Hell, J. W., Starr, T. V., Snutch, T. P. and Catterall, W. A. (1995). "Immunochemical identification and subcellular distribution of the alpha 1A subunits of brain calcium channels." J Neurosci **15**(10): 6403-18.

Wilkinson, M. and Barnes, S. (1996). "The dihydropyridine-sensitive calcium channel subtype in cone photoreceptors." Journal of General Physiology **107**(5): 621-630.

Williams, M. E., Brust, P. F., Feldman, D. H., Patthi, S., Simerson, S., Maroufi, A., McCue, A. F., Velicelebi, G., Ellis, S. B. and Harpold, M. M. (1992). "Structure and functional expression of an omega-conotoxin-sensitive human N-type calcium channel." Science **257**(5068): 389-95.

Williams, M. E., Feldman, D. H., McCue, A. F., Brenner, R., Velicelebi, G., Ellis, S. B. and Harpold, M. M. (1992). "Structure and functional expression of alpha 1, alpha 2, and beta subunits of a novel human neuronal calcium channel subtype." Neuron **8**(1): 71-84.

Wong-Riley, M. T. (1974). "Synaptic orgnization of the inner plexiform layer in the retina of the tiger salamander." J Neurocytol **3**(1): 1-33.

Wu, L. G., Borst, J. G. and Sakmann, B. (1998). "R-type Ca2+ currents evoke transmitter release at a rat central synapse." Proc Natl Acad Sci U S A **95**(8): 4720-5.

Yagi, T. and Macleish, P. (1994). "Ionic conductances of monkey solitary cone inner segments." Journal of Neurophysiology **71**(2): 656-665.

Yamashita, M. and Wässle, H. (1991). "Responses of rod bipolar cells isolated from the rat retina to the glutamate agonist 2-amino-4-phosphonobutyric acid (APB)." Journal of Neuroscience **11**(8): 2372-2382.

Yau, K. W. and Nakatani, K. (1984). "Electrogenic Na-Ca exchange in retinal rod outer segment." Nature **311**(5987): 661-3.

Yau, K. W. and Nakatani, K. (1985). "Light-induced reduction of cytoplasmic free calcium in retinal rod outer segment." Nature **313**(6003): 579-82.

Young, H. M. and Vaney, D. I. (1991). "Rod-signal interneurons in the rabbit retina: 1. Rod bipolar cells." J Comp Neurol **310**(2): 139-53.

Yuste, R. and Denk, W. (1995). "Dendritic spines as basic functional units of neuronal integration." Nature **375**(6533): 682-4.

Zhang, J. F., Randall, A. D., Ellinor, P. T., Horne, W. A., Sather, W. A., Tanabe, T., Schwarz, T. L. and Tsien, R. W. (1993). "Distinctive pharmacology and kinetics of cloned neuronal Ca2+ channels and their possible counterparts in mammalian CNS neurons." Neuropharmacology **32**(11): 1075-88.

Zucker, R. S. (1996). "Exocytosis: a molecular and physiological perspective." Neuron **17**(6): 1049-55.

Appendix

Response characteristics and receptive field widths of on-bipolar cells in the mouse retina

Amy Berntson and W. Rowland Taylor

Division of Neuroscience and Centre for Visual Sciences, John Curtin School of Medical Research, Australian National University, Canberra, ACT 2600, Australia

(Received 20 October 1999; accepted after revision 10 January 2000)

1. Voltage-clamp and current-clamp recordings were made from bipolar cells in dark-adapted mouse retinal slices. Light-evoked responses fell into three groups corresponding to the rod bipolar cells, on-cone bipolar cells and off-cone bipolar cells. The morphology of the recorded cells confirmed this classification.

2. Intensity–response relations were well fitted by a Michaelis saturation function with Hill coefficients of 1·15 ± 0·11 ($n = 6$) for rod bipolar cells and 2·33 ± 0·06 ($n = 4$) for cone inputs onto on-cone bipolar cells.

3. In the absence of antagonists for GABA or glycine receptors, light-evoked synaptic currents for all cells displayed linear current–voltage relations that reversed near 0 mV, indicating that very little inhibition was activated under dark-adapted recording conditions. Saturating light stimuli evoked conductances of 0·81 ± 0·56 nS ($n = 4$) in rod bipolar cells and 1·1 ± 0·8 nS ($n = 4$) in on-cone bipolar cells.

4. Receptive field widths were estimated by flashing a vertical light bar at various locations along the slice. Rod and on-cone bipolar cells had receptive field widths of 67 ± 16 μm ($n = 6$) and 43 ± 7 μm ($n = 5$), respectively. The maximum spatial resolution of an array of such cone bipolar cells was estimated to be 0·3 cycles deg^{-1}, compared with a maximum resolution of 0·5 cycles deg^{-1} obtained from behavioural studies in mice. Our results suggest that this limit to spatial resolution could be imposed early in the visual system by the size of the bipolar cell receptive fields.

The first synapse in the vertebrate visual system occurs between the photoreceptors and bipolar cells in the retina. Two classes of bipolar cell split the visual signals into separate pathways. Off-bipolar cells hyperpolarise while on-bipolar cells depolarise in response to increases in light intensity. This dichotomy is achieved by virtue of the glutamate receptors expressed by the cells. Off-bipolar cells express excitatory AMPA/kainate receptors (Slaughter & Miller, 1983; Sasaki & Kaneko, 1996; DeVries & Schwartz, 1999) while on-bipolar cells express inhibitory metabotropic glutamate (mGluR6) receptors (Nawy & Jahr, 1990; Shiells & Falk, 1990). The two pathways are also separated morphologically. Off- and on-bipolar cells have axon terminal systems stratifying in the outer and inner halves of the inner plexiform layer, respectively.

Within these two broad classes there is further morphological diversity. In every mammalian retina studied to date eight to ten morphological subclasses of bipolar cell have been proposed (Famiglietti, 1981; Boycott & Wässle, 1991; Kolb *et al.* 1992; Grünert *et al.* 1994; Euler & Wässle, 1995). Two of these subclasses have known physiological roles. The rod bipolar cells are the only bipolar cells known to make direct synaptic connections with rod photoreceptors. All other bipolar cells, collectively the cone bipolar cells, connect exclusively to cone photoreceptors. A blue on-cone bipolar cell is known from anatomical studies in primate (Mariani, 1984; Kouyama & Marshak, 1992) to connect exclusively to short-wavelength-sensitive 'blue' cones, and thus is involved in transmitting colour signals. It is not known whether the remaining subclasses of cone bipolar cells have other physiological specialisations. To date there have been no detailed physiological analyses of bipolar cell function in a mammalian retina. One aim of this study was to look for possible physiological heterogeneity by characterising the light-evoked responses in identified subclasses of bipolar cells. We also wanted to develop the mouse as a model system for neurophysiological investigations in the retina, because of the potential for using transgenic and gene knock-out techniques to study neural function.

There have been as yet no detailed analyses of the extent of bipolar cell receptive fields in mammals. A further aim of this study was to measure the centre sizes of bipolar cell receptive fields and compare them with the measured acuity of the mouse visual system. Behavioural experiments

peak photocurrents recorded at each position were fitted to a Gaussian function:

$$I_{peak} = I_{min}\exp(-(x - c)^2/w^2), \quad (2)$$

where I_{min} is the minimum current value, c denotes the centre of the profile and w is a measure of the half-width of the profile. Responses at the central location were repeated during the data collection run to ensure that the sensitivity of the cell did not change significantly (< 10 %).

RESULTS

We recorded light responses from 95 cells, 67 of which were visually identified as bipolar cells. Cells that could not be conclusively identified were excluded from the analysis.

Classes of bipolar cells

Bipolar cells in the mammalian retina have been divided morphologically into about ten different classes, and so we began by examining the hypothesis that the light-evoked physiological responses might display a variability that reflects the morphological diversity (Hare *et al.* 1986; DeVries & Schwartz, 1999). Analysis of photocurrents in response to flashes and steps of light (Fig. 1) revealed only three functionally distinct groups: rod bipolar cells (RBPs, $n = 30$), on-cone bipolar cells (on-CBPs, $n = 22$) and off-cone bipolar cells (off-CBPs, $n = 15$).

RBPs, which had narrow axonal arbors stratifying deep in the inner plexiform layer at the border with the ganglion cell layer, were always depolarising or on-type cells (i.e. inward photocurrents, Fig. 1*A*). RBPs invariably displayed a pronounced sag during responses to saturating light steps. The presence of the sag could be used as a first indication that the cell recorded from was a RBP and not an on-CBP. On-CBPs, which had axonal arbors stratifying in the inner half of the inner plexiform layer, displayed step responses which were generally more sustained (Fig. 1*B*). Light responses in both RBPs and on-CBPs, which are mediated by metabotropic glutamate receptors (Nawy & Jahr, 1991), ran down within the first 10–15 min of recording, presumably due to wash out of a soluble second messenger. Off-CBPs, which had axonal arbors restricted to the outer half of the inner plexiform layer, produced sustained outward currents in response to light steps (Fig. 1*C*). These light-evoked responses, which are mediated by shutting off tonically activated ionotropic glutamate receptors, did not wash out during the recording period.

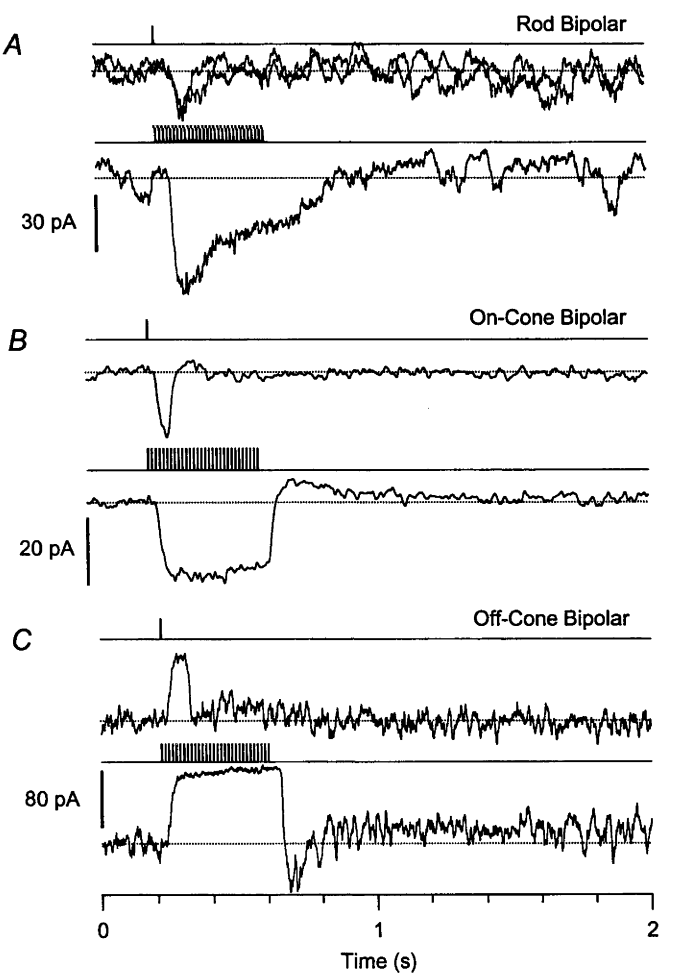

Figure 1. Three classes of bipolar cell
Whole-cell voltage-clamp responses to flashes (upper traces) and steps (lower traces) of light in rod and cone bipolar cells. Holding potential, −70 mV. The light intensity produced saturating responses in all cases except the flash responses for the RBP, which were subsaturating. The light stimulus monitor traces above the records show the timing of the light flashes. *A*, RBP. Two flash responses have been superimposed. Stimulus intensity, 0·1 lm m^{-2}. Despite the characteristically high dark noise (and low signal:noise ratio of ~3) the timing of the responses to the two flashes is very accurately registered. Note the strong suppression of current noise during the light step (stimulus intensity, 0·35 lm m^{-2}). *B*, on-CBP. The dark noise was lower in on-CBPs than in RBPs. *C*, off-CBP. The dark noise was strongly suppressed by light. Stimulus intensity in *B* and *C*, 14·4 lm m^{-2}.

cell photocurrents (Fig. 2*A*) and photovoltages (Fig. 2*B*) evoked in the same RBP by 390 ms light steps of increasing intensity (top to bottom). The pronounced sag and long tails seen for the brighter steps are reminiscent of photovoltages evoked by 10 ms light flashes in mammalian rods (Schneeweis & Schnapf, 1995), as is the progressively more rapid activation of the photocurrent (Fig. 2*C*). The rate of activation was similar for the current and the voltage (Fig. 2*D*), indicating that the membrane time constant does not significantly filter the light-evoked signals. The sag in the photovoltages during the largest responses was less pronounced than that seen for the photocurrents (Fig. 2*D*), probably due to the decrease in the driving force as the cell is depolarised during the light stimulus.

Normalised data for six RBPs were well described by eqn (1) with $h = 1{\cdot}15 \pm 0{\cdot}11$ (Fig. 3*A*). The values for L_0 for the individual cells averaged $0{\cdot}072 \pm 0{\cdot}039$ lm m^{-2}. The L_0 value for each cell has been normalised to this average value in Fig. 3*A*. Similarly the photovoltages in another group of five RBPs were well described by eqn (1), with h taking the slightly higher value of $1{\cdot}46 \pm 0{\cdot}11$. The values of L_0 for the individual cells averaged $0{\cdot}028 \pm 0{\cdot}006$ lm m^{-2}, and were also normalised to the average value in Fig. 3*B*.

Intensity–response relations were also measured in four on-CBPs. In one cell the data were well described by eqn (1); however, in contrast to the RBPs the Hill coefficient was 2·38. Three other cells displayed more complex intensity–response relations (Fig. 4). There was a distinct shoulder at lower intensities, followed by a sharper rise at higher intensities. If the shoulder at lower intensities was due to rod input, either through gap junctions between rods and cones or via the RBP to A-II amacrine cell pathway, then the intensity–response relation should be described by the sum of two eqn (1), with the L_0 and h values for the shoulder component being similar to those obtained for the RBPs above (Fig. 3). To test this we fitted the data to the sum of two eqn (1). There were six parameters, $R_{\max(1)}$, $R_{\max(2)}$, $L_{0(1)}$, $L_{0(2)}$, h_1 and h_2. Based on the results in Fig. 3*A* we set $h_1 = 1{\cdot}15$ for the putative rod component and allowed the other parameters to vary during the fitting procedure. For the two cells illustrated in Fig. 4, the L_0 values were very similar to the average L_0 obtained for the RBPs.

The difference in $L_{0(1)}$ and $L_{0(2)}$ also supports the idea that the two inputs arise from rods and cones. The half-activation intensities for putative rod inputs in the three cells were 1·6, 1·2 and 1·9 log intensity units lower than the cone inputs. A similar difference in half-maximal activation intensities occurs for macaque rods and cones (Schneeweis & Schnapf, 1995). Despite this variability in the half-activation intensities, the amplitude ratios (rod:cone) of the two inputs were very similar, being 0·29, 0·34 and 0·26 for the three cells. The Hill coefficients measured for the cone inputs in four cells (one cell lacked the rod input) were also highly reproducible ($h_2 = 2{\cdot}33 \pm 0{\cdot}06$, $n = 4$).

Response characteristics: synaptic conductance

The results presented thus far were recorded at a holding potential of −70 mV, close to the reversal potential for chloride conductances, and therefore inhibitory inputs, if present, might not have been detected. Current–voltage relations of the light-activated responses were measured to test for the presence of light-activated inhibition and also to estimate the magnitude of the excitatory conductances in the cells. Photocurrents were recorded at a range of holding potentials in RBPs (Fig. 5*A*) and on-CBPs (Fig. 5*C*). The light-evoked conductance had a reversal potential close to 0 mV (RBP, $V_{\text{rev}} = -1{\cdot}7$ mV, $n = 4$; on-CBP, $V_{\text{rev}} = -0{\cdot}70$ mV, $n = 4$) and a linear current–voltage relation, consistent with the photocurrents being almost

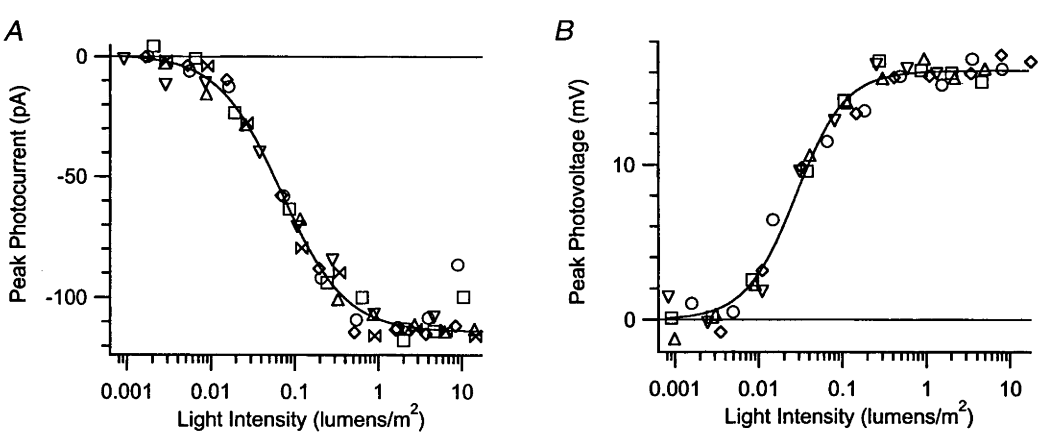

Figure 3. Normalised intensity–response plots for RBPs

For each cell the data have been normalised to have the same half-maximal light intensity and maximum amplitude. *A*, intensity–response relation obtained from the peak photocurrents in six cells, including those illustrated in Fig. 2*A* and *C*. The line though the points was fitted to eqn (1) where $h = 1{\cdot}15$, $L_0 = 0{\cdot}070$ lm m^{-2} and $I_{\min} = -115$ pA. *B*, intensity–response relation obtained from the peak photovoltages in four cells, including the cell shown in Fig. 2*B*. The line though the points was fitted to eqn (1) where $h = 1{\cdot}46$, $L_0 = 0{\cdot}028$ lm m^{-2} and $V_{\max} = 16{\cdot}1$ mV.

field profiles were 67 ± 16 μm ($n = 6$) for the RBPs and 43 ± 7 μm ($n = 5$) for the on-CBPs. No evidence for the activation of surround inhibition was seen during these experiments.

DISCUSSION

This study represents the first detailed analysis of light-evoked inputs to bipolar cells in a mammalian retina. A notable finding is that the properties of the light-evoked responses for individual cells within the three broad groups (RBPs, off- and on-CBPs) were similar, independent of the diverse morphologies. A similar conclusion was reached from a study of light-evoked responses in visualised salamander bipolar cells (Hare *et al.* 1986) and also from an analysis of synaptic responses in off-CBPs in squirrel (DeVries & Schwartz, 1999). This suggests that further functional specialisation must arise at the level of the inner plexiform layer, where the different subclasses of bipolar cell make connections with specific classes of amacrine and ganglion cells.

Recent studies have reported the presence of ionotropic glutamate receptors on RBPs and on-CBPs (Hughes, 1997; Morigiwa & Vardi, 1999) which would produce off-type responses if they were activated by the glutamate released from the photoreceptors. However, we found no evidence that these receptors are activated by physiological stimuli. During recordings from 30 morphologically identified RBPs we only encountered depolarising responses to light. These results accord with other physiological data from dissociated cells (Yamashita & Wässle, 1991; de la Villa *et al.* 1995) and

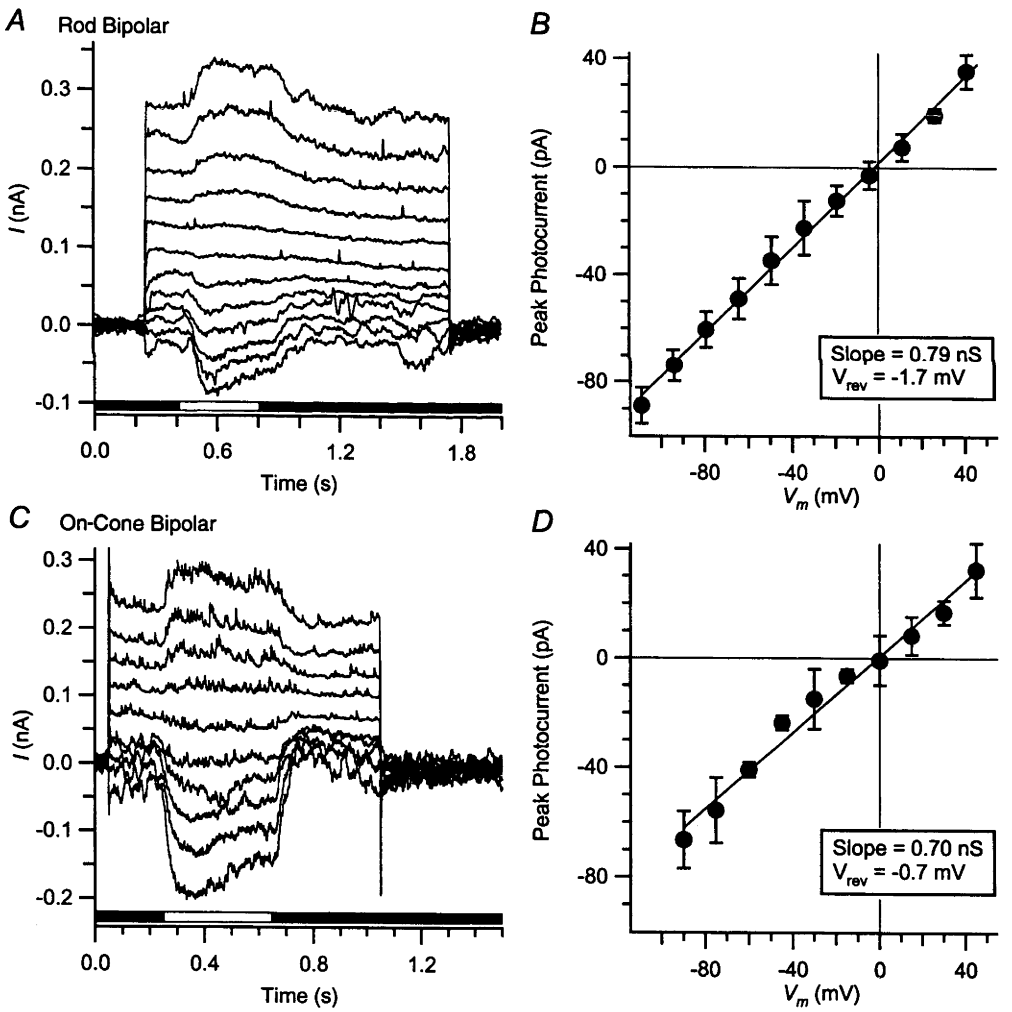

Figure 5. Current–voltage relations recorded from RBPs and on-CBPs

The holding potential was −70 mV. The membrane potential was stepped from −109 to +41 mV and ganzfeld light stimuli (390 ms; open bar in *A* and *C*) were delivered 150 ms after establishing the new potential. The peak amplitude of the light-evoked current was measured at each potential. *A* and *C*, light-evoked currents in one RBP and one on-CBP, respectively. *B* and *D*, averaged peak current–voltage relations from light-evoked currents measured in four RBPs and four on-CBPs, respectively, including the cells shown in *A* and *C*.

visual threshold when the RBPs are responding to only one or a few photons. We did not observe such behaviour in our experiments, but the presence of the 'dark noise' referred to above suggests that under the present recording conditions the stray light levels were significant, and thus the synapses may not have been operating at close to receptor saturation.

The Hill coefficient of the on-CBPs (2·33) was consistently higher than the value of 1 reported for photovoltages of dark-adapted monkey cones (Schneeweis & Schnapf, 1995). If cones in mice are similar, then the larger Hill coefficient must be due to processes subsequent to the photoreceptor voltage change. One possibility is that at the relatively low light intensities the mGluR6 receptors in on-CBPs display a dose–response relation similar to that just discussed for the RBPs and this may underlie the high Hill coefficient observed. In future experiments it will be interesting to see whether the Hill coefficient for CBPs declines to values closer to 1 at higher mean light levels.

Current–voltage relations

The current–voltage relations revealed that bipolar cells almost exclusively received glutamatergic inputs. Given that bipolar cells also receive inhibitory inputs via glycine receptors (Suzuki *et al.* 1990; Gillette & Dacheux, 1995) and GABA receptors (Feigenspan & Bormann, 1993; Gillette & Dacheux, 1995; Hartveit, 1997; Lukasiewicz & Wong, 1997; Euler & Wässle, 1998; Lukasiewicz & Shields, 1998), it is surprising that we did not see light-evoked GABA-mediated inhibitory inputs. It seems likely that GABA receptors in the inner plexiform layer contribute to the generation of surrounds in ganglion cells due to activity of the amacrine cells possibly feeding onto bipolar cell terminals (Cook & McReynolds, 1998; Taylor, 1999). The lack of inhibition in the bipolar cells cannot be attributed to inactivity of the amacrine cells, since under the same recording conditions light responses can be obtained from amacrine cells in mouse (A. Berntson & W. R. Taylor, unpublished observations) and rabbit retina (Taylor & Wässle, 1995; Taylor, 1996).

The absence of the surround could in part be a result of the tissue preparation and stimulus conditions. The slices were about 200 μm thick, and the extent of the ganzfeld stimulus was about 500 μm along the slice. Surrounds in amacrine and ganglion cells extend for hundreds of micrometres (Taylor & Wässle, 1995; Taylor, 1996), and preliminary results from peripheral monkey retina indicate that the surrounds of bipolar cells are similarly extensive (Packer *et al.* 1999). Thus, whereas the centre mechanism will be essentially intact, much of the surround might well be lost when making the slices. This, coupled with the restricted stimulus and lower sensitivity of the surround mechanism (Barlow & Levick, 1976; Ashmore & Falk, 1980), may explain the absence of strong inhibitory responses in the present experiments.

Receptive field profiles

At present the only estimates for the width of bipolar cell receptive fields in mammalian retinae come from cat (Nelson & Kolb, 1983) where widths of around 300–600 μm were obtained, although a recent abstract provides estimates of 90 μm for peripheral monkey retina (Packer *et al.* 1999). Similar widths have been obtained in non-mammalian vertebrates (Werblin & Dowling, 1969; Kaneko, 1973; Ashmore & Copenhagen, 1983; Hare *et al.* 1986; Hare & Owen, 1990). Rod and cone bipolar cells in rat have dendritic spreads of 20–40 μm (Euler & Wässle, 1995; Hartveit, 1997). Observation of our lucifer yellow-filled cells indicated that dendritic spread is similar in mouse, although it was often difficult to see clearly the finest dendritic processes. If the morphologies were similar in the mouse and the receptive fields were delineated by the reach of the dendritic processes, then the bipolar cell receptive fields in mouse retina also should have diameters of 20–40 μm.

The width of the receptive field profiles observed here was similar to or perhaps slightly larger than the dendritic spread of the bipolar cells, consistent with the idea that the bipolar cells contact the photoreceptors within reach. It also indicates that there is not extensive signal spread in the outer plexiform layer through gap junction connections between the terminals of the photoreceptors. Gap junction coupling between bipolar cells has been reported previously in vertebrate retinae (Umino *et al.* 1994; Vaney, 1994) including New World monkeys (Luo *et al.* 1999), but the results presented here indicate that if such coupling exists in mice, it is functionally weak.

The receptive fields measured here were all fairly similar in size, even though no attempt was made to control for retinal eccentricity of the recorded cells. This is to be expected since the density gradients of bipolar cells across the retina are shallow (Jeon *et al.* 1998) and thus receptive field sizes should also be fairly constant. For an eye 3 mm in diameter, an average on-CBP receptive field of 40 μm diameter covers about 1·5 deg of visual angle. Thus if the acuity of the mouse visual system was limited by the bipolar cell receptive field size, the highest spatial frequency that mice could resolve would be about 0·3 cycles deg^{-1}. Sinex and co-workers (Sinex *et al.* 1979) have used a behavioural measurement to estimate acuity. Consistent with our results, they found that behavioural responses peaked at 0·125 cycles deg^{-1} and declined to zero when the spatial frequency of the gratings reached 0·5 cycles deg^{-1}. Together these results imply the presence of an array of ganglion cells which are able to preserve the spatial acuity of the bipolar cells, presumably by making one-to-one connections with them.

In conclusion, we have established the mouse retinal slice as a viable preparation for making recordings of light-evoked responses in a mammalian retina. The mouse was chosen because it is currently the best-developed mammalian model for performing genetic manipulations and in the future we will be able to combine genetic and physiological techniques to study retinal function.

SIMON, E. J., LAMB, T. D. & HODGKIN, A. L. (1975). Spontaneous voltage fluctuations in retinal cones and bipolar cells. *Nature* **256**, 661–662.

SINEX, D., BURDETTE, L. & PEARLMAN, A. (1979). A psychophysical investigation of spatial vision in the normal and reeler mutant mouse. *Vision Research* **19**, 853–857.

SLAUGHTER, M. M. & MILLER, R. F. (1983). An excitatory amino acid antagonist blocks cone input to sign-conserving second-order retinal neurons. *Science* **219**, 1230–1232.

SUZUKI, S., TACHIBANA, M. & KANEKO, A. (1990). Effects of glycine and GABA on isolated bipolar cells of the mouse retina. *Journal of Physiology* **421**, 645–662.

TAYLOR, W. (1996). Response properties of long-range axon-bearing amacrine cells in the dark-adapted rabbit retina. *Visual Neuroscience* **13**, 599–604.

TAYLOR, W. (1999). TTX attenuates surround inhibition in rabbit retinal ganglion cells. *Visual Neuroscience* **16**, 285–290.

TAYLOR, W. & WÄSSLE, H. (1995). Receptive field properties of starburst cholinergic amacrine cells in the rabbit retina. *European Journal of Neuroscience* **7**, 2308–2321.

UMINO, O., MAEHARA, M., HIDAKA, S., KITA, S. & HASHIMOTO, Y. (1994). The network properties of bipolar-bipolar cell coupling in the retina of teleost fishes. *Visual Neuroscience* **11**, 533–548.

VANEY, D. I. (1994). Patterns of neuronal coupling in the retina. *Progress in Retinal and Eye Research* **13**, 301–355.

WERBLIN, F. S. & DOWLING, J. E. (1969). Organization of the retina of the mudpuppy, *Necturus maculsus* II: intracellular recording. *Journal of Neurophysiology* **32**, 339–355.

YAMASHITA, M. & WÄSSLE, H. (1991). Responses of rod bipolar cells isolated from the rat retina to the glutamate agonist 2-amino-4-phosphonobutyric acid (APB). *Journal of Neuroscience* **11**, 2372–2382.

Acknowledgements

We wish to thank Drs J. Bekkers, C. Morgans and P. Sah for critical comments on the manuscript, and Erika van de Pol for technical assistance.

Corresponding author

W. R. Taylor: Division of Neuroscience and Centre for Visual Sciences, John Curtin School of Medical Research, Australian National University, Canberra, ACT 2600, Australia.

Email: rowland.taylor@anu.edu.au